2006

Developmental and Neurogenetic Studies on the Peptidergic Nerve System in *Drosophila*

Youn-Jeong Choi
University of Tennessee - Knoxville

To the Graduate Council:

I am submitting herewith a dissertation written by Youn-Jeong Choi entitled "Developmental and Neurogenetic Studies on the Peptidergic Nerve System in *Drosophila*." I have examined the final electronic copy of this dissertation for form and content and recommend that it be accepted in partial fulfillment of the requirements for the degree of Doctor of Philosophy, with a major in Biochemistry and Cellular and Molecular Biology.

Jae H. Park, Major Professor

We have read this dissertation and recommend its acceptance:

Ranjan Ganguly, Bruce Mckee, Rebecca Prosser, Albrecht von Arnim

Accepted for the Council:

Carolyn R. Hodges

Vice Provost and Dean of the Graduate School

(Original signatures are on file with official student records.)

To the Graduate Council:

I am submitting here with a dissertation written by Youn-Jeong Choi entitled "Developmental and Neurogenetic Studies on the Peptidergic Nerve System in *Drosophila*." I have examined the final electronic copy of this dissertation for form and content and recommend that it be accepted in partial fulfillment of the requirements for the degree of Doctor of Philosophy, with a major in Biochemistry, Cellular and Molecular Biology.

Jae H. Park
Major Professor

We have read this dissertation
and recommend its acceptance:

Ranjan Ganguly

Bruce Mckee

Rebecca Prosser

Albrecht von Arnim

Accepted for the Council:

Linda Painter
Interim Dean of Graduate Studies

(Original signatures are on file with official student records.)

Developmental and Neurogenetic Studies on the Peptidergic Nerve System in *Drosophila*

A Dissertation

Presented for the

Doctoral philosophy

Degree

The University of Tennessee Knoxville

Youn-Jeong Choi

December 2006

Dedication

To my husband Joonho and my son Edward, the most precious persons in my life

Acknowledgments

I would like to thank my advisor, Dr. Jae Park for providing me scientific supports, guidance, and his time. I am thankful for all the members of my dissertation committee: Dr. Ranjan Ganguly, Dr. Bruce Mckee, Dr. Rebecca Prosser, and Dr. Albrecht von Arnim. I am grateful for encouragement, academic support, and guidance. I am also thankful for all members in Dr. Park's laboratory including Dr. Gyunghee Lee, who gave me scientific support.

Last, I would like to thank my husband Joonho and son Edward for their patience and love. Without their help, I could not succeed in my study.

Abstract

Neuropeptides in insects act as neurotransmitters and neuromodulators in the central nervous system (CNS) and as regulatory hormones released to the circulation. To gain insight into the mechanisms of tissue-specific *Corazonin* (*Crz)* regulation and functions in *Drosophila*, I cloned *Crz*-encoding genes from different species, and performed the phylogenetic analysis of *Crz*-encoding genes as well as Crz primary structures. To compare Crz expression patterns among different species, I performed *in situ* hybridization and immunohistochemistry to detect *Crz* expression in the CNS. Although *Crz* gene sequences reveal a great deal of diversity, Crz expression patterns are conserved among different species. In the larval CNS, Crz expression is observed in 4 pairs of cells in the cerebral lobes as well as in 8 pairs of bilateral cells in the ventral nerve cord (vCrz). During larval-to-pupal metamorphosis, vCrz neurons die of programmed cell death (PCD) while brain neurons in the pars lateralis undergo significant remodeling to form adult-specific structures. Neurites stemming from the remodeled Crz neurons project to the corpora cardiaca, a neurohemal organ, suggesting Crz's endocrine function. The finding that somata of Crz neurons are located in the proximity of nerve terminal emanating from Pdf-expressing clock pacemaker neurons suggests that Crz neurons have a functional connection to the circardian clock.

To determine neuronal cell death mechanisms, I utilize two different peptidergic neurons as model systems: vCrz and CCAP neurons. The vCrz neurons die within 6 hours after puparium formation while subsets of crustacean cardioactive peptide (CCAP)

neurons die shortly after adult eclosion. The loss of Crz and CCAP signals was prevented by ectopic expression of the baculovirus apoptotic inhibitor, *p35*, indicating caspase-dependent PCD. The vCrz cell death is triggered by ecdysone signaling mediated via EcR-B1 and EcR-B2. The vCrz PCD is prevented in a *rpr*-null mutant, however, targeted knockdown of *diap1* does not accelerate PCD, suggesting that vCrz cell death occurs via a *diap1*-independent *rpr* activation. The vCrz cell death was delayed in *dronc* and *dark* mutants, suggesting apoptosome formation during the death program. By comparison, CCAP cell death was induced by both *rpr* and *hid*, and required *dronc*. The vCrz PCD was delayed but CCAP PCD was not affected by *dcp-1*-null mutation, supporting the presence of differential caspase machinery between the two different peptidergic neurons.

Table of Contents

List of Tables

List of Figures

Figure

Figure

List of abbreviations

20-HE: 20-HydroxyEcdysone

aCCAP: abdominal ganglia CCAP

AE: After Eclosion

AEL: After Egg Laying

AKH: Adipokinetic Hormone

AO: Aorta

AP: Alkaline Phosphate

Apaf-1: Apoptotic Protease Activating Factor-1

APF: After puparium Formation

APR: Accessary Planta Reactor

Br: Brain

BR-C: Broad Complex

C. elegans: *Caenorhabditis elegans*

CAP: Crz-Associated Peptide

CC: Corpora Cardiaca

CCAP: Crustacean CardioActive Peptide

CLK: Clock

CNS: Central Nervous System

Crz: Corazonin

CYC: Cycle

Cyt-c: cytochrome-c

D. melagnogaster: *Drosophila melanogaster*

Dark: *Drosophila* Apaf-1-Related Killer

dCCAP: dorsal CCAP

Dcp-1: *Drosophila* caspase-1

DIAP: *Drosophila* Inhibitor of Apoptosis

DL: Dorsal Lateral

DLP: Dorsal-Lateral-Posterior

DM: Dorsal Medial

drICE: *Drosophila* Interleukin-1β-Converting Enzyme

EcR: Ecdysone Receptor

ELAV: Embryo Lethal Abnormal Vision

GFP: Green Fluorescent Protein

GMR: Glass Multiple Repeat

Hid: Head Involution Defective

IAP: Inhibitor of Apoptosis

IHC: Immunohistochemistry

ISH: In Situ Hybridization

IR: Immunoreactive

IRy: Immunoreactivity

JH: Juvenile Hormone

M. sexta: *Manduca sexta*

MB: Median Bundle

MB: Mushroom Body

mCCAP: Medial protocerebrum CCAP

Met: Methoprene

PCD: Programmed Cell Death

Pdf: Pigment Dispersing Factor

PG: Prothoracic gland

PLT: Posoterior Lateral Tract

RHG: Rpr, Hid, Grim

Rpr: Reaper

sCCAP: subesophageal ganglia CCAP

SCP: Small Cardioactive Peptide B

SG: Salivary Gland

Skl: Sickle

s-LNv: Small Ventro-Lateral Neuron

SOG: Subesophageal Ganglia

TH: Thyroid Hormone

UTR: UnTranslated Region

vCCAP: ventral CCAP

vCrz: Crz in the ventral nerve cord

VNC: Ventral Nerve Cord

Chapter One

Background and Significance

I. History of programmed cell death

Since the mid-nineteenth century, many observations have indicated that programmed cell death plays considerable roles in physiological processes such as metamorphosis and embryogenesis. The suicidal cell death idea was not generalized until the middle of the twentieth century. In 1951, Glücksmann assembled a long list of examples of cell death, which he classified according to their functions (Glücksmann, 1951).

The term, programmed cell death, was adopted by Lockshin and Williams (1964), in order to indicate that cell death occurs via programmed biological plan. In 1972, Kerr et al., first coined 'apoptosis' to describe distinct morphological characteristics of certain types of cell death. Apoptosis is of Greek origin, meaning "falling off or dropping off", in analogy to leaves falling off trees or petals dropping off flowers. They observed that dying cells of tadpole tissues during metamorphosis resembled each others; they are rounded, dense, and blebbed. Their nuclei becomes rounded or fragmented, and the chromatin is very condensed and pushes against the nuclear membrane. Such morphological features of cellular degeneration are distinct from those of necrotic cell death.

Genetic dissection of programmed cell death was first accomplished in *C. elegans* (Ellis and Horvitz, 1986). Since then, the molecular mechanisms by which cell death is regulated have been extensively studied, notably in the nematode, fruit fly and mammals. These studies revealed that fundamental death pathways are remarkably conserved in remotely related organisms. Despite this fact, however, it is not surprising that a number of studies witnessed that molecular death mechanisms are significantly diverse depending on types of cells, nature of the death inducing signals, and developmental status. In the following sections, I will review apoptotic cell death mechanisms identified in *Caenorhabditis elegans*, *Drosophila melanogaster*, and vertebrates.

II. Biological significance of programmed cell death

Programmed cell death (PCD) is a widespread phenomenon, occuring in all kind of metazoans such as in mammals, insects, nematodes, and cnidaria. Moreover, PCD is manifest in plants and single-cell organisms. PCD contributes to a series of biological events related to embryonic development, postembryonic development (*e.g.* metamorphosis) as well as pathology.

Appropriate execution of PCD is essential for normal developmental processes such as sculpturing bodies and metamorphosis. For example, the formation of free and independent digits requires timely elimination of the interdigital mesenchymal tissue (Zuzarte-Luís and Hurlé, 2002). It is also well known that degeneration of tail and dorsal muscles of *Xenopus* tadpole during metamorphosis is accomplished by the programmed cell death (Dodd and Dodd, 1976). In nematodes, the sculpturing process gives rise to species-specific organs and body structures. For example, in *C. elegans*, two distal tip

cells guide the extension of the anterior and posterior ends of the developing gonads, resulting in the formation of two symmetric gonadal arms, whereas in females of another nematode species, *Panagrellus redivivus*, the posterior distal tip undergoes programmed cell death, leading to the development of a one-armed gonad (Sternberg and Horvitz, 1981). During the development of the vertebrate nervous system, half or more of many types of neurons normally die soon after they form synaptic connections with their target cells (Raff et al., 1993). This programmed cell death is considered to result from the failure of these neurons to receive neurotropic signals from target cells which they innervate. By this neurotropic signaling, neurons which project to an inappropriate target are automatically eliminated, thus the number of neurons can be appropriately matched to the number of target cells (Raff et al., 1993). PCD also contributes to the formation of sex-specific organs. Structures which are required in one sex but not in the other are deleted later by PCD. For example, the Müllerian duct forms the uterus and oviduct in female mammals, but it is not needed in males and is considered to be removed by PCD. On the other hand, the Wolffian duct forms the vas deferens, epididymis, and seminal vesicle in males but it is not needed in females, thus is removed later by PCD (Jacobson et al., 1997).

PCD plays a critical role in lymphocyte development and homeostasis (Rathmell and Thompson, 2002). During lymphocyte development, the majority of cells die. Each cell must create a unique antigen receptor to provide antigen specificity to the adaptive immune system. The lymphoid cells that fail to generate antigen receptors lose developmental cues, and finally undergo PCD (Melchers et al., 2000). Furthermore,

lymphocyte numbers are tightly regulated and remain relatively constant in mature animal despite expansion during immune responses (Rathmell and Thompson, 2002).

Inappropriate PCD is involved in pathological conditions. For example, cells with severely damaged DNA that cannot be repaired appropriately usually are removed by apoptosis (Nagata, 2005). Failure of the elimination of such damaged cells may cause autoimmune diseases. For example, Autoimmune Lymphoproliferative Syndrome is due to defects in Fas (a member of tumor necrosis factor receptor family)-mediated extrinsic cell death pathways (See IV-3 in Chapter 1), leading to autoimmunity (proliferative expansion of lymphocytes reactive to self antigens) (Kiess and Gallaher, 1998; Wang et al, 1999a). PCD is also implicated in tumorigenesis since oncogenes and tumor suppressors often affect apoptotic pathways and lack of apoptosis leads to cancer (Rathmell and Thompson, 2002). Conversely, the excessive apoptosis causes neurogenerative diseases, like Alzheimer's disease, and immunodeficiency through cell loss (Huang et al., 2005; Thevissen et al., 2006).

III. The types of cell death

Kerr et al. (1972) described two distinct types of cell death: necrosis and apoptosis. Necrotic death is induced by physical injury or severe metabolic poisons, which causes abrupt and uncontrolled simultaneous damage of clumps of cells in a tissue, and leads to inflammatory responses (Trump et al., 1973; Wyllie et al., 1980). Necrotic cells are featured by an overall increase in cellular size, with little change in the chromatin initially. Organelles within the cytoplasm become disorganized, and mitochondria begin to undergo distinct changes, including the accumulation of lipid-rich

particles within the mitochondria and swelling, with the inner mitochondrial membrane shrinking from the outer membrane. At a later stage, the chromatin becomes loose and disperse and, the rupture of the cell membrane occurs and leads to release of protease, nucleases, and the cellular contents as well as inflammatory cytokines which recruit monocytes and macrophages to the site of death, thereby often causing inflammatory responses (Trump et al., 1973; Wyllie et al., 1980).

Compared to the necrotic death, apoptosis is induced by developmental processes or external stimuli, which turn on programmed events of cellular destruction, and does not lead to inflammatory responses. Unlike cellular swelling in necrotic death, apoptotic cells shrink in size, and exhibit marked alterations in their chromatin structures at an early stage (Kerr et al., 1972). Initial shrinkage of the cell causes disruption of cell-to-cell contact with neighbors and rounding up. The chromatins become highly condensed within the nucleus. Since cytoplasmic size is shrunken and thus the volume of organelles becomes smaller, the organelles look darker. However, structure of the organelles remain intact and show little changes except some swelling of the endoplasmic reticulum. Intact plasma membrane retains cytoplasmic constituents within the cell and thus an inflammatory response does not take place. Externally the cell appears to boil as the membrane becomes convoluted, thus this phase is often refered to as 'blebbing'. Concomitant with the condensation of chromatin, DNA becomes fragmented by endonuclease which cleaves DNA between nucleosomes and produces multiples of about 200 bp of DNA (Arends et al., 1990). While DNA breakdown takes place, the nucleus begins to break into fragments and the cell likewise splits into pieces. The resulting cellular fragments, called 'apoptotic bodies', are membrane-bound vesicles containing

intact cellular organelles and sometimes condensed chromatin. Finally these apoptotic bodies are phagocytosed by macrophages or neighboring epithelium cells (Kerr et al., 1972).

Another type of the programmed cell death is autophagy, which is characterized primarily by the formation of autophagosome prior to death (Klionsky and Emr, 2000). During this process, cytoplasm and organelles are enclosed in double-membrane structures called autophagic vacuoles, which then dock against the lysosome vesicles. The fusion of the outer autophagic vacuole membrane with the lysosomal membrane releases the inner membrane-bound cytoplamsic contents into the lysosome where degradation occurs (Klionsky and Emr, 2000; Baehrecke, 2003). Autophagic structures were first observed during developmental programmed cell death in insects (Schin and Clever, 1965), and later recognized as an important type of cell death in diverse organisms including humans (Baehrecke 2002).

IV. Molecular PCD mechanisms in worm, flies, and mammals

IV-1. Programmed cell death in *C. elegans*

During the development of *C. elegans*, 131 cells out of 1090 cells are fated to die via apoptosis (Sulston, 1976). Genetic studies identified more than a dozen genes that are involved in programmed death of these cells (Ellis and Horvitz, 1986). Mutations in two genes, *ced-3* and *ced-4,* prevent almost all of the programmed cell death in *C. elegans*, suggesting that functions of these two genes are crucial for the execution of cell death. Mosaic analysis of *ced-3* and *ced-4* mutants suggests that both genes act cell autonomously within dying cells (Ellis and Horvitz, 1986; Yuan and Horvitz, 1990).

Subsequent molecular and biochemical analyses revealed that *ced-3* encodes a caspase that is related to mammalian caspase-3 (Yuan et al., 1993; Xue et al., 1996), while *ced-4* encodes an ortholog of the mammalian Apaf-1 (apoptotic protease activating factor 1) that is required for the activation of CED-3 (Yang et al., 1998).

Further genetic screening identified two other death regulators, *ced-9* (Hengartner et al., 1992) and *egl-1* (Conradt and Horvitz, 1998). *ced-9* was initially identified by a gain-of-function mutation that prevents most cell death. In *ced-9* loss-of-function mutants, many cells that normally remain alive undergo PCD, suggesting that *ced-9* acts to protect cells from PCD and thus functions as an anti-apoptotic factor (Hengartner et al., 1992). The *egl-1* was also originally defined by several gain-of-function mutations that cause inappropriate death of HSN (hermaphrodite-specific neurons) (Conradt and Horvitz, 1998). A loss-of-function *egl-1* mutation prevents most somatic programmed cell deaths, suggesting that *egl-1* is an important proapoptotic factor (Conradt and Horvitz, 1998). The *egl-1* encodes a 91aa-long protein that has no sequence similarity to any other protein except for a nine-amino-acid stretch that resembles the BH3 motif of the Bcl-2 protein family (Conradt and Horvitz, 1998). Several BH3-only proteins have been known to induce apoptosis either by binding to pro-apoptotic proteins such as Bax and activating them, or by binding to and antagonizing anti-apoptotic proteins such as Bcl-X_L and Bcl-2 (see IV-3 section in Chapter 2). Similarly, EGL-1 binds CED-9 in a BH3 domain-dependent manner *in vitro* (Conradt and Horvitz, 1998).

The proposed model of the PCD occurring in *C. elegans* is as follows (Fig. 1-1). In cells that normally live, CED-3, CED-4, and CED-9 form a ternary protein complex associated with mitochondria, in which CED-3 caspase remains inactive. CED-3 may

C.elegans

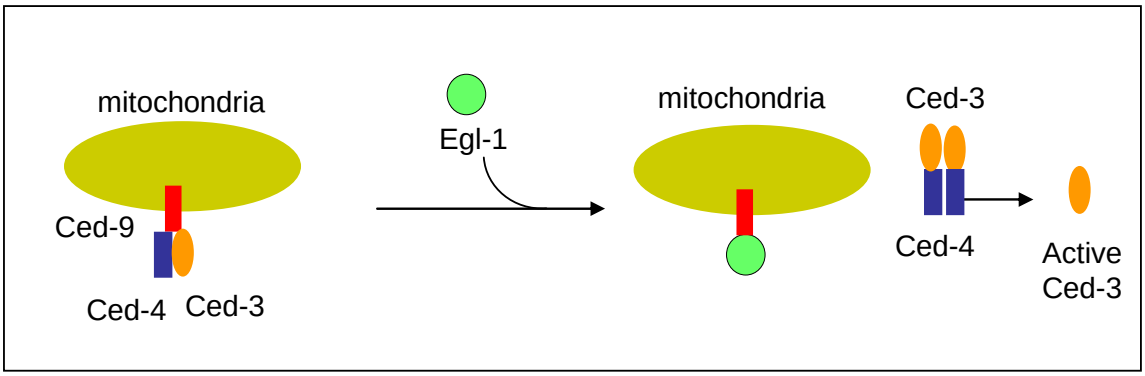

Figure 1-1. Programmed cell death pathways in *C. elegans*. In normal cells, CED-9, CED-4, and CED-3 form complexes which are associated with mitochondria. When death signals arrive, EGL-1 interacts with CED-9, then releasing CED-3/CED4. The oligomerization of CED-3 and CED-4 activates processing of CED-3 which in turn executes cell death.

also directly contact CED-9 given that CED-9 has two CED-3 cleavage sites. In cells that are fated to die, EGL-1 binds to CED-9 and displaces the CED-4/CED-3 complex from CED-9 (Yan et al., 2004), leading to the oligomerization of the CED-4/CED-3 complex. This molecular complex facilitates processing and activation of CED-3, which then executes cell death (Chinnaiyan et al., 1997, Wu et al., 1997, Yang et al., 1998, Fig. 1-1). Since *egl-1* is the most upstream activator of general cell death pathways in *C. elegans*, *egl-1* may play a crucial role in receiving cell death signals and initiating the activation of the cell death program (Conradt and Horvitz, 1998).

IV-2. Programmed cell death in *Drosophila*

Cell death genes and IAP proteins: During embryonic development, a number of cells undergo PCD to sculpt final larval form. A genomic region represented by a deletion of the chromosomal interval 75C1-2 (called *H99*) was found to be essential for embryonic cell death, as embryos homozygous for *H99* deletion are lethal due to complete lack of normal cell death (White et al., 1994). Analysis of the *H99* region revealed three important proapoptotic gene cell death genes: *reaper* (*rpr*) (white et al., 1994), *grim* (Chen et al., 1996), and *head involution defective* (*hid*) (Grether et al., 1995) (Table 1-1, 1-2). Surprisingly, *rpr*-null mutant embryos do not show significant deficit of the PCD and are viable throughout adult stage (Peterson et al., 2002). During metamorphosis, however, apoptotic death of neuroblasts and obsolete larval neurons was prevented in this mutant background, suggesting a role for *rpr* in the death of specific tissue types. Perhaps abnormal CNS structure resulting from such defective neuronal apoptosis might be a cause of sterility of *rpr* mutant males (Peterson et al., 2002). By

Table 1-1. The effect of genes on *rpr*, *grim*, and *hid*-induced PCD in the eye

Cell death gene expression	mutant background	Phenotype	Reference
GMR-rpr	+/+ (wild-type)	eye defect	
	th^{-}/+	+	Lisi et al., 2000
	GMR-gal4:UAS-diap1	–	Lisi et al., 2000
	dBruce gain of function	–	Vernooy et al., 2002
	$dark^{-}$/$dark^{-}$	–	Rodriguez et al., 1999
	$dronc^{-}$/+	–	Daish et al., 2004
	$drICE^{-}$/$drICE^{-}$	–	Muro et al., 2006
	GMR-dcp-1/+	+	Song et al., 2000
	GMR-drICE/+	+	Song et al., 2000
GMR-grim	+/+	eye defect	
	th^{-}/+	+	Lisi et al., 2000
	GMR-gal4:UAS-diap1	–	Lisi et al., 2000
	dBruce gain of function	–	Vernooy et al., 2002
	$dark^{-}$/ $dark^{-}$	–	Rodriguez et al., 1999
	$dronc^{-}$/+	–	Daish et al., 2004
	$drICE^{-}$/$drICE^{-}$	–	Muro et al., 2006
	GMR-dcp-1/+	+	Song et al., 2000
	GMR-drICE/+	+	Song et al., 2000
	GMR-p35/+	–	Chen et al., 1996
GMR-hid	+/+	eye defect	
	th^{-}/+	+	Lisi et al., 2000
	GMR-gal4:UAS-diap1	–	Lisi et al., 2000
	dBruce gain of function	No effect	Vernooy et al., 2002
	$dark^{-}$/$dark^{-}$	–	Rodriguez et al., 1999
	$dronc^{-}$/+	–	Daish et al., 2004
	$drICE^{-}$/$drICE^{-}$	–	Muro et al., 2006
	GMR-dcp-1/+	No effect	Song et al., 2000
	GMR-drICE/+	No effect	Song et al., 2000
	GMR-p35/+	–	Grether et al., 1995

th^{-}: th^{4}, th^{5}, th^{7}, $th^{109.07}$
$dark^{-}$: $dark^{CD4}$
$dronc^{-}$: $dronc^{51}$, $dronc^{I24}$, $dronc^{I29}$
$drICE^{-}$: $Ice^{\Delta 1}$
dBruce gain of function: GMREP-86A-1-5 lines (*P*-element insertion)
+: enhancement of eye defect, –: suppression of eye defect

Table 1-2. The genes essential for cell death during embryogenesis and irradiation-induced cell death

Gene	Loss-of-function mutant	Organ	Reference
Embryogenesis			
H99 (rpr, grim, hid)	Complete lack of apoptosis	Embryo	White et al., 1994
th	Increased apoptosis	Embryo	Wang et al., 1999
dronc	Reduced apoptosis	Embryo	Chew et al., 2004 Xu et al., 2005
dark	Reduced apoptosis	Embryo	Rodriguez et al., 1999
drICE	Reduced apoptosis	Embryo	Muro et al., 2006
Irradiation (IR)			
Rpr	Lack of X-ray-induced PCD	Embryo	Peterson et al., 2002
Dronc	Lack of gamma-ray-induced PCD	Eye disc	Daish et al., 2004
Dark	Lack of gamma-ray-induced PCD	Brain lobes	Mills et al., 2006
	Lack of gamma-ray-induced PCD	Eye disc	Mills et al., 2006
	Lack of gamma-ray-induced PCD	Wing disc	Mills et al., 2006
drICE	Lack of X-ray-induced PCD	Wing disc	Muro et al, 2006

comparison, homozygous *hid* loss-of-function mutants are mostly embryonic lethal, and display reduced levels of cell death (Grether et al., 1995). It is likely that *rpr*, *hid*, and *grim* cooperatively function to instruct appropriate cell death in developing embryos (e.g. Zhou et al., 1997). Genetic functions of *grim* awaits the identification of mutant variants of this gene.

Since not all types of the PCD requires REAPER, HID, and GRIM (RHG) functions (e.g. Foley and Cooley, 1998), the presence of other apoptosis activators has been proposed. Consistent with this prediction, two other death activators have been identified either through database search for proteins containing a consensus domain among RHG proteins or microarray screening (*sickle*; Christich et al., 2002; Wing et al., 2002; Srinivasula et al., 2002) or through biochemical screening of proteins that bind to inhibitor of apoptotic proteins (*Jafrac 2*; Tenev et al., 2002). Like *grim*, mutational effects of these genes on specific cell death phenotypes remains elusive.

In contrast to likely redundant actions of RHG, ectopic expression of each of these genes is sufficient for inducing cell death in a cell culture system or of specific tissues using targeted promoters (Christich et al., 2002; Srinivasula et al., 2002; Tenev et al., 2002; Wing et al., 2002). Interestingly, alignment of the aforementioned proapoptotic proteins revealed a consensus N-terminal motif, which is referred to as RHG domain (Fig. 1-2). Structure-function analysis demonstrated that this specific motif is essential for their functions as death activators (Srinivasula et al., 2002; Bergmann et al., 2003).

In contrast to the pro-death factors, a group of proteins are known to be prosurvival factors that protect cells from the death. The first identified member of this

Reaper	M**AVAF**YIPDQATLL
Grim	M**AIAY**FIPDQAQLL
Hid	M**AVPF**YLPEGGADD
Sickle	M**AIPF**FEEEHAPKS
Jafrac2	-**AKPE**

Figure 1-2. RHG motif of cell death activators. The RHG motif (in bold) is essential for the ability of the RHG proteins to induce apoptosis. The tetrapeptide motif is located at N-termini of RHG proteins and Sickle whereas it is at residue 18 of Jafrac2 precursor.

family is DIAP1 (Drosophila inhibitor of Apoptosis 1), which was shown to suppress *rpr*- or *hid*-induced degeneration of the compound eyes (Hay et al., 1995, Table 1-1). Database search for proteins similar to DIAP1 identified another member, called DIAP2 in *Drosophila*. As expected from antiapoptotic functions of DIAP1 (encoded by the *thread* (*th*) locus), homozygous *th*-null mutant embryos exhibit developmental arrest and die of massive ectopic cell death (Wang et al., 1999b; Lisi et al., 2000). However, analysis of *diap2*-null mutant showed that DIAP2 functions are not required for overall development but for innate immunity (Leulier et al., 2006a; Huh et al., 2006). These *in vivo* data suggest that DIAP2 is not a necessary component for normal apoptotic cell death, although ectopic *diap2* expression is capable of inhibiting RPR and HID-dependent cell death (Wing et al., 1998).

Sequence alignments of DIAP1 and DIAP2 together with previously described viral and mammalian IAPs revealed a consensus domain, called BIR (Baculovirus IAP repeat) (Hay et al., 1995). This ca. 70 aa long domain is present from one to three among members of the IAP family (for a review, Bergmann et al., 2003). Complete transgenic rescue of RPR- and HID-induced eye cell death by BIR of DIAP1 suggested that the BIR motifs are essential for the antiapoptotic functions of DIAPs (Hay et al., 1995). Interestingly, IAPs antagonize proapoptotic RHG proteins via physical interactions between RHG motif of RHG and BIR domains of IAPs (Vucic et al., 1997, 1998; McCarthy and Dixit, 1998; Wang et al., 1999b; Goyal et al., 2000, Fig. 1-3). In addition to the BIR, C-termini of several IAPs feature the RING (really interesting new gene) motif, which has an E3-ubiquitin ligase activity. Upon binding to proapoptotic RHG proteins, this activity is elevated to cause autoubiquitination, thereby facilitating

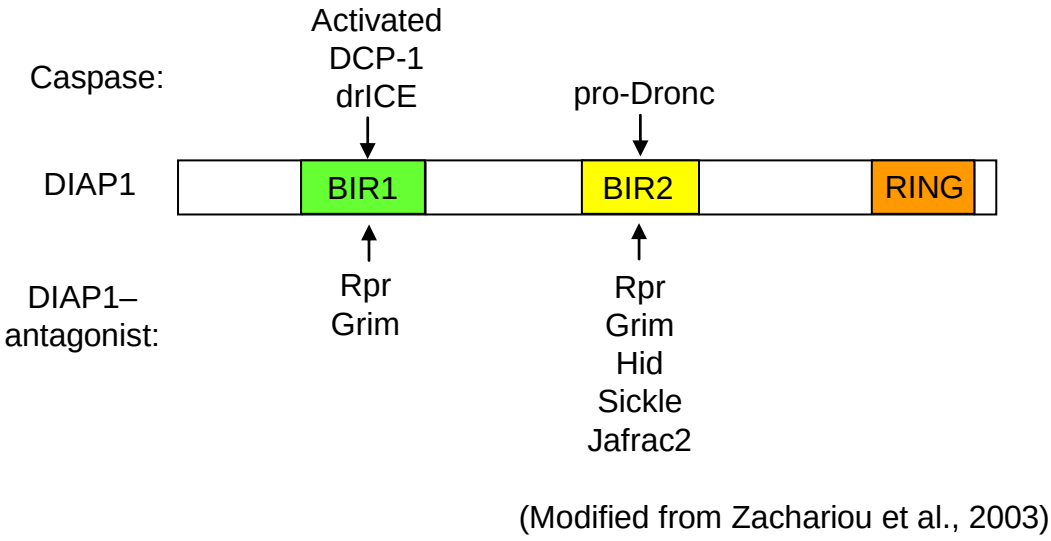

Figure 1-3. The binding of specific DIAP1 BIR domains to caspases and DIAP1-antagonists. Rpr and Grim are able to bind to both BIR domains of DIAP1. Processed forms of DCP-1 and drICE can bind to BIR1 domain of DIAP1 and unprocessed Dronc containing CARD binds to BIR2 domain. Different DIAP1-antagonists compete with distinct caspases for DIAP1 binding. RING domain of DIAP1 contains E3-ubiquitin ligase activity. The binding of the RHG proteins to DIAP1 induce E3-ligase activity of the RING domain, causing auto-ubiquitination of DIAP1.

degradation of DIAP1 (Ryoo et al., 2002; Yoo et al., 2002). Such self-degradation of DIAP1 further ensures one-way of cellular degeneration in response to death signals. Further study discovered another DIAP family, Bruce (Vernooy et al., 2002). Although Bruce has anti-apoptotic function, the regulation of cell death by Bruce is likely to be different from that of DIAP1, since Bruce inhibits cell death induced by *rpr* and *grim* but not *hid* (Table 1-1).

Caspase: Disintegration of cellular components during apoptosis is catalyzed by active caspases (Cys-Asp-protease). Therefore, tight regulation of caspase activity is crucial to determine life or death of cells. *Drosophila* genome encodes 7 caspases, which can be grouped into 2 classes, class I (initiator caspase) and class II (effector caspase) (Kumar and Doumanis, 2000). Class I caspases (DRONC, DREDD, STRICA) are characterized by a long prodomain, whereas class II caspases (DCP-1, DRICE, DECAY, DAMM) have a short or no prodomain. The long prodomain usually contains protein-protein interaction motifs, CARD (caspase recruitment domain) and DED (death effector domain), that help recuit class I caspases to specific death complexes. Class II caspases cleave a number of cellular proteins such as nuclear lamins, and they cause most of the changes that are characteristics of apoptotic cell death.

DRONC is the only known initiator caspase containing a CARD motif. *dronc* mutant embryos essentially lack most, but not all, apoptosis. In addition, *dronc* mutants affect salivary gland histolysis but not midgut degeneration (Chew et al., 2004; Daish et al., 2004; Xu et al., 2005). These observations suggest that DRONC is essential for most developmental cell death, however, also suggests for the existence of *dronc*-independent cell death pathways. Ectopic *dronc* expression induces eye ablation (Meier et al., 2000)

and RPR-, GRIM-, HID-induced eye ablation is suppressed in *dronc* mutants (Chew et al.,2004; Daish et al., 2004,; Xu et al., 2005), suggesting that *dronc* is a death executor downstream of *rpr*, *grim*, and *hid*.

DREDD is an apical caspase containing DED motifs (Chen et al., 1998). Ectopic expression of the *dredd* in *Drosophila* cells is not sufficient to induce apoptosis on its own. However, *rpr*- and *grim*-induced eye defects are suppressed in flies heterozygous for *dredd* loss-of-function, and ectopic expression of *rpr* and *grim* accumulated *dredd* mRNA in the embryos, suggesting that *dredd* is a downstream effector of these apoptotic activators (Chen et al., 1998). Furthermore, *dredd* loss-of-function mutations blocks expression of the genes related to antibacterial activity, thus indicating that *dredd* is also essential for immune responses to bacterial pathogens (Leulier et al., 2000).

Among effector caspases, *dcp-1* and *drICE* have been studied relatively well for their functions associated with PCD. *dcp-1*-null mutations did not cause significant defect on embryonic cell death and homozygotes for this mutation are viable and fertile, suggesting the existence of additional caspases (Song et al., 1997, Laundrie et al., 2003). Furthermore, *dcp-1* loss-of-function mutation disrupted germline cell death at mid-oogenesis in response to nutrient depreviation, therefore suggesting *dcp-1* is essential for mid-oogenesis (Laundrie et al., 2003). *dcp-1* overexpression does not significantly induce apoptosis in the compound eyes, yet it enhances *rpr*, *grim*-induced eye ablation but not that induced by *hid* (Song et al., 2000).

Loss-of-function *drICE* mutants have defects in PCD during embryogenesis and post-embryonic development of the pupal retina, suggesting *drICE* is essential for many

apoptotic cell deaths (Muro et al., 2006). Most of *drICE* mutants die during the pupal stage and only 20 % can survive to adulthood. *drICE* mutants do not show any inductions of cell death in response to X-irradiation, suggesting that drICE is required for X-ray-induced cell death (Table 1-2). Rpr-, Grim- and Hid-induced eye ablations are suppressed in *drICE* mutants (Muro et al., 2006) while *drICE* overexpression enhances *rpr*-, *grim*-induced eye ablation, but not *hid*-induced one (Song et al., 2000).

Drosophila Apaf-1-related killer (*dark*) is a homolog of *C. elegans* ced-4 and mammalian Apaf-1 (Rodriguez et al, 1999). Homozygous *dark* mutants reduce apoptosis significantly during embryogenesis (Rodriguez et al., 1999; Akdemir et al., 2006). This mutation partially suppresses *rpr*, *hid*, and *grim*-induced retinal degeneration, indicating a function of *dark* in RPR/HID/GRIM-mediated apoptosis (Rodriguez et al, 1999). A *dark*-encoded protein has a putative CARD motif which allows it to interact with DREDD and DRONC (Rodriguez et al, 1999)

PCD mechanisms: In healthy cells, DIAP1 binds to caspases DRONC, DCP-1, DRICE and prevent them from being activated (Kaiser et al., 1998; Meier et al., 2000; Quinn et al., 2000). However, in response to the death signal, the expressions of *rpr*, *grim*, and *hid* are transcriptionally induced, and RHG proteins bind to DIAP1 molecule and derepress caspase activity (Wang et al., 1999b). Since it is widely accepted that RPR/HID/GRIM competes with caspases for binding to BIR domains of IAP molecules, binding of RPR/HID/GRIM to DIAP1 sets caspases free to execute cell death (Zachariou et al., 2003, Fig. 1-4). Dark also interacts with Dronc, inducing caspase activity (Quinn et al., 2000; Rodriguez et al., 2002). Like *rpr*, *dark* is also activated transcriptionally in response to X-ray and UV irradiation (Zhou et al., 1999). Therefore, it is possible that

D. melanogaster

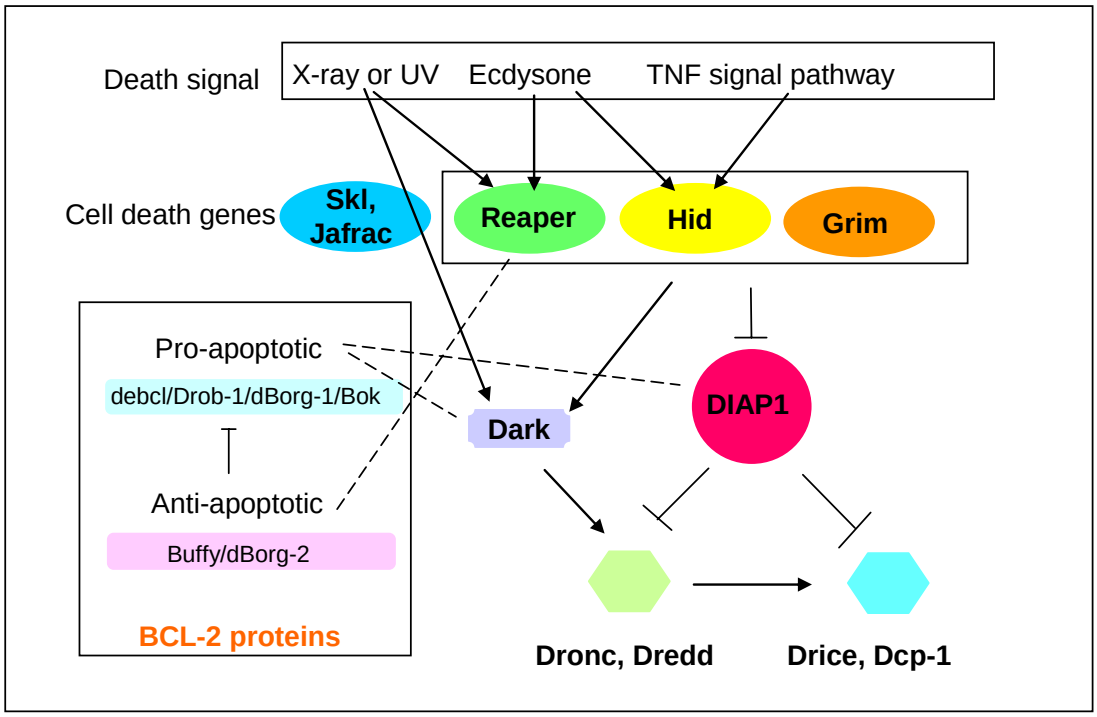

Modified from Danial and Korsmeyer (2004)

Figure 1-4. Apoptosis in *Drosophila.* Multiple upstream pathways regulate expression and activation of Reaper, Hid, and Grim (RHG), three proapoptotic proteins central to regulation of cell death in *Drosophila*. RHG proteins appear to control caspase activation by multiple mechanisms, including of Dark-dependent pathways as well as dark-independent activation of downstream caspases through antagonizing caspase inhibitors such as DIAP1. Anti- and proapoptotic BCL-2 family homologs in *Drosophila* might reside downstream or in parallel to RHG proteins and further influence caspase activation. Dashed lines represents genetic interaction between genes and biochemical interactions were not determined yet.

there are two pathways for *dark* action: direct activation from irradiation or RPR-, GRIM-, HID-mediated activation. RPR and GRIM-induced apoptosis requires DCP-1 and drICE while Hid-induced cell death does not need DCP-1 (Song et al., 2000; Leulier et al., 2006b), suggesting that two pathways are mechanistically different from each other.

Bcl-2 family: The activity of Apaf-1 is tightly regulated by Bcl-2 family members in mammals. Two Bcl-2 family genes in *Drosophila* have been identified: *debcl* (Brachmann et al., 2000; Colussi et al., 2000; Igaki et al., 2000) and *buffy* (Quinn et al., 2003). *debcl* is a proapoptotic gene and genetically interacts with *dark* and *diap1*, however, any genetic interaction with *rpr, grim,* and *hid* has not been observed yet (Colussi et al., 2000). *buffy* is an antiapototic gene and acts downstream of *rpr, grim,* and *hid* (Quinn et al., 2003).

IV-3. Programmed cell death in mammals

Mammalian PCD machineries are composed of extrinsic and intrinsic pathways. Extrinsic apoptotic signaling is mediated by the activation of death receptors (cell surface receptors) that transmit apoptotic signals upon binding to specific ligands. These death receptors belong to the tumor necrosis factor receptor (TNFR) superfamily, including TNFR-1 (Tartaglia et al., 1993), FAS/CD95 (Suda et al., 1993), and TRAIL receptors DR4/5 (Ashkenazi and Dixit, 1998). All members have extracellular domains which interacts with specific ligands, resulting in trimerization and activation of the respective death receptors. Subsequent signaling is mediated by a conserved sequence, called death domain (DD), which is part of cytoplasmic region of death receptors. Adaptors, such as

FADD or TRADD, also have a DD and they are recruited to the death receptors through DD-DD homotypic interaction, thereby forming death inducing signaling complex (DISC) (Muzio et al., 1996). In addition to DD, adaptors also have a death effector domain (DED) by which procaspase-8 is recruited through DED-DED interaction (Kischkel et al., 1995). The procaspase-8 at DISC is then activated and processes other downstream caspases in a cascade, leading to cell death.

In other cases, such a mainly caspase-dependent extrinsic apoptotic pathway is not sufficient to cause apoptosis, thus the signal needs to be amplified by mitochondria-mediated intrinsic pathways in which BCL-2 family proteins play roles (Fig. 1-5). The founding member of this family, BCL-2, product of the proto-oncogene *bcl-2*, was first discovered in the human follicular B cell lymphoma (Bakhshi et al., 1985; Cleary and Sklar, 1985; Tsujimoto et al., 1985). However, unlike other oncogene products, which stimulate cell proliferation, expression of the *bcl-2* did not promote cell proliferation, but inhibited apoptotic cell death following various death stimuli (Vaux et al., 1988; McDonnell et al., 1989). As expected from antiapoptotic functions of BCL-2, *bcl-2*-deficient mice displays apoptosis of lymphocytes, developmental renal cell death, and loss of melanocytes, suggesting the role of BCL-2 for maintaining cellular homeostasis (Veis et al., 1993). Remarkably, BCL-2 was identified to interact with another member of the BCL-2 family, BAX (Oltvai et al., 1993). Null-mutant mice lacking *bax* function showed hyperplasia of selective tissues, suggesting that Bax plays an important role as a proapoptotic factor.

To date, mammalian genome analysis has discovered entire members of BCL-2 family, which are grouped into three main subfamilies defined by the number of the

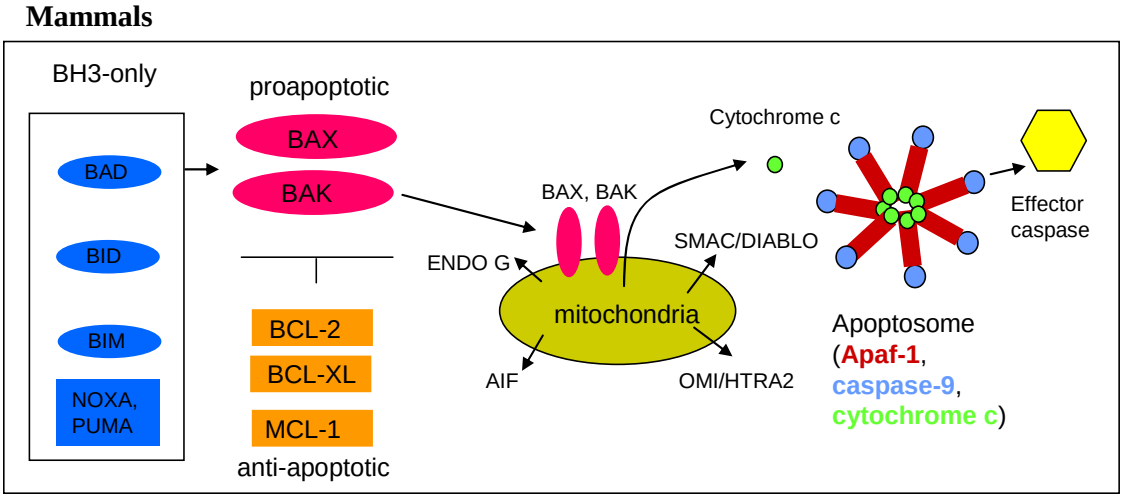

Modified from Danial and Korsmeyer (2004)

Figure 1-5. Mammalian intrinsic PCD pathways. In viable cells, proapoptotic proteins Bax and Bak are antagonized by antiapoptotic Bcl-2 members. In response to various death signals, BH3-only proteins are activated. Subsequently they activate and insert Bax to mitochondria outer membrane as oligomers. Inactive Bak, which resides at the mitochondria, becomes oligomerized in response to death signal. The resulting conformational change of proapoptotic proteins induces permeabilization of the mitochondria, releasing cytochrome c (cyt-c) from mitochondria. In turn, Apaf-1 binding of cyt-c induces the formation of apoptosome complexes, then activating the processing of caspase-9. Not only cyt-c but other apoptogenic factors (SMAC, OMI, ENDO G, AIF) are also released from the mitonchondria, executing cell death.

conserved region, called BCL-2 homology (BH) 1-4 domains (Fig. 1-6). The antiapoptotic members, BCL-2, BCL-X_L (Boise et al., 1993), and MCL-1 (Kozopas et al., 1993) contain all BH1-4 domains while the proapoptotic members, BAX and BAK, have BH1-3 domains. Members of the last subclass, represented by BID, BAD, BIM, NOXA and PUMA, display only BH3 domain, thus termed BH3-only members**.**

BCL-2 was shown to be localized to the mitochondria, indicating a role of this organelle in the regulation of cellular suicide (Janiak et al., 1994; Cory and Adams**,** 2002). Consistent with this notion, upon receipt of a death signal, proapoptotic BAX and BAK proteins are oligomerized and inserted into the mitochondrial outer membrane, thereby facilitating the release of cytochrome-c (cyt-c) from the intermembrane space. The cyt-c then binds to an adaptor molecule, called Apaf-1 (Apoptotic protease activating factor-1) via WD40 domains. This binding helps Apaf-1 to recruit an initiator caspase, caspase-9, via homotypic interactions between CARD domains in the presence of ATP/dATP. As a consequence, Apaf-1 undergoes a conformational change, which then promotes formation of heptameric complex, better known as apoptosome (Acehan et al., 2002). Upon formation of this complex, procaspase-9 is believed to be autocatalytically activated. The active caspase-9 then proteolytically activates downstream effector caspases (caspase-3, -6, -7), which subsequently process specific target protein substrates, thereby leading to the death.

Activation of the proapoptotic BCL-2 members is a key molecular event that is held in check by the prosurvival members, BCL-2 and BCL-$X_{L,}$ in live cells. In response to death signals, activities of proapoptotic BH3-only members are elevated either by transcriptional control (NOXA, PUMA; *e.g.* Nakano and Vousden, 2001) or by

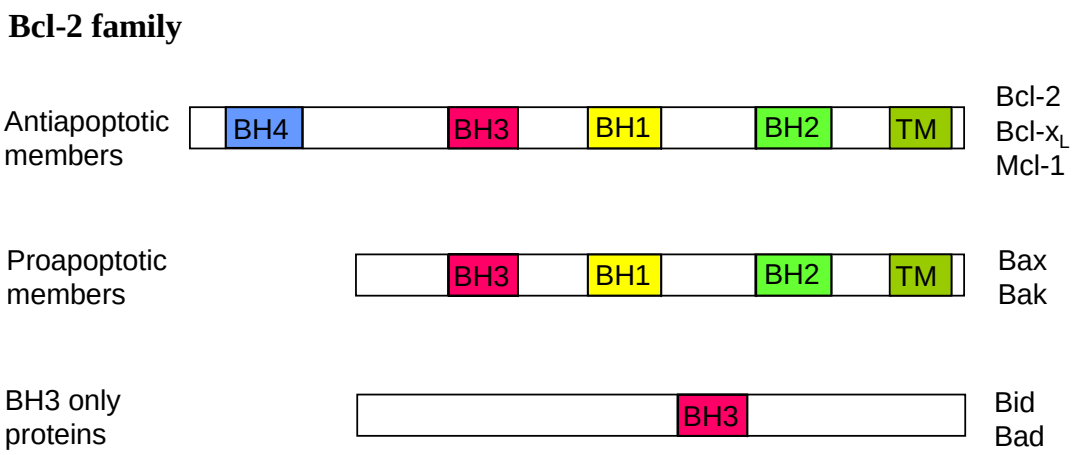

Figure 1-6. Classification of the Bcl-2 family of proteins based on domain organization. BH, Bcl-2 homology (BH) domains; TM, transmembrane domains.

posttranslational modification (*e.g.* BAD by dephosphorylation; Zha et al., 1996). These activated BH3-only factors are likely to bind to BAX/BAK, which then oligomerize and permeabilize the mitochondrial outer membrane to induce the release of the cyt-c (*e.g.* Desagher et al., 1999). In some cases, this intrinsic cell death pathway is intimately connected to the extrinsic pathway. For instance, activated caspase-8, through interactions between cell surface receptors and death ligand, cleaves BH3-only member BID. The truncated BID is then translocated and targeted to mitochondria and triggers the oligomerization of BAK or BAX, which in turn stimulates the release of cyt-c from the mitochondria (Luo et al., 1998, Fig. 1-5).

Apoptosome formation is a core process in mitochondria-mediated cell death in mammals; however, apoptosis can be enhanced by apoptosome-independent machineries. In response to death signals, fly RHG-like IAP antagonists, SMAC/DIABLO (Du et al., 2000) and OMI/HTRA2 (Suzuki et al., 2001), are released from mitochondria and inhibit IAP function, thus liberating caspases.

V. Developmental programmed cell death associated with metamorphosis

Life of most multicellular organisms can be divided into two distinct stages: growth phase and reproductive phase. After embryonic development is finished, juveniles are dedicated to increase their body size to accommodate physiological and behavioral demands as reproductive adults. Once they attain critical a body mass, then substantial changes of the body plan takes place to sculpt the final adult form. Such biological process is referred to as metamorphosis.

Conspicuous morphological changes from juveniles to adults are most prominent in insects and amphibians (Hartenstein, 1993; Nakajima et al., 2005). In both groups of animals, metamorphosis is completed through three major events: removal of unwanted juvenile structures, *de novo* formation of adult-specific structures, and respecification of juvenile structures. These overall reorganization processes are induced by timely release of lipophilic hormones: thyroid hormone in amphibians, and ecdysteroids in insects. Here I will briefly review the overall developmental switch associated with metamorphosis, and molecular events associated with developmentally controlled cell death occurring in the frog *Xenopus* and in the fruit fly *Drosophila*.

V-1. Amphibian programmed cell death

V-1-1. Thyroid hormone-induced amphibian metamorphosis

Among all processes of vertebral postembryonic development, amphibian metamorphosis displays the most prominent morphological transformation which includes the typical programmed cell death in regressing or remodeling organs (Dodd and Dodd, 1976). Thyroid hormone (TH) is apparently the most important endocrine cue that initiates and orchestrates overall metamorphic development of amphibian (Dodd and Dodd, 1976). The first hint of the role of TH in the amphibian metamorphosis came from the observation in which tadpoles fed with equine thyroid extract accelerate their metamorphosis (Gudernatsch, 1912). Further evidence showed that the metamorphosis is prevented by extirpation of the tadpole thyroid glands (Dodd and Dodd, 1976) or treatment with TH synthesis inhibitor (Gordon et al., 1943) or congenital defect of thyroid gland function (Rot-Nikcevic and Wassersug, 2003). Consistent with a role of

TH as the inducer of metamorphosis, it is observed that the progression of metamorphosis correlates with increasing amounts of TH (Dodd and Dodd, 1976).

Metamorphosis of the African clawed toad *Xenopus laevis* is composed of three consecutive developmental periods, premetamorphosis, prometamorphosis and climax. Such developmental periods are conveniently staged from 1 to 66 by Nieuwkoop and Faber (1956). In *Xenopus*, the premetamorphic period covers from hatching up to Nieuwkoop and Faber (NF) stage 54, at which thyroid hormone starts to be secreted from the developing thyroid gland. During prometamorphosis (NF stage 55-57), the endogenous thyroid hormone level rises and a series of morphological changes begin to occur. The most prominent change during this period is the development of hind-limbs. During climax (NF stage 58-66), when the thyroid hormone level is at peak, tadpoles undergo rapid metamorphic changes: the eruption of front-limbs from the opercular fold, shrinkage of the head, the resorption of gills and tails, and the remodeling of intestine and skin.

V-1-2. Mechanisms of thyroid hormone-induced programmed cell death.

Transcriptional control of specific sets of genes is the primary event of TH-induced metamorphosis. TH signaling is mediated by heterodimeric nuclear receptor complexes, consisting of TH receptors (TR) and retinoic acid receptor (RXR). TRs are encoded by two TR gene loci, designated TR-α and TR-β.

Distinct expression profiles of these two TR isoforms suggest isoform-specific functions during metamorphosis. For instances, a high level of TR-α expression before the onset of metamorphosis and in the tissues that develop into adult structures suggest

that TR-α is particularly important for the growth and differentiation of adult tissues. By comparison, developmental profile of TR-β transcript levels overlaps with that of TH levels. Of particular interest, TR-β is highly induced in the tadpole tissues that degenerate via programmed cell death, suggesting that TR-β isoform plays a critical role for the signal transduction of TH-induced cell death (Wang and Brown, 1993; Furlow and Neff, 2006).

Analysis of TH-regulated genes may provide insight into cell death mechanisms in regressing tissues. Up- or down-regulated genes in amputated tail treated with TH were characterized by a gene expression screen (Brown et al., 1996). A member of the matrix metalloproteinase family, stromelysin-3, and the delayed response genes encoding collagenase-3 and serine dipeptidyl peptidases were induced in regressing tails. In the proposed 'murder' model of cell death, the secretion of TH-induced extracellular matrix-degrading proteinases from subepidermal fibroblasts, adjacent to muscle cells, proteolyzes the extracellular matrix, resulting in the death of muscle cells. Since death signals come from neighboring cells, this type of PCD is called 'murder'. In tail epidermal cells, however, expression of these proteinases is low, thus the death of epidermal cells is likely to result from cell-autonomous death excecutors (suicide model) (Berry et al., 1998).

Expressions of caspases and BCL-2 family proteins were examined in the *Xenopus* tadpole. The activation of caspase-3, -6, and -7 is observed in apoptotic tail-derived cells, regressing tail and remodeling dorsal skin (Nakajima et al., 2000; Schreiber and Brown, 2003). Expression of Xenopus BCl-X_L can inhibit the cell death of neurons and tail muscle cells during metamorphosis (Cruz Reyes and Tata, 1995). The expression

profile of *bax* mRNA suggests that Bax is induced in regressing tail and thyroid hormone-treated tail, leading to muscle cell death (Sachs et al., 1997). Taken together, fundamental PCD mechanisms occurring during amphibian metamorphosis are quite similar to those in mammalian cells.

V-2. Programmed cell death in *Drosophila* metamorphosis

V-2-1. Ecdysone-induced metamorphosis

The *Drosophila* life cycle is composed of embryo, larva, pupa, and adult flies. Once 1st instar larvae hatch from embryos, they start feeding and grow through two consecutive moltings (escaspe of a new larva from old cuticle). The last 3rd instar larvae continue to feed to attain a critical body mass, and then cease feeding, and crawl out of the food, and wander to find an appropriate site for metamorphosis (wandering 3rd instar larvae). Soon the wandering larva becomes immobile, the anterior spiracles are everted and its cuticle becomes hardened. This event is called pupariation. Approximately 10-12 hours after pupariation, prepupa to pupa formation, called pupation, takes place with the feature of head eversion toward the anterior. The adult organs are generated and differentiated inside the pupal case until adult flies finally emerge from the pupal case (eclosion) (Riddford, 1993).

Ecdysteroid hormone (also ecdysone) is a critical developmental signal in insects including *Drosophila* (Riddford, 1993). During the larval stage, a small peak of ecdysone is observed just prior to each molting but the ecdysone level is low compared to that at the end of the 3rd instar larva. During larval-to-pupal transformation, two sequential pulses of ecdysone direct the transformation from a crawling larva to an

immobile pupa. The first peak of ecdysone at the end of the third instar larva induces pupariation, and then the second peak, which occurs approximately 10 hours after pupariation, induces pupation. During such early metamorphic transitional period, most of the obsolete larval tissues are completely degenerated via PCD, while dormant stem cells begin to proliferate and differentiate to form adult structures. A decline in the ecdysone level at the late pupal stage induces eclosion. As in amphibians, these developmental switches are orchestrated by transcriptional regulation of specific ecdysone-induced genes.

V-2-2. Molecular programmed cell death mechanism during *Drosophila* metamorphosis

Ecdysone induces stage-specific destruction of obsolete larval tissues. The anterior muscles and larval midgut die in response to the late larval ecdysone peak (first peak) while the larval salivary gland and abdominal muscles degenerate in response to the prepupal peak (second peak) (Jiang et al., 1997).

Ecdysone signaling is transduced via the ecdysone receptor complex, a heterodimer of two nuclear receptors: ecdysone receptor (EcR) and ultraspiracle (USP), the fly retinoid X receptor ortholog (Riddiford et al., 2001). The ecdysone/EcR/USP complex regulates expression of primary-response genes, which in turn regulates the expression of secondary-response genes (Thummel, 1996). The primary-response genes include *Broad Complex* (*BR-C*), which encodes several isoforms of BTB-zinc finger transcription factors, *E74,* which encodes an ETS-domain transcription factor, and E93 which encodes a novel site-specific DNA binding protein.

Activated ecdysone signaling also induces transcription of proapoptotic genes. Immediately prior to the death of the midgut and salivary gland, ecdysone upregulates the transcriptions of the death activators, *reaper* (*rpr*) and *head involution defective* (*hid*), the caspase *dronc*, the *Apaf-1* homolog *dark*, and the CD36 homolog *croquemort* (*crq*), a marker for phagocytes (Jiang et al., 1997). These data suggest that *rpr* and *hid* are important for activation of the death cascade. Surprisingly, however, a *rpr*-null mutant shows no defect in the death of both larval tissues, while reduction of *hid* function by RNAi causes partial defects in the salivary gland cell death. However, loss-of-function of both *rpr* and *hid* shows strong deficit in the larval salivary gland (SG) and midgut cell death, indicating *hid* acts in consert with *rpr* for the destruction of larval tissues (Yin and Thummel, 2004).

As in developing embryos, RPR/HID promote cell death by antagonizing DIAP1 functions. Yin and Thummel (2004) showed precocious death of the larval tissues by RNAi-mediated knockdown of *diap1*, pointing to the roles of DIAP1 as a central regulator of ecdysone-triggered cell death. DIAP1 is likely to prevent PCD by suppressing activation of an initial caspase, Dronc (Meier et al., 2000; Muro et al., 2002). Recently identified *dronc*-null mutations show substantial attenuation of the SG cell death; however, the same genetic lesion does not affect normal death of the midgut, suggesting that Dronc function is required for the death of specific tissues (Daish et al., 2004). Similar differential tissue-specific death was observed for mutants lacking Dronc activator *dark* (Akdemir et al., 2006; Mills et al., 2006). These findings, therefore, suggest essential roles of 'Dronc-Dark' for the histolysis of the SG, but not for the midgut. PCD of the midgut perhaps requires caspase functions other than Dronc. In

addition, recent microarray and SAGE (serial analysis of gene expression) assay detected up-regulation of caspase-encoding genes by ecdysone including *drICE* and *dream* (Strica) during the salivary gland histolysis (Gorski et al., 2003; Lee et al., 2003). This result suggests that these two caspases may be important for SG histolysis.

V-2-3. Transcriptional regulation of programmed cell death machinery by ecdysone-signaling pathways.

Ecdysone-induced *rpr*, *hid*, and *dronc* expression have a role in the larval tissue cell death. Ecdysone directly induces *rpr* and *dronc* expression in the larval salivary gland through a EcR/USP response element in their promoters (Jiang et al., 2000; Cakouros et al., 2004a). Studies in tissue culture cells suggest that this action is mediated by an EcR-interacting factor, the *Drosophila* homolog of the arginine-histone methyltransferase CARM1, which appears to be required for maximal death gene transcription (Cakouros et al., 2004b).

The activation of *rpr* and *dronc* by ecdysone is also induced indirectly. *BR-C* is required for *rpr* and *hid* transcription since *rpr* and *hid* expression is reduced in BR-C loss-of-function mutants. *E74* is required for the maximal expression of *hid* (Lee et al., 2002b). *BR-C* appears to directly regulate *dronc* transcription as mutagenesis of *BR-C* binding sites within the *dronc* promoter leads to significantly reduced promoter activity in transfected tissue culture (Cakouros et al., 2002). *E93* displays the most global effect among early ecdysone-inducible genes, since this mutant shows reduced levels of *rpr*, *hid*, *dronc* and *crq* (Lee et al., 2002b, See the illustration at p. 170).

Interestingly, *dark* transcription is not significantly affected by mutations in *BR-C*, *E74*, or *E93*, although its expression is induced in the salivary gland prior to cell death, suggesting *dark* induction might be mediated by another pathway other than involvement of transcription factor BR-C, E74, and E93 (Lee et al., 2002b). Therefore, programmed cell death of the salivary gland by ecdysone encompasses two steps of regulatory hierarchies in which ecdysone-induced transcription factors coordinate the induction of key death activators.

The genetic interaction of ecdysone response genes during midgut degeneration shares common pathways with salivary gland histolysis, although there are some differences (Lee et al., 2002a). First, E74 is not involved in the midgut degeneration. Second, E93 is not required for *rpr* and *hid* expression since *rpr* and *hid* transcriptions are not affected in E93 mutants.

VI. Ecdysone-dependent neuronal cell death associated with metamorphosis

Neuronal programmed cell death (PCD) in insects has been extensively studied in the tobacco hornworm *Manduca sexta* and *Drosophila melanogaster* due to easy identification of neurons. In *M. sexta* larvae, abdominal segments A3-A6 bear a pair of prolegs. These prolegs are used to grasp the foliage of plants while feeding, and in behaviors such as crawling and ecdysis (Weeks and Truman, 1984a). The musculature of each proleg includes an accessory planta retractor muscle (APRM) which is innervated by a pair of excitatory accessory planta reactor (APR) motoneurons (Weeks and Truman, 1984b). The APRs located in larval prolegs are known to undergo PCD in response to ecdysone (Weeks, 2003). The death of APR neurons is a stage- and segment-specific

phenomenon; APRs in segments A5 and A6 die after the rise of the prepupal peak of ecdysone, while APRs in segments A3 and A4 survive, however, die later at the end of pupal stage in response to the decline in ecdysone levels. ARP neurons in segments A3 and A4 during pupation are re-specified to pump hemolymph to the developing wings and legs, or innervate new abdominal extensor muscles, respectively (Fig. 1-7). Cell culture studies further verified that a rise in 20-hydroxyecdysone (HE) level triggers APR6 neuronal death during pupation while a fall in 20-HE level triggeres APR4 neuronal death after adult eclosion (Streichert et al., 1997; Zee and Weeks, 2001).

During metamorphosis of *D. melanogaster*, neuronal death is prominent mostly in the thoracic and abdominal neuromeres of the CNS (Kimura and Truman, 1990; Robinow et al., 1993; Tissot and Stocker 2000). As seen in *M. sexta* APR neurons, a peak of ecdysone stimulates neuronal cell death during prepupal development, while a fall of ecdysone level triggers death of other neurons immediately after adult eclosion. Ecdysone signaling is mediated by three different isoforms: EcR-A, EcR-B1, and EcR-B2, which share C-terminal DNA- and ligand binding domains, but are variable in their N-termini (Talbot et al., 1993). In the CNS, differential expression of EcR isoforms correlates with stage-specific responses to ecdysone (Talbot et al., 1993; Truman et al., 1994). Interestingly, at the onset of metamorphosis, EcR-B isoform is produced predominantly in the larval tissues, while EcR-A expression is restricted to dormant tissues, such as imaginal discs that will differentiate and form adult structure (Talbot et al., 1993). In the CNS, many larval neurons initially express EcR-B isoform and undergo remodeling process throughout pupal development. During this process, they switch to

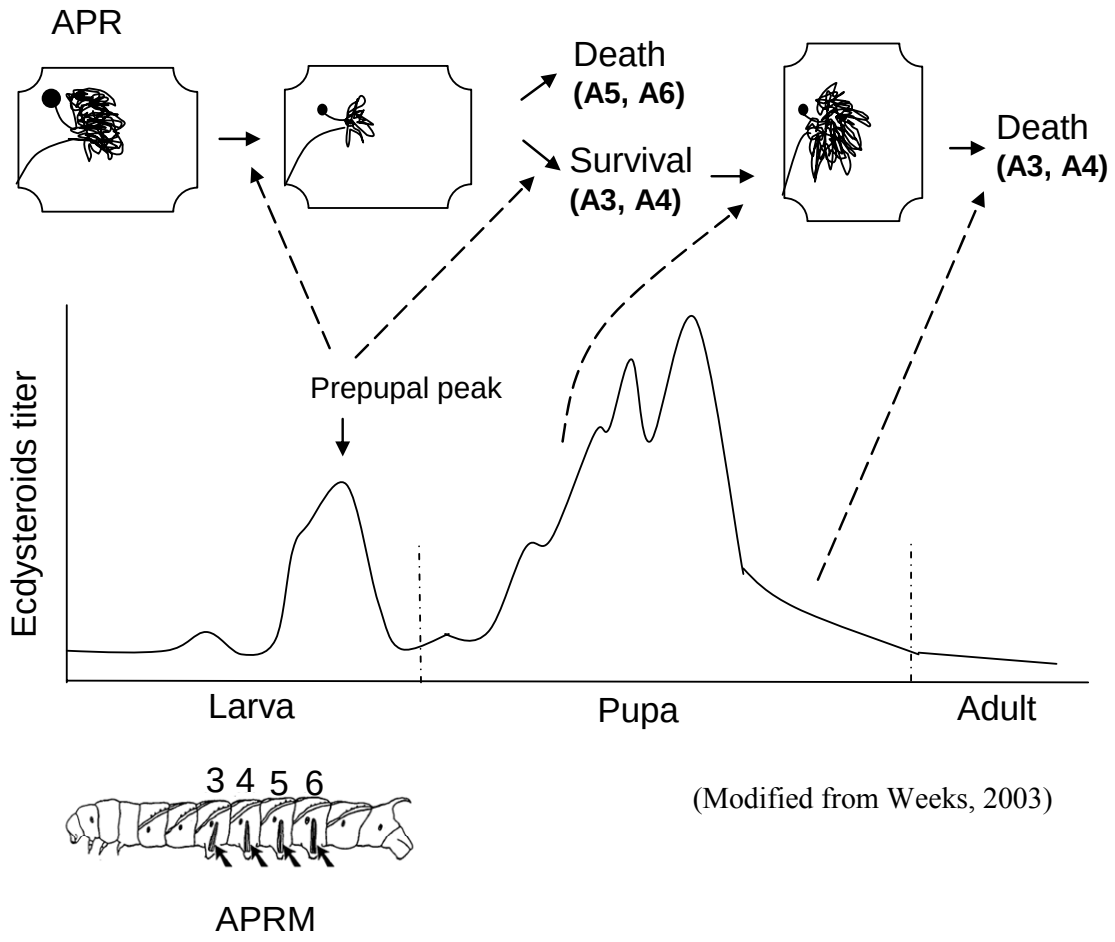

Figure 1-7. Neuronal remodeling and programmed cell death of APR neurons in *Manduca sexta*. Top row is the drawing of abdominal ganglia (anterior up). One APR neuron is illustrated. In response to the prepual peak of ecdysteroid, dendritic regression and segment-specific PCD (A5, A6) occur during larval-pupal transition. When the ecdysteroid titer rises, dendritic re-growth takes place in the survived neurons (A3, A4). After adult eclosion, these neurons die. At the bottom of drawing, larval A3-A6 segments are labeled and arrows indicate APR muscles (APRM) (left is anterior).

EcR-A expression, which is then likely to mediate differentiation of these neurons into the adult-specific neuronal form (Truman et al., 1994). A subset of these neurons, called type-II, hyperexpresses EcR-A and these neurons are programmed to die following adult emergence (Robinow et al., 1993). Further analysis showed that *rpr* and *grim* genes are transcriptionally induced prior to the death of these doomed neurons (Robinow et al., 1997). Therefore, overproduced EcR-A in response to decline of ecdysone somehow activates PCD via transcriptional activation of the proapoptotic genes. Little is known about the molecular mechanisms underlying such activation process.

VII. Clearance of cells by phagocytosis

Once cells are dead via programmed cell death, their corpses need to be cleared in order not to cause any inflammatory responses (Savill and Fardok, 2000). Such clearance is largely accomplished by macrophages and phagocytes. Unlike *D. melanogaster* and mammals, *C. elegans* does not have professional phagocytes that recognize and phygocytose dying cells. Instead, cell corpses are engulfed by neighboring cells (Reddien and Horvitz, 2004). In *C. elegans*, the clearance of cell corpses involves at least seven genes, which have homologs in higher organisms. These genes are divided into two categories: One helps recognize apoptotic cells and the other influences cyoskeketal remodeling. The former includes *ced-1* which encodes an engulfment receptor (Zhou et al., 2001), *ced-6,* a homolog of the mammalian PTB domain-bearing adaptor GULP (Liu and Hengartner, 1998), and *ced-7* which encodes a protein with homology to ABC-1 transporter (Wu and Horvitz, 1998a). The latter includes *ced-2*

(Reddien and Horvitz, 2000), *ced-5* (Wu and Horvitz, 1998b), *ced-10* (Reddien and Horvitz, 2000), and *ced-12* (Gumienny et al., 2001).

Phagocytes recognize the surface of the dying cells most likely via 'eat-me' signals. In mammalian cells, the best studied 'eat-me' signal is phosphatidylserine (PS) displayed on the plasma membrane of dying cells (Fadok et al., 2000). The disposal of the apoptotic corpse is plotted once 'eat me' signals on its surface are engaged by engulfment receptors. In *C. elegans*, the receptor encoded by *ced-1* in engulfing cells clusters around the dying cell (Zhou et al., 2001). *ced-7* is the only engulfment gene expressed in both dying cells and engulfing cells. It is proposed that CED-7 expresssed in dying cells is involved in presenting a cell corpse signal, perhaps PS, to the surface of the dying cells, while CED-7 expressd in engulfing cells assists CED-1 to recognize its ligand PS or to cluster around the dying cells (Zhou et al., 2001). Subsequently, binding of engulfment receptors to PS triggers cytoskeletal remodeling events to engulf dying cells.

In mammals, phagocytic cells, such as macrophages, dispose of cell corpses by interaction between 'eat- me' signals and receptors and subsequent cytoskeletal events as observed in *C. elegans*. Furthermore, the phagocytic clearance also regulates inflammatory responses (Savill and Fardok, 2000). By releasing anti-inflammatory factor including TGFβ and IL-10, macrophages suppress inflammatory responses during engagement in corpse engulfment. Defect in clearance of corpses are predicted to create a proinflammatory environment that may predispose to autoimmune disorders (Savill and Fardok, 2000).

In *D. melanogaster, croquemort*, a member of the scavenger receptor family, is required for the engulfment of apoptotic corpses by macrophages (Franc et al., 1999).

VIII. Corazonin overview

Corazonin (Crz) neuropeptide was initially identified as a cardioactive peptide from the corpora cardiaca (CC) of the American cockroach, *Periplaneta americana* (Veenstra, 1989). The author measured the rate of cockroach heart beat in the presence of corazonin neuropeptide *in vitro* and found that the pulses are increased in a Crz dose-dependent manner, suggesting that Crz possesses a cardiostimulatory effect (Veenstra, 1989).

Crz was also identified in other insects such as locust, grasshoppers, crickets (Hua et al., 2000), moths, and fruitflies (Nässel, 2002), therefore forming a distinct peptide family. Members of this family are all C-terminally amidated 11 aa-long neuropeptides and consist of three types of peptides, two of which have only one dissimilar residue (His or Arg) at the 7^{th} amino acid, named His^7 and Arg^7. The former was found in locusts (Veenstra, 1991; Tawfik et al., 1999) and the latter in American coachroach (Veenstra, 1989), cricket, silkworm (Hua et al., 2000), waxmoths (Hansen et al., 2001), and *Drosophila* (Veenstra, 1994). A third type is [Thr^4, His^7]-Crz, which was recently found in the honey bee *Apis mellifera,* has threonine and histidine at 4^{th} and 7^{th} amino acid positions, respectively (Verleyen et al., 2006).

Interestingly, Crz has been found to have diverse biological functions in a species-specific manner. For example, neither His^7- nor Arg^7-Corazonin has cardioacceleratory effects in insects except cockroaches (Veenstra, 1991). Even in the

cockroach species, *P. americana*, Crz did not elicit a cardioactive effect *in vivo* (Slama et al., 2006). Instead of such dubious cardioactive roles, Crz has been found to induce the dark pigmentation in the body of locusts. In the migratory locust *L. migratoria,* albino mutants were discovered, originating from an Okinawa (Japan) laboratory strain and this albinism is caused by a single recessive gene (Hasegawa and Tanaka, 1994). Of interest, implantation of the CC from a normally pigmented locust into albino mutants induces dark pigmentation, suggesting that the CC contains dark-color-inducing activity (Tanaka and Pener, 1994). Tawfik et al. (1999) subsequently identified Crz as the dark-color-inducing factor.

Crz plays roles in development and behavior in lepidopteran insects. When the silkworm *Bombyx mori* larvae stop feeding, they started wandering, and then spinning to produce cocoon layers until pupal ecdysis. Injection of Crz to *B. mori* larvae reduced the weight of cocoon layers as well as prolonged the spinning period, indicating that Crz reduces the spinning rate and delays pupal ecdysis (Tanaka et al., 2002). The tobacco hornworm, *Manduca sexta*, Crz induces ecdysis behavior (Kim et al., 2004). The authors identified a Crz receptor in this species, and found that it is expressed specifically in the Inka cells, the sites of synthesis of preecdysis-triggering hormone (PETH) and ecdysis-triggering hormone (ETH). Injection of the Crz to larvae elicits release of PETH and ETH from the Inka cells, which in turn stimulates precocious preecdysis and ecdysis behaviors. Biological roles played by Crz are yet to be determined in dipteran insects including *D. melanogaster*.

Crz expression patterns in the nervous systems were observed in insects including blow fly, wax moth, and American cockroach (Cantera et al., 1994; Hansen et al., 2001;

Roller et al., 2003; Veenstra and Davis, 1993). The most consensus expression site among diverse insect species is the pars lateralis of the protocerebrum (Roller et al., 2003). Crz-expressing neuronal death in the ventral nerve cord was first described from the expression analyses of the blow fly, *Phormia terraenovae* (Cantera et al., 1994). The Crz-immunoreactive neurons against cockroach Crz peptide present in the thoracic-abdominal ganglion of the larva disappear during metamorphosis while new Crz immunoreactive neurons in the brain are added to those that persist from larval stages.

In my dissertation, I will focus on two areas. One is neurogenetic characterization of Crz-expressing neurons involving comparative genomics and histological analyses (Chapter 2). With these background studies, I further delved into the programmed cell death mechanisms of two separate groups of peptidergic neurons (Chapter 3 and 4).

Chapter Two

Comparative analysis of Corazonin-Encoding Genes (Crz's) in Drosophila Species and Functional Insights into Crz-Expressing Neurons

*This chapter is modified from Choi et al., 2005 in the Journal of comparative neurology.

Youn-Jeong Choi, Gyunghee Lee, Jeffrey C. Hall, Jae H. Park. (2005). Comparative Analysis of *Corazonin*-Encoding Genes (*Crz*'s) in *Drosophila* species and Functional Insights into *Crz*-Expressing Neurons. *The Journal of Comparative Neurology* 482:372-385.

I am the co-first author of the paper above and contributed by generating most results, cooperating to create ideas, writing a draft, editing a manuscript, reviewing, and publishing.

I. Abstract

To gain insight into regulatory mechanisms of tissue-specific *Corazonin* (*Crz*) gene expression and its functions in *Drosophila*, we cloned the *Crz* genes from four *Drosophila* species (*D. melanogaster*, *D. simulans*, *D. erecta*, and *D. virilis*) and performed comparative analyses of *Crz* gene sequences and expression patterns using *in situ* hybridization and immunohistochemistry. Although *Crz* gene sequences showed a great deal of diversity, its expression patterns in the CNS were highly conserved in

Drosophila species examined here. In *D. melanogaster* larva, *Crz* expression is evident in four neurons per cerebral lobe and in eight pairs of bilateral neurons in the ventral nerve cord; in adult, the number of *Crz*-producing neurons is 6-8 in the pars lateralis of each brain lobe, whereas neurons in the ventral nerve cord are no longer detectable. Such adult-like spatial *Crz* expression is established within 48 hours after the onset of metamorphosis. Somata of *Crz* neurons in the pars lateralis are located in the vicinity of terminals emanating from PDF-containing pacemaking neurons, indicating a functional connection between the two peptidergic nervous systems. Two pairs of ectopic *Crz* cells are detected in the adult brains of behaviorally arrhythmic $Clock^{Jrk}$ or $cycle^{02}$ mutants, suggesting that CLOCK and CYCLE proteins negatively regulate *Crz* transcription in a cell-specific manner.

II. Introduction

Corazonin (Crz) is an amidated undecapeptide originally isolated from the corpora cardiaca (CC) of the American cockroach, *Periplaneta americana*, as a potent cardioactive peptide (Veenstra, 1989). Similar or identical peptides have been discovered in other insect species including grasshoppers, crickets, and moths, thereby forming a neuropeptide family (Nässel, 2002). Interestingly, Crz has been shown to effect diverse physiological functions in a species-specific manner. For instance, unlike in cockroaches, no obvious cardiostimulatory roles played by this peptide were observed in other insect groups (Veenstra, 1991; Predel et al., 1994; Tanaka et al., 2002; Kim et al., 2004). Instead, Crz induces dark cuticular pigmentation exclusively in several orthopteran species, including the migratory locust, *Locusta migratoria* (Tawfik et al.,

1999; Hua et al., 2000; Tanaka, 2000a). A genetic variant of this species is characterized by an albino phenotype, which follows Mendelian inheritance as a recessive trait, suggesting that the albinism is caused by a single gene mutation (Hasegawa and Tanaka, 1994). Interestingly, albino animals developed dark pigmentation in response to Crz injection (Tawfik et al., 1999). These results along with the lack of detectable Crz peptide in the albino locusts (Schoofs et al., 2000) strongly support that Crz is a causative neural substance for this particular physiological event. By comparison, Crz has an effect on animal's developmental processes, since the peptide was shown to elongate larval spinning period prior to pupation in the silkworm, *Bombyx mori* (Tanaka et al., 2002, 2003) and to induce ecdysis behavior in the moth, *Manduca sexta* (Kim et al., 2004). In a crustacean species, Crz promotes pigment migration in the integument (Porras et al., 2003).

Lack of consensus physiological functions shown by the aforementioned studies could possibly indicate distinct biological roles played by Crz in dipteran insects including the fruit fly, *Drosophila melanogaster*. Although a Crz-encoding gene sequence was first cloned in this species (Veenstra, 1994), no further attempts have been made to elucidate *Crz* gene's function. One important step toward this aim is to identify *Crz* gene expression sites, since anatomical characteristics of peptidergic neurons often lead to the revelation of neuropeptide gene functions (***e.g.***, Helfrich-Förster, 1995; Renn et al., 1999).

In this study, we used comparative approaches involving *Crz* gene sequences as well as its expression patterns in several *Drosophila* species. Thus, we first cloned and characterized *Crz* genes from four members of the *Drosophila* genus, and then species-

specific *Crz* expression patterns were compared in larval and adult stages. Comparative analyses using four related *Drosophila* species have several advantages. First, preexisting information on *D. melanogaster Crz* gene sequence can facilitate identification of the *Crz* genes in related species, since homologous gene sequences are likely to be conserved in such members. Second, overall anatomical similarities in the CNS structures among these species enable us to perform cell-to-cell comparison of *Crz*-expressing neurons (*e.g.*, Taghert and Schneider, 1990). Third, comparative expression data could provide an important clue about molecular mechanisms underlying cell-specific *Crz* gene expression. For instance, comparable *Crz* expression patterns among different fly species may suggest a conserved mode of transcriptional activation resulting from specific interactions between *trans*-acting regulators and their cognate binding sites. The latter *cis*-acting elements, which are presumably conserved in those species, can be revealed by interspecific comparison of regulatory sequences of the *Crz* genes (Ludwig, 2002; Zhang and Gerstein, 2003).

Here we report that *Crz* gene sequences and structures have diverged significantly during evolution of *Drosophila* species. Despite this diversity, comparable expression patterns suggest that *Crz* functions and its transcriptional regulatory mechanisms remain unchanged among dipteran insects. We predict multiple physiological functions of *Crz* in *Drosophila*, on the bases of developmental stage-specific *Crz* expression patterns, intimate association of *Crz* neurons with other functionally known peptidergic neurons, and diverse targets of *Crz* neurons.

III. Materials and methods

Drosophila strains and species

Flies were raised at 25°C under 12-h:12-h light:dark cycles on food containing dextrose, cornmeal, agar, yeast, and methyl paraben as a preservative. Canton-S was used as a wild-type strain of *D. melanogaster*, and behaviorally arrhythmic mutants (per^{01}, tim^{01}, cyc^{02}, and Clk^{Jrk}) used in this study were as described and applied previously (Park et al., 2000). Other *Drosophila* species (*D. simulans*, *D. virilis*, and *D. erecta*) were obtained from the Tucson stock center. The following transgenic lines were used: *Pdf-gal4* (Park et al., 2000); *UAS-mCD8-GFP* (a membrane targeted green fluorescent protein, Lee and Luo, 1999); $Crz\text{-}gal4^{T2a}$ (Choi, et al., 2006). The *Crz-gal4* transgene is described in Chapter 3.

Cloning the *Crz* gene

Total RNAs were purified from adult fly heads of *D. melanogaster*, *D. simulans*, and *D. erecta* or from ~100 dissected larval CNSs of *D. virilis* using TRIZOL Reagent (Gibco BRL) according to the manufacturer's instruction. First strand cDNAs were synthesized from 20 μg of total RNA using oligo-dT-adaptor primer, and then the cDNAs were employed as a template for 5'- and 3'-RACE (rapid amplification of cDNA ends) in order to define the transcription unit of the *D. melanogaster Crz* gene (*Dm-Crz*) (for detailed reaction conditions, see Park and Hall, 1998). A given PCR product was subcloned into the pGEM-T vector (Promega) and sequenced using a dideoxy Dye-terminator kit (ABI Prism).

To clone *D. simulans Crz* cDNA (*Ds-Crz*), we carried out PCR using *simulans*-specific cDNAs as a template and various *Dm-Crz* gene specific primer pairs. One such pair yielded a PCR product, whose sequence was similar to *Dm-Crz*. Subsequently, *Ds-Crz* specific primers were employed to perform RACEs in order to determine 5'- and 3'-termini of *Ds-Crz* mRNA. To isolate *Crz* cDNAs from *D. virilis* (*Dv-Crz*) and *D. erecta* (*De-Crz*), 3'-RACE was performed using degenerate primers whose sequences were deduced from conserved Crz amino acid residues. The resulting PCR products were subcloned and sequenced as above. Subsequently, 5'-RACE was performed using gene-specific primers to define the transcription start sites. PCR primer sequences are presented in Table 2-1, and PCR conditions and parameters are summarized in Table 2-2.

Reverse transcription (RT)-PCR and PCR of genomic DNA

Full-length *Crz* cDNAs were obtained by RT-PCR using primers corresponding to 5'- and 3'-terminals for each specific *Crz* cDNA (designated 5'- and 3'-end primers, respectively) (Tables 2-1, 2-2). A given PCR product was subcloned into pGEM-T, and at least three plasmid clones were sequenced to detect any nucleotides mis-incorporated by *Taq* polymerase.

Genomic DNA was purified from five female flies of each species using DNAzol reagent (Gibco BRL) according to manufacturer's recommendation. *Crz* genomic materials were amplified by PCR in the same manner as RT-PCR, except for the use of genomic DNA as templates; resulting PCR products were subcloned and sequenced as above. The sequence data were compared to cDNA sequences to define intron-exon boundaries.

Table 2-1. PCR primer sequences used for cloning *Crz* cDNAs from different *Drosophila* species

Primer	Sequence (5' to 3')
Crz-5'end	AGACGCAGTTGTGATTCGAAC
Crz-1	ATGTTGCGCCTCCTGCTGCT
Crz-2	CTGCCCCTCTTCCTCTTCAC
Crz-3R	AACACATTGGGTTCGGCGGA
Crz-4R	TGCTCCTCCAGCGGCACTCA
Crz-6R	CGCTCGAGCCTACGATCGCT
Crz-7R	CGTAGAGATCCGTGAGTCCC
Ds-8R	CGACAGACAGCGCTCCAGCC
Dm-3'end	AATTCATAAAAATCCTGTGTT
Ds-3'end	AGTTCATAAAAATCGAGTGTTTTAT
Crz-dg-1	ATGGGICARACITTYCARTA
Crz-dg-2	GIGGITGGACIAAYGGIAAR
Dv-5R	GTCGGGCCTGCTCGCACT
Dv-6	GGATTCTTGAATCTGCTATCTA
Dv-7R	GCCAATATCAATTAGTTTCTTC
Dv-8R	CGGTGGGCCTATCCTGAATA
Dv-5'end	AGACGTTGCTTCAGCCTGC
Dv-3'end	CTTCAGATTTTCCATTTTCTTTTTTATTAA
De-1R	GGTCGGTACATTGGCACTGG
De-2R	CTCTCAGGATCCGGATCCAC
De-3'end	AATTCATAAAAATCCTCTGTTT
Ad-d(T)	GACTCGAGTCGACATCGAT$_{20}$
Ad-I	CGCTCTAGAGACTCGAGTCGACATCGA
Ad-II	CGCGAGCTCGAGTCGACATCGATTT

Primer sets for each specific PCR are described in Table 2-2. In the case of degenerate primers (Crz-dg-1 and -2), 'I' indicates inosine, 'R' purine nucletides (A or G), and 'Y' pyrimidine nucleotides (C or T).

Table 2-2. Primers, templates, and PCR conditions for sequential PCR steps to obtain full-length *Crz* cDNA clones from each *Drosophila* species

species	PCR	Forward primer	Reverse primer	Template	Denaturation		Annealing		Extension		Cycle
					°	sec	°	sec	°	sec	
melanogaster	I 3′RACE	1st:Crz-1	Ad-I	cDNA	94	45	55	45	72	45	30
		2nd: Crz-2	Ad-II	1st PCR	94	45	55	45	72	45	30
	II 5′RACE	1st: Ad-d(T)	Crz-3R	Poly (A) added cDNA	94	45	55	45	72	45	30
		2nd: Ad-I	Crz-4R	1st PCR	94	45	55	45	72	45	30
	III RT-PCR	Crz-5′end	Dm-3′end	cDNA	94	45	55	45	68	90	30
simulans	I 3′RACE	1st: Crz-1	Ad-I	cDNA	94	45	55	45	72	45	30
		2nd: Crz-2	Ad-II	1st PCR	94	45	55	45	72	45	30
	II 5′RACE	1st: Ad-d(T)	Ds-8R	Poly (A) added cDNA	94	45	55	45	72	45	30
		2nd: Ad-I	Crz-7R	1st PCR	94	45	55	45	72	45	30
	III RT-PCR	Crz-5′end	Ds-3′end	cDNA	94	45	55	45	68	90	30
virilis	I 3′RACE	1st: Crz-dg-1	Ad-I	cDNA	94	45	50	45	72	55	30
		2nd: Crz-dg-2	Ad-II	1st PCR	94	45	50	45	72	55	30
	II 5′RACE	1st: Ad-d(T)	Dv-5R	Poly (A) added cDNA	94	45	55	45	72	45	30
		2nd: Ad-I	Dv-8R	1st PCR	94	45	55	45	72	45	30
	III RT-PCR	Dv-5′end	Dv-3′end	cDNA	94	45	55	45	68	90	30
erecta	I 3′RACE	1st: Crz-dg-1	Ad-I	cDNA	94	45	50	45	72	55	30
		2nd: Crz-dg-2	Ad-II	1st PCR	94	45	50	45	72	55	30
	II 5′RACE	1st: Ad-d(T)	De-1R	poly (A) added cDNA	94	45	55	45	72	45	30
		2nd: Ad-I	De-2R	1st PCR	94	45	55	45	72	45	30
	III RT-PCR	Crz-5′end	De-3′end	cDNA	94	45	55	45	68	90	30

In situ Detection of *Crz* mRNA

For whole-mount *in situ* localizations of *Crz* mRNA, digoxigenin-labeled sense and antisense RNA probes were prepared from full-length *Crz* cDNAs using an RNA labeling kit (Roche). The template pGEM-T vectors containing a full-length *Crz* cDNA obtained from each species were digested with 5'-overhang producing enzymes. The resulting linearized DNAs were purified using a PCR purification kit (Qiagen), and then the eluted solution was completely dried, and the precipitant DNA was resuspended with 13 μl of H_2O. Subsequently, 1 μl of RNase inhibitor, 2 μl of 10 x transcription buffer, 2 μl of NTP labeling mixture, and 2 μl of RNA polymerase (RNA labeling kit from Roche) were added and mixed briefly, and then incubated for 2 hours at 37°C to produce digoxigenin-labeled RNA probes. To remove DNA template, 2 μl of DNase I was added and incubated for 15 minutes more. To precipitate RNAs, 1.3 μl of 8 M LiCl and 75 μl of pre-chilled 100% ethanol were added, mixed, and stored overnight at -20°C. RNAs were precipitated by centrifugation for 15 minutes at 12,000 x g and washed with 75% ethanol. RNA precipitants were dried completely and dissolved in 20 μl of hydrolysis buffer (4 mM $NaHCO_3$ and 6 mM Na_2CO_3) to produce 100-base RNA fragments. For storage at -20°C, 10 μl of 1 M Tris (pH 7.5), 300 μl of Hybrix buffer (50% deionized formamide, 5x SCC, 100 μg/ml transfer RNA, 100 μg/ml salmon sperm DNA, 50 μg/ml heparin, and 0.1% Tween-20), and 1 μl of RNase inhibitor were added to the hydrolyzed solution.

To quantify RNA, the sample solution and control dig-labeled RNA was serially diluted in RNase-free water, and 1 μl of each diluted solution was spotted to nylon

membrane and UV cross-linked. The membrane was briefly wet in buffer-1 (0.1M Tris-HCl pH 7.5, 0.15 M NaCl), blocked in buffer-2 (1% blocking reagent in buffer-1) for 30 minutes, and rinsed in buffer-1 two times for 15 minutes each. The alkaline phosphatase (AP)-conjugated anti-digoxigenin antibody at a dilution factor 1:5000 in buffer-1 was applied to the membrane. Subsequently the membrane was rinsed in buffer-1 and buffer-3 (100 mM Tris-HCl pH 9.5, 100mM NaCl) and AP substrates were applied. The RNA concentration was calculated by comparison of the color intensity of the sample to that of the control.

For *In situ* hybridization, dissected larval or adult CNSs were fixed in fixative (4% paraformaldehyde, 0.1% sodium deoxycholate in PBTw (PBS solution containing 0.1% Tween-20)) for about 1 hour on ice. The fixed tissues were rinsed 5 times in PBTw for 5 minutes each, once in 1:1 PBTw: Hybrix for 10 minutes, and then once in Hybrix for 10 minutes to equilibrate the tissues. After prehybridization of the tissue in Hybrix at 60°C for 2 hours, denatured RNA probes were added to a final concentration of 0.25 ng/μl to the prehybridized tissues for hybridization overnight at the same temperature. The hybridized CNSs were washed in the solutions (Hybrix: PBTw= 4:0, 3:1, 2:2, 1:3, 0:4) and in PBTw 4 times for 20 minutes each at room temperature. The hybridization signals were detected immunologically as described above for the quantification of digoxigenin-labeled RNA probes.

Immunohistochemistry

Crz-specific antibodies were obtained from rats that had been immunized with synthetic Crz peptides conjugated separately to three different carrier proteins (bovine

serum albumin, ovalbumin, and Keyhole Limpet Hemocyanin). Anti-CAP was generated in rabbits by injecting synthetic peptide corresponding to a part of the Crz precursor (VDPDPENSAHPRLSN, Fig. 2-1) conjugated to Keyhole Limpet Hemocyanin (Genemed synthesis). These primary antibodies were applied at a dilution of 1:500-1:1,000 for whole-mount immunohistochemistry (IHC).

For IHC, dissected CNSs were fixed in fixative (4% paraformaldehyde in PBS) for 30 minutes and rinsed in PBS solution containing 1% Triton three times for 15 minutes each. After incubating in blocking buffer (0.4 % normal donkey serum in TNT (0.1 M Tris, 0.3 M NaCl, 0.5 % Triton X-100, pH 7.4)) for 30 minutes, primary antibodies as above were applied and incubated overnight at 4°C. The CNSs were then rinsed in TNT 6 times for 10 minutes each at room temperature. The primary immunoreactive signals were detected by fluorescein isothiocyanate (FITC)-, TRITC-, or horse-radish peroxidase (HRP)-tagged secondary antibodies, each used at a dilution of 1:200 (Jackson ImmunoResearch) by 2-hour incubation. Fluorescently labeled tissues were cleared in 30% and 60% glycerol for 10 minutes each, and then mounted in Vectashield medium (Vector laboratory). For HRP-conjugated secondary antibody, 0.25 mg/ml DAB (3, 3'-diaminobenzidine) was used as a substrate. NiCl was added to DAB to enhance staining intensities (Nässel and Ekström, 1997). After optimal color development was achieved, tissues were dehydrated in a graded ethanol series (60-100%), cleared in methyl salicylate, and mounted in a mixture of methyl salicylate:permount (1:6). Images were acquired by Olympus BX-61 microscope equipped with a CCD camera and processed by Adobe Photoshop. In an experiment, fluorescent immunosignals were quantified using Adobe Photoshop software as described

Figure 2-1. Comparisons of genomic sequences and putative translation products encoded by the *Dm-Crz* (m) and *Dv-Crz* (v) genes. Dashes are introduced for regions of no homology. The transcription start site is indicated by +1, and canonical polyadenylation signals (AATAAA) are underlined. Lower-case letters represent intervening sequences, and splice junctions (gt-ag) are bold-faced. An additional intron present in the 5'-UTR of the *Dv-Crz* is designated by [gc···ag]. Most of intronic sequences are omitted and represented by dots. A sequence previously assigned as a stop codon (taa) (Veenstra, 1994) is shown in the box. Nucleotides underscored by stars in the 5'- and 3'-UTRs indicate sequences conserved between the two *Crz* genes. Italics indicate putative signal peptide regions predicted by a web-based software (www.cbs.dtu.dk/services/SignalP/), and amino acids in three-letter symbols represent the mature Crz peptide. Consensus GKR processing sites (see Results) and residues used to produce anti-CAP (VDPDPENSAHPRLSN) are bold-faced.

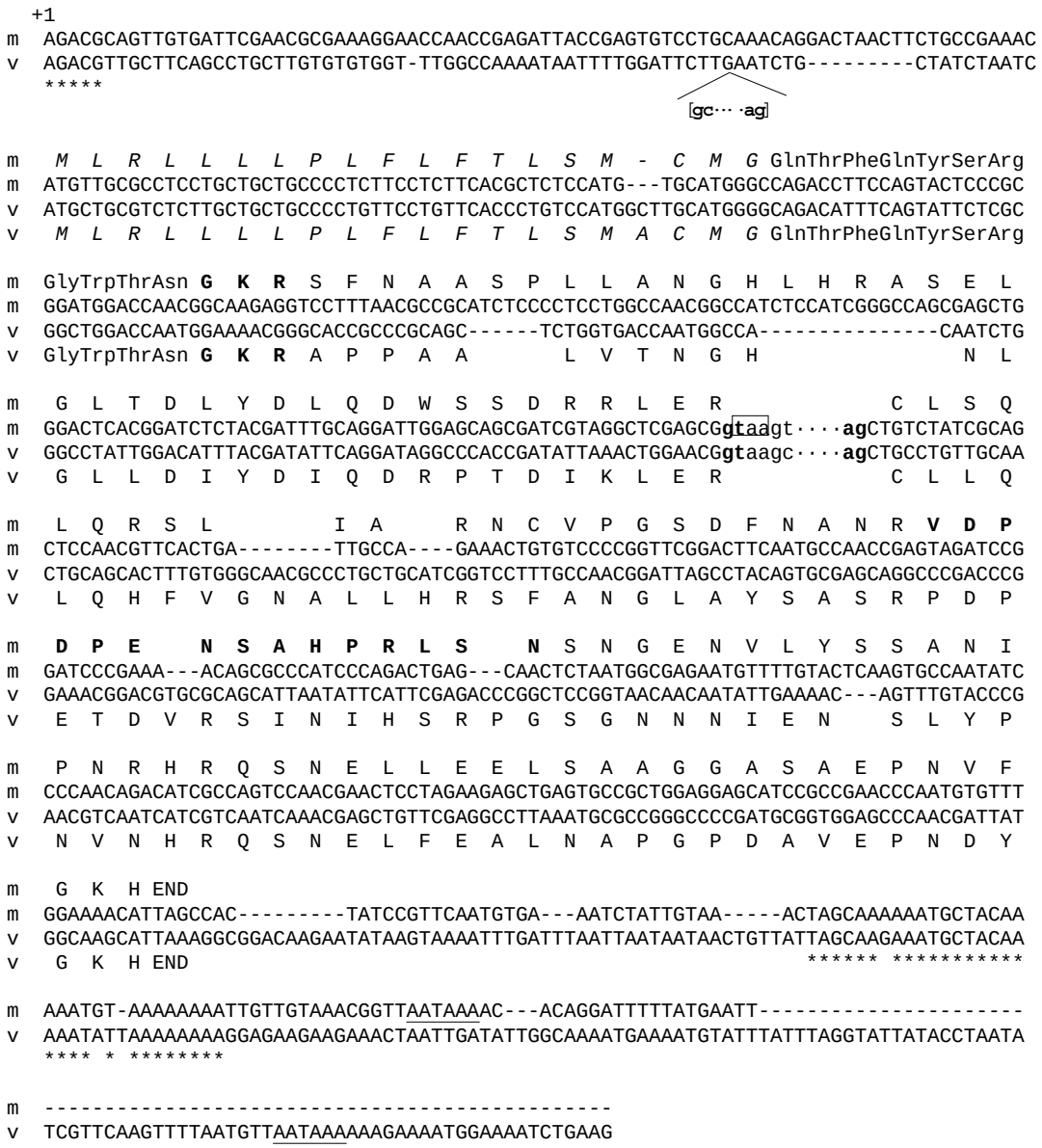
+1
m AGACGCAGTTGTGATTCGAACGCGAAAGGAACCAACCGAGATTACCGAGTGTCCTGCAAACAGGACTAACTTCTGCCGAAAC
v AGACGTTGCTTCAGCCTGCTTGTGTGTGGT-TTGGCCAAAATAATTTTGGATTCTTGAATCTG---------CTATCTAATC
*****
[gc··· ·ag]
m M L R L L L L P L F L F T L S M - C M G GlnThrPheGlnTyrSerArg
m ATGTTGCGCCTCCTGCTGCTGCCCCTCTTCCTCTTCACGCTCTCCATG---TGCATGGGCCAGACCTTCCAGTACTCCCGC
v ATGCTGCGTCTCTTGCTGCTGCCCCTGTTCCTGTTCACCCTGTCCATGGCTTGCATGGGGCAGACATTTCAGTATTCTCGC
v M L R L L L L P L F L F T L S M A C M G GlnThrPheGlnTyrSerArg
m GlyTrpThrAsn G K R S F N A A S P L L A N G H L H R A S E L
m GGATGGACCAACGGCAAGAGGTCCTTTAACGCCGCATCTCCCCTCCTGGCCAACGGCCATCTCCATCGGGCCAGCGAGCTG
v GGCTGGACCAATGGAAAACGGGCACCGCCCGCAGC------TCTGGTGACCAATGGCCA---------------CAATCTG
v GlyTrpThrAsn G K R A P P A A L V T N G H N L
m G L T D L Y D L Q D W S S D R R L E R C L S Q
m GGACTCACGGATCTCTACGATTTGCAGGATTGGAGCAGCGATCGTAGGCTCGAGCGgtaagt····agCTGTCTATCGCAG
v GGCCTATTGGACATTTACGATATTCAGGATAGGCCCACCGATATTAAACTGGAACGgtaagc····agCTGCCTGTTGCAA
v G L L D I Y D I Q D R P T D I K L E R C L L Q
m L Q R S L I A R N C V P G S D F N A N R V D P
m CTCCAACGTTCACTGA--------TTGCCA----GAAACTGTGTCCCCGGTTCGGACTTCAATGCCAACCGAGTAGATCCG
v CTGCAGCACTTTGTGGGCAACGCCCTGCTGCATCGGTCCTTTGCCAACGGATTAGCCTACAGTGCGAGCAGGCCCGACCCG
v L Q H F V G N A L L H R S F A N G L A Y S A S R P D P
m D P E N S A H P R L S N S N G E N V L Y S S A N I
m GATCCCGAAA---ACAGCGCCCATCCCAGACTGAG---CAACTCTAATGGCGAGAATGTTTTGTACTCAAGTGCCAATATC
v GAAACGGACGTGCGCAGCATTAATATTCATTCGAGACCCGGCTCCGGTAACAACAATATTGAAAAC---AGTTTGTACCCG
v E T D V R S I N I H S R P G S G N N N I E N S L Y P
m P N R H R Q S N E L L E E L S A A G G A S A E P N V F
m CCCAACAGACATCGCCAGTCCAACGAACTCCTAGAAGAGCTGAGTGCCGCTGGAGGAGCATCCGCCGAACCCAATGTGTTT
v AACGTCAATCATCGTCAATCAAACGAGCTGTTCGAGGCCTTAAATGCGCCGGGCCCCGATGCGGTGGAGCCCAACGATTAT
v N V N H R Q S N E L F E A L N A P G P D A V E P N D Y
m G K H END
m GGAAAACATTAGCCAC---------TATCCGTTCAATGTGA---AATCTATTGTAA-----ACTAGCAAAAAATGCTACAA
v GGCAAGCATTAAAGGCGGACAAGAATATAAGTAAAATTTGATTTAATTAATAATAACTGTTATTAGCAAGAAATGCTACAA
v G K H END ****** **********
m AAATGT-AAAAAAAATTGTTGTAAACGGTTAATAAAAC---ACAGGATTTTTATGAATT----------
v AAATATTAAAAAAAAGGAGAAGAAGAAACTAATTGATATTGGCAAAATGAAAATGTATTTATTTAGGTATTATACCTAATA
**** * ********
m ----------
v TCGTTCAAGTTTTAATGTTAATAAAAAAGAAAATGGAAAATCTGAAG

Figure 2-1.

(Lee et al., 2000a). As a negative control, immunohistochemistry was performed in the absence of primary antibodies, which did not produce any signals.

For a double labeling of *Crz* and *Pdf* neurons, a *Pdf-gal4* line was crossed to the *UAS-mCD8-GFP*; the resulting double transgenic adults were immunolabeled with anti-CAP. To determine types of cells that express *Crz* transcripts in the optic lobe medulla, GFP-labeled Crz cells were immunolabeled with anti-ELAV, a neuronal marker (Robinow and White, 1991). To examine whether *Crz*-neurons project to the CC in adults, a CC specific *Akh-gal4* driver was crossed to a UAS-*lacZ*; the adult progeny bearing both transgenes were doubly immunolabeled with anti-β-GAL (Sigma) and anti-CAP. Differential fluorescent signals were captured by Olympus BX-61 microscope, and then co-labeling patterns were obtained by merging two relevant channels.

Green fluorescent protein (GFP) staining for whole-mount embryo

Crz-gal4/UAS-mCD8-GFP flies were allowed to lay eggs on grape juice plate, and staged embryos were collected with a brush from juice plates and transferred to a microcentrifuge tube containing water. To dechorionate embryos, water in the tube was replaced by fresh 50% bleach in PBS containing 0.5% Triton X-100, the tubes were shaken for 5 minutes, and the embryos in the tube were rinsed with embryo washing solution (0.12 M NaCl, 0.02% Triton X-100) three times. To fix embryos, the embryos were transferred to a 4-well plate (Nunc) containing fixative (4% paraformaldehyde in PBS) and incubated for 30 minutes at room temperature. Subsequently the embryos were washed 3 times in PBS for 5 minutes each, cleared in 30% and 60% glycerol in PBS, and mounted using vectashield (Vector Laboratory).

IV. Results

Molecular characteristics of the *Crz* gene in *D. melanogaster*

Crz-encoding gene sequence in *D. melanogaster* (*Dm-Crz*) was previously reported by Veenstra (1994); however, lack of information about its transcription unit prompted us to perform RACEs to determine 5'- and 3'-termini of the *Crz* transcript. As a result, we obtained a 654-bp full length *Dm-Crz* cDNA sequence that encodes conceptual 154-amino acid-long product (Fig. 2-1). Comparison of the cDNA sequence with corresponding genomic DNA sequence revealed a single 209-bp intron containing canonical splicing donor (GT) and acceptor (AG) sites (Reed and Maniatis, 1985). Such genomic organization is in good agreement with annotation for the *Crz* gene (CG3302) reported in the *Drosophila* genome database (flybase.bio.indiana.edu/.bin/fbidq.html?FBgn0013767).

Crz genes in other *Drosophila* species

Our previous northern hybridization result indicates that under high-stringency conditions, the *Dm-Crz* probe hybridized significantly less to *D. simulans* transcripts compared with *Dm-Crz* mRNAs and almost not at all to *D. erecta* transcripts (Choi et al., 2005). Such reduced levels of cross-specific hybridization could indicate that *Crz* gene sequences are not well conserved in these species. Since comparative studies on the gene structures and expression patterns could provide important information about the molecular mechanisms of *Crz* gene regulation and functions (*cf.* O'Neil and Belote, 1992), we cloned the *Crz*-homologous genes in the two *Drosophila* species just noted and

from *D. virilis*. *D. simulans* and *D. erecta* are close relatives of *D. melanogaster* and belong to the *Sophophora* subgenus, whereas *D. virilis* is a member of the *Drosophila* subgenus; these two subgenera are estimated to have radiated approximately 60 million years ago (Powell, 1997).

Using RACE and PCR (as summarized in Table 2-1 and 2-2), we isolated *Crz* genes from *D. simulans*, *D. erecta*, and *D. virilis*; these genes are hereafter referred to as *Ds-Crz*, *De-Crz*, and *Dv-Crz*, respectively. Sequence alignment analyses show that the nucleotide sequence of *Dm-Crz* cDNA is 93% identical to *Ds-Crz*, 89% to *De-Crz*, and 53% to *Dv-Crz* (Table 2-3). Identities are nearly absent between *Drosophila* and moth (*Galleria mellonella*) gene sequences (Hansen et al., 2001). The results verify that degrees of *Crz* sequence similarities correlate with phylogenetic relatedness of these species (Fig. 2-3B).

We compared nucleotide sequences of the untranslated regions (UTRs) separately to determine whether the non-coding regions are less constrained to evolutionary selection than are coding sequences. Nucleotide lengths of the 5'-UTRs are more or less uniform (72-85 nt) (Fig. 2-2C); however, the 5'-UTR of *Dv-Crz* shows only 9-11% of identities to the corresponding regions of Sophophoran *Crz* genes (Table 2-3). Interestingly, the first five nucleotides in the 5'-UTR are invariable in all four *Drosophila Crz* genes (AGACG, Fig. 2-1), indicating that this consensus sequence may play a role in specifying *Crz* transcription start site. Alternatively, this conserved motif may be a regulatory element for tissue-specific *Crz* expression, since *Crz* mRNA expression patterns in *D. virilis* are mostly consistent with those observed in Sophophoran species (see *Dv* Crz expression at p. 64).

Table 2-3. Interspecific comparisons of the *Crz* gene and Crz precursor sequences

			Percentage of identity				
			Dm	Ds	De	Dv	Gm
Nucleotide sequence	Entire cDNA	Dm	-	93	89	53	5
		Ds	-	-	89	53	5
		De	-	-	-	51	4
		Dv	-	-	-	-	5
	ORF	Dm	-	93	89	62	10
		Ds	-	-	90	62	9
		De	-	-	-	63	9
		Dv	-	-	-	-	11
	5'-UTR	Dm	-	95	89	9	13
		Ds	-	-	86	9	12
		De	-	-	-	11	9
		Dv	-	-	-	-	27
	3'-UTR	Dm	-	90	87	28	49
		Ds	-	-	82	28	18
		De	-	-	-	24	44
		Dv	-	-	-	-	50
	Intron	Dm	-	87	31	33	NA
		Ds	-	-	16	46	NA
		De	-	-	-	16	NA
Amino acid sequence	Entire precursor	Dm	-	98	92	54	15
		Ds	-	-	92	52	15
		De	-	-	-	55	15
		Dv	-	-	-	-	23
	CAP region	Dm	-	97	90	41	7
		Ds	-	-	90	38	7
		De	-	-	-	42	7
		Dv	-	-	-	-	13

Dm-*D. melanogaster*; Ds-*D. simulans*; De-*D. erecta*; Dv-*D. virilis*; Gm-*G. mellonella*; UTR-Untranslated Region; CAP-Crz associated peptide. Numbers are pairwise percentages of identity between species. Intron-II in the *Dv-Crz* gene was compared to introns in other species due to their identical genomic location. All sequences were analyzed by CLUSTAL W sequence alignment software (www.ebi.ac.uk/clustalw). Relatively higher percentages of identity between Gm and *Drosophila* 3'-UTRs are likely due to AT-rich nature of the 3'-UTRs.

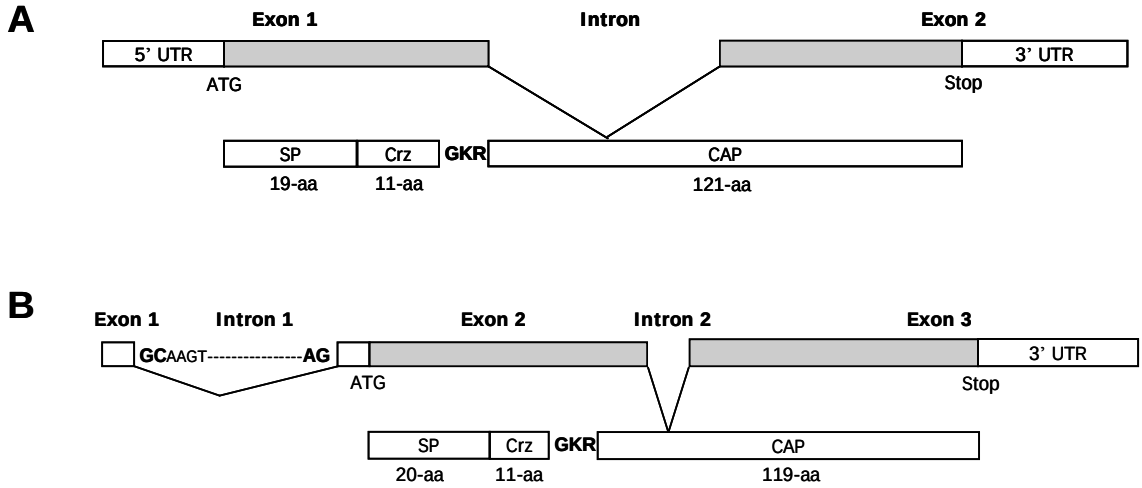

C

species	Full-length cDNA	5' UTR	ORF	3' UTR	intron
D. melanogaster	654	82	465	107	209
D. simulans	659	85	465	109	186
D. erecta	668	82	465	121	316
D. virilis	731	72	462	197	I-408, II-71
G. mellonella *	927*	161	342	424	NA

Figure 2-2. Comparisons of *Corazonin* gene organization and prepro-corazonin structures. **(A)** *D. melanogaster*, *D. simulans*, and *D. erecta*. **(B)** *D. virilis*. Open reading frames are shaded in gray. Prepro-Crzs consist of a signal peptide (SP) and Crz, followed by Crz-associated peptide (CAP). A consensus post-translational processing site (GKR) is present in all precursors. The *Dv-Crz* gene contains an additional intron within the 5'-UTR of the mRNA. This intron has a non-canonical 5'-splicing site (GC) flanked by consensus sequence (see Results text). **(C)** Comparisons of base-pair lengths for each sequence motif. *The cDNA length shown here for the wax moth, *G. mellonella*, is shorter than the original report (*cf.* Hansen et al., 2001), since we discounted putative poly-A tail, as were done for fly cDNAs. Degrees of identities involving the sequences diagrammed here are shown in Table 2-3.

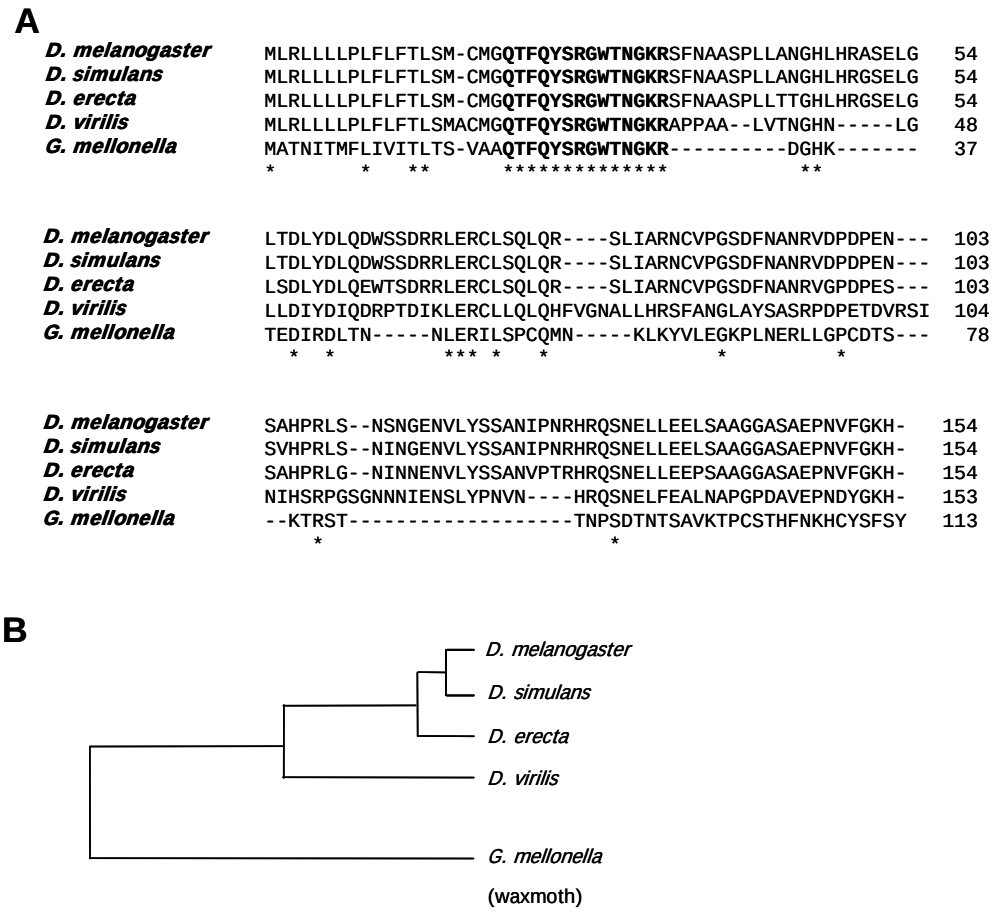

Figure 2-3. Comparison of Crz precursors. **(A)** Sequence alignment of Crz precursors of four Drosophila species and the wax moth *Galleria mellonella* (Hansen et al., 2001). Numbers in the right-most column denote amino acid lengths. Asterisks indicate identical amino acid residues occurring in all species, and dashes for gaps are inserted with respect to regions of no homology. The Crz peptide and GKR processing site (bold-face letters) are invariable in all species, whereas the *C*-terminus CAP regions are significantly diverged. Degrees of homology in the CAP region correlate with phylogenetic relationships of these species, as shown in **(B)**. For instance, there are only 3 amino-acid differences between *D. melanogaster* and *D. simulans* Crz precursors, compared with 14 between *D. melanogaster* and *D. erecta*. The *G. mellonella* precursor shows essentially no similarity to *Drosophila* precursors except with regard to Crz itself. Additional features of these data are presented in Table 2-3.

In contrast to the 5'-UTRs, nucleotide lengths of the 3'-UTRs are quite diverse; for instance, *Dv-Crz* 3'-UTR is almost twice as long as *Dm-Crz* 3'-UTR (Figs. 2-1, 2-2C). However, a stretch of 33 nucleotides is found to be highly conserved in the 3'-UTRs of all *Drosophila Crz* genes examined here (***e.g.***, Fig. 2-1), indicating a functional significance of this element in the regulation of *Crz* expression. Introns are also not well conserved with respect to their numbers, nucleotide lengths, and compositions. The Sophophoran *Crz* genes contain a single intron at identical location within the conceptual open reading frame; however, nucleotide lengths of the introns are highly variable (209-bp in *Dm-Crz*, 186-bp in *Ds-Crz*, 316-bp in *De-Crz*) (Fig. 2-2). Unlike in Sophophoran *Crz* genes, there are two introns found in the *Dv-Crz* gene; the first one (408-bp) is located within the 5'-UTR; the second, much shorter one (71-bp) is situated where the Sophophoran introns are found (Fig. 2-2). Interestingly, the first intron contains an unusual 'GC-AG' splice junction rather than consensus 'GT-AG'. This type of non-canonical splice site occurs in an appreciable number of mammalian introns (126 cases out of 22,489 entries examined; Burset et al., 2001). Consensus sequence flanking 'GC' splice site (GCAAGT; Burset et al., 2001) is also found in the *Dv-Crz* intron (Fig. 2-2B). Overall, the results show that non-coding regions of the *Crz* gene have diverged more rapidly than do coding sequences during the course of evolution. This agrees with a general pattern of gene evolution in which noncoding regions are less constrained to evolutionary selection (Graur and Li, 1999).

Comparative analyses of Corazonin precursors

The 154 amino-acid Crz precursor (prepro-CRZ) predicted from the *Dm-Crz* cDNA sequence is composed of a putative signal peptide (presumably for secretory pathway), the Crz peptide itself, followed by a *C*-terminal peptide which we call here Crz-associated peptide (CAP) (Figs. 2-1, 2-2). The presence of consensus processing site (GKR) between Crz and CAP suggests that Crz is separated from its precursor and further modified by α-amidation at its *C*-terminus (Bradbury et al., 1982). A biochemical separation analysis revealed the Crz peptide in a CNS extract of *D. melanogaster*, supporting the notion that Crz is released from a larger precursor via post-translational processing (Baggerman et al., 2002). The tri-domain structure is also conserved in precursors from three other *Drosophila* and Lepidopteran species (Figs. 2-2, 2-3).

The putative prepro-Crz is much longer than the previously reported one (Veenstra, 1994). We found that the previously assigned termination codon, which would result in a much shorter open reading frame overall, is actually located within the intronic sequence (Fig. 2-1). Our prediction of prepro-Crz structure was verified by the detection of CAP-immunoreactivity using antibodies raised against a region of the CAP domain, which was excluded from the previously reported Crz precursor structure (Fig. 2-1).

Sequence alignment of the precursors was carried out to compare their primary structures by using a web-based program (ClustalW; www.ebi.ac.uk/clustalw/) (Fig. 2-3). Amino-acid residues for the predicted signal peptides are identical among fly precursors except for an additional residue in *D. virilis*. In all cases, Crz peptides *per se* are the same, which speaks to a "constrained" biological function for this substance. Fly Crz

belongs to the [Arg^7]-CRZ subfamily, since the 7th amino acid residue is an arginine, whereas Crz isolated from locusts are referred to as [His^7]-Crz due to the histidine residue at this position (Tawfik et al., 1999). A third isoform was recently found in the honey bee *Apis mellifera* as [Thr^4, His^7]-Crz which have threonine and histidine at the 4th and 7th amino acid positions, respectively (Verleyen et al., 2006). As in *D. melanogaster*, the four other Crz sequences are flanked by a consensus post-translational processing site (GKR).

The largest domain in the prepro-Crz (*i.e.*, CAP) appears to be rapidly evolving. For instance, Sophophoran CAP sequences share only 38-42% identities with *D. virilis* CAP, and there is essentially no similarity of this domain between flies and moth (Fig. 2-3A, Table 2-3). Moreover, our BLAST search for each species-specific CAP sequence found no significant homology with any known polypeptides. Because of such dissimilarities, biological activities (if any) of the CAP are a matter of conjecture. Nevertheless, a similar tendency was also observed in members of other neuropeptide families (*e.g.*, Bogerd et al., 1995; Park and Hall, 1998). In the case of adipokinetic hormone (AKH) precursors, the AKH-associated peptide domain is important for the formation of precursor dimers, which are subsequently processed to produce bioactive AKHs in locusts (O'Shea and Rayne, 1992). In this context, the associated peptide could be necessary for the formation of tertiary structure of the precursor molecules, which hypothetically permits the precursors to be processed in an optimal manner.

Conservation of *Crz* expression patterns in larval CNS of *Drosophila* species

In an attempt to gain insight into biological functions and regulatory mechanisms of the *Crz* gene in *Drosophila*, we examined *Crz* expression patterns in the CNS using *in situ* hybridization for the detection of *Crz* mRNA and immunohistochemistry for Crz product. Based on our Northern hybridization results (Choi et al., 2005) and sequence data (Fig. 2-1), we expected that the *Dm-Crz* specific probe would not hybridize well to *Crz* mRNAs in other fly species. Thus, species-specific cRNA probes were generated.

In each brain lobe of wandering 3rd instar larvae of *D. melanogaster*, strong hybridization signals were detected in a cluster of three neurons in the dorso-lateral region of the protocerebrum (referred to as DL neurons); a weaker signal in a neuron located more medially (dorso-medial neurons; abbreviated DM) (Fig. 2-4A, B). In addition to these brain cells, *Crz* mRNAs were localized in eight pairs of bilateral neurons in the ventral nerve cord (VNC). None of these expression sites were detectable with the application of the sense probe (n=12, data not shown). Identical *Crz* expression patterns were observed in *D. simulans* and *D. erecta* (not shown; at least five CNS specimens were examined for each species). Although such larval expression sites (*i.e.*, DL and DM neurons) were also well conserved in the CNS of *D. virilis* larvae, we found additional *Crz* mRNA expression in a pair of cells located in the medial brain region (arrowheads in Fig. 2-4C); however, these signals were very faint and detectable only in a half of specimens examined (n=29).

To determine whether *Crz* mRNAs are translated into protein products and to reveal neural circuits formed by *Crz*-neurons, whole-mount immunohistochemistry was performed using Crz-specific antibody. In *D. melanogaster* larvae, somata of Crz-

Figure 2-4. *In situ* hybridizations of *Crz* transcripts. (**A)** Schematic representation of *Crz* mRNA expression sites within the larval CNS of *D. melanogaster*, and **(B)** a representative CNS specimen (n=10) displaying this pattern (*i.e.*, one dorso-medial (DM) and three dorso-lateral (DL) neurons in a brain lobe and eight pairs of bilateral neurons within the ventral nerve cord (VNC)). The expression patterns were identical in larval CNSs of *D. simulans* (n=7) and *D. erecta* (n=5) (not shown). **(C)** *D. virilis* larval CNS (n=6). *Crz* expression patterns are identical to those of *D. melanogaster*, except for a pair of faintly stained cells that are occasionally observed within medial brain region (arrowheads). **(D-G)** *Crz* mRNA expression patterns in adult CNS. (D) A diagram illustrating *Crz*-neurons in adult brain. *Crz* mRNA is localized in a cluster of 6-8 neurons within dorso-latero-posterior region of each hemi-brain (DLP-neurons). (E) A representative *D. melanogaster* adult CNS (n=16). Notice that *Crz* expression is absent in the VNC. Similar expression patterns were observed for *D. simulans* (n=10) and *D. erecta* (n=12) (data not shown). (F) Anterior view of 2-day-old *D. melanogaster* adult brain (n=6). Widespread signals on the anterior surface of the medulla optic lobes (arrowheads) were detected only in *D. melanogaster*. (G) *D. virilis* adult brain (n=14), showing DLP-like *Crz*-expressing neurons. *Crz* expression is undetectable in the medulla (*cf*. Fig. 2-4F). Scale bar: 100 μm.

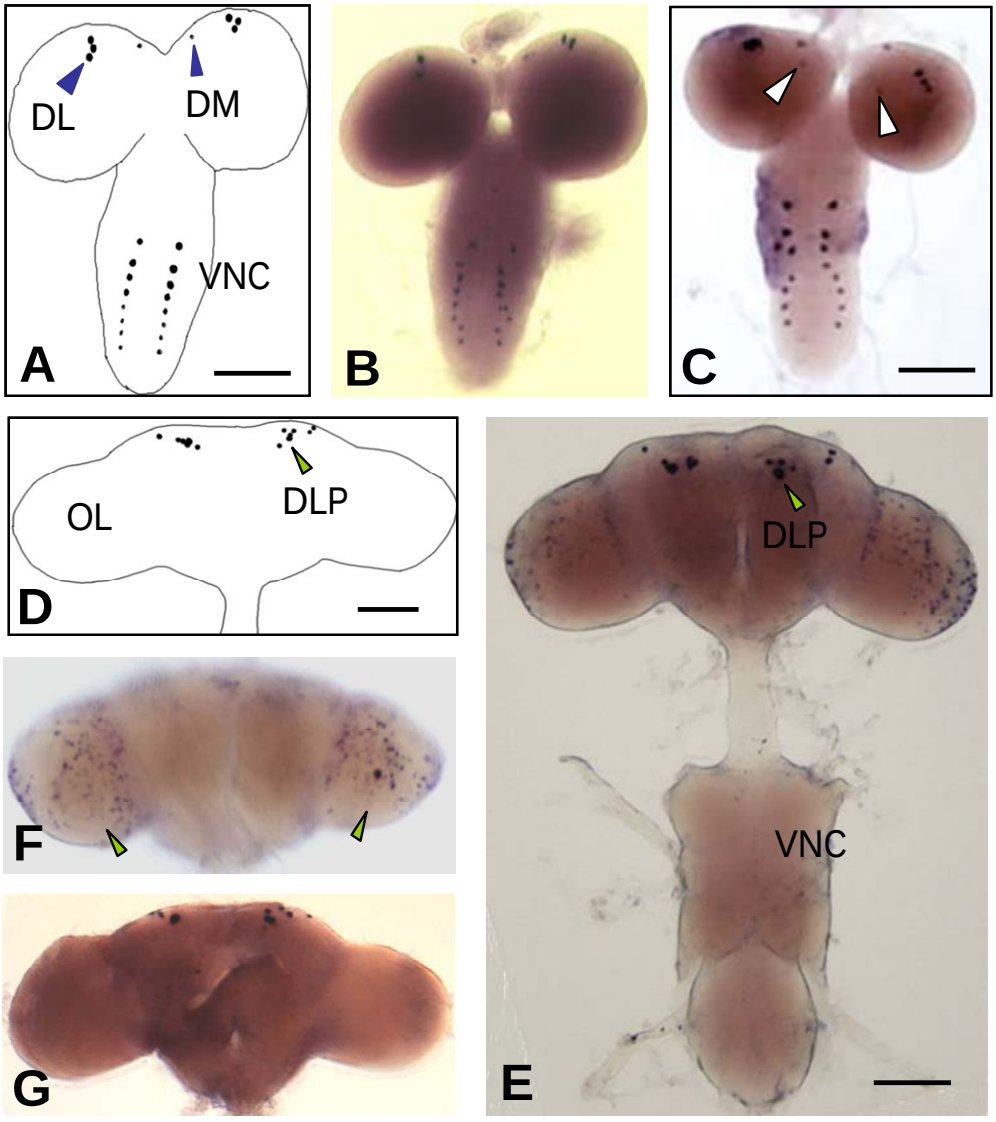

Figure 2-4.

immunoreactive neurons were detected in the same locations as cells labeled by *in situ* hybridization with antisense *Crz* probe (Figs. 2-5A *vs.* 2-4B). Consistent *Crz*-expressing neurons revealed by two independent methods that detect different gene products (*i.e.*, peptide by immunohistochemisty and mRNA by *in situ* hybridization) strongly corroborate that *Crz* gene activities are restricted to those nerve cells in the larval CNS. The results also mutually validate specificity of the probes employed for both techniques (*i.e.*, antisense RNA for *in situ* hybridization and antibody for immunohistochemistry).

Since antibodies can readily detect neuronal processes of cytoplasmically expressed gene products, we traced neurite pathways emanating from the Crz-immunoreactive neurons. Axonal projections from the DL neurons initially extend to the medial brain region and then bifurcate into two branches; one of them continues projecting medially up to the midline, just dorsal to the esophagus foramen, and then it turns abruptly and extends ventrally, bordering the esophageal foramen. The other branch travels ventrally, and then it makes a dorsal turn forming a loop, and finally terminates at the ring gland and aorta (Fig. 2-5B, C). Since the latter two structures are major neurohemal organs in insects (*e.g.*, Predel, 2001), Crz peptides are likely to be secreted into the circulatory system to function as a neurohormone. Within the ring gland, DL terminals arborize in the corpora cardiaca (CC), and occasionally one or two axonal branches extend farther to the area where the prothoracic gland cells are located (Fig. 2-5C). Neurites from the DM neurons project contralaterally across the midline; further tracing was in vain due to faint immunosignals.

In the ventral ganglia, somata of Crz-immunoreactive neurons are ventrally located. One prominent projection from these cells runs contralaterally to their bilaterally

Figure 2-5. Crz immunohistochemistry. **(A-C)** Whole-mount Crz-immunostainings in *D. melanogaster* larvae. (A) A representative confocal image shows three DL neurons (solid arrowhead) in a hemi-brain and eight pairs of bilateral neurons in the VNC. Axon terminals stemming from VNC neurons are designated by an open arrowhead. (B) Schematic diagram of Crz-immunoreactive neurons. Anatomical positions of Crz-immunoreactive neurons are comparable to those observed by *in situ* hybridization (*cf.* Fig. 2-4A). (C) Crz-immunoreactive arborizations. The staining was elicited colorimetrically with DAB/NiCl. Extensive Crz-immunoreactive terminals stemming from DL neurons are displayed in the corpora cardiaca (CC) and aorta (AO), and one or two fibers (arrowheads) extend to the prothoracic glands (PG). **(D-E)** Crz-immunoreactive patterns in adult brain. (D) A representative confocal image. Mean immunosignal intensities (arbitrary unit ± SD) were not significantly different between males (1015 ± 334, n=13 hemispheres) and females (1043 ± 353, n=10 hemispheres). (E) A diagram illustrating neurite pathways involving DLP neurons. (EF-Esophagus Foramen; PLT-Posterior Lateral Tract; SOG-Subesophageal Ganglia; MB-Median Bundle). Scale bar: 100 μm.

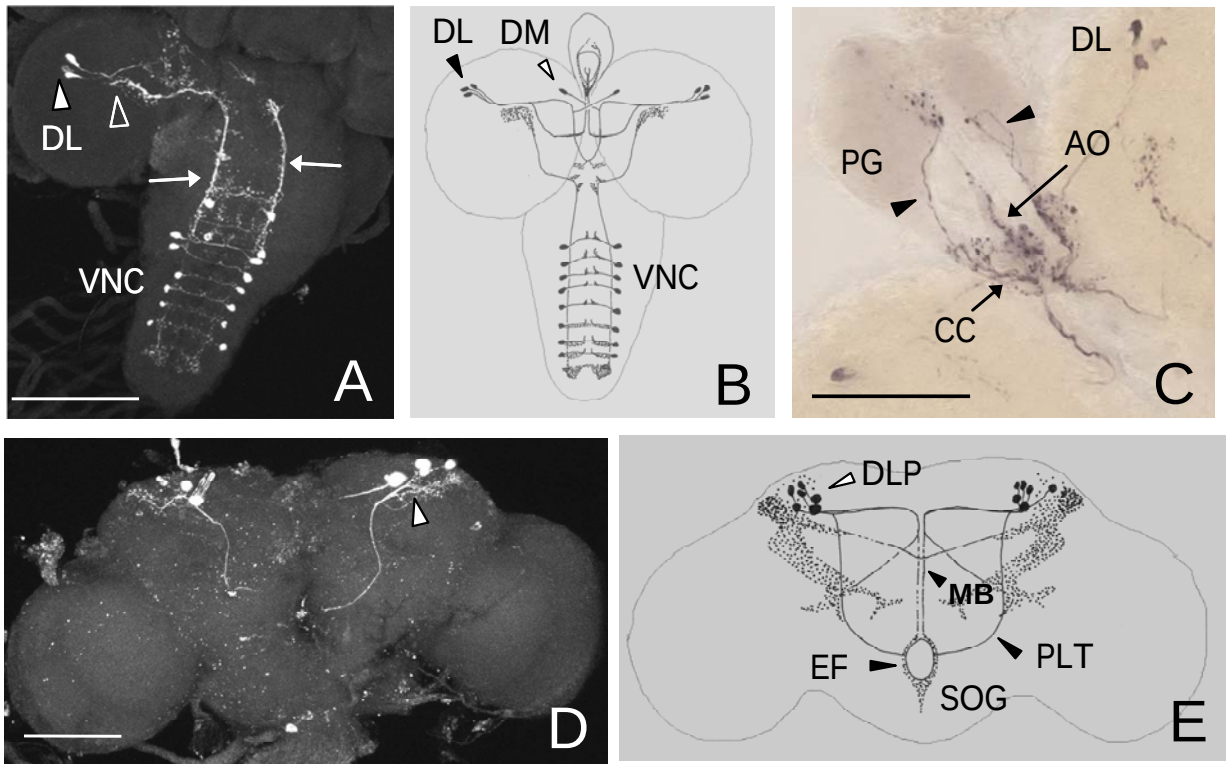

Figure 2-5.

symmetrical cells across the midline; short branches from these projections direct dorsally, just before reaching the midline, as illustrated in Fig. 2-5B. Another projection from the somata run dorsally, bifurcates, and then extends both anteriorly and posteriorly. These projections appear to fasciculate with neurites originating from other ipsilaterally located somata, giving rise to a longitudinal tract in each side of the VNC (arrows in Fig. 2-5A). The anterior end of this tract arborizes in a brain region where DL fibers bifurcate (open arrowhead in Fig. 2-5A), indicating possible interactions between DL and VNC neurons. The other end of the tract orients posteriorly and terminates in caudal region of the abdominal ganglia. Identical Crz-immunoreactive patterns were also observed in the CNSs of wandering *D. virilis* larvae (not shown; n>5).

Crz expression patterns in adult and pupal CNSs

We extended our expression analyses to the adult stage to look for changes of *Crz* expression patterns during metamorphosis. In *D. melanogaster*, we detected 6-8 loosely clustered *Crz* mRNA expressing-neurons positioned in the dorso-latero-posterior area of the protocerebrum (DLP neurons) in each hemi-brain (Fig. 2-4D, E). Comparable expression patterns were observed in adult brains of *D. virilis* (Fig. 2-4G) and other Sophophoran species (not shown; at least 10 specimens were examined for each species). Since anatomical locations of DLP neurons are similar to those of larval DL neurons, some of adult DLP neurons are likely to be derived from persisting larval DL neurons. In contrast, *Crz* expression in larval DM and VNC neurons was no longer detected in corresponding regions of adult nervous system (Fig. 2-4E). This could be due to either inactivation of the *Crz* gene or programmed death of these neurons during

metamorphosis. Our further analyses, as described in Chapter 3, reveal that at least the VNC neurons are genetically programmed to die during early metamorphosis. Nevertheless, different *Crz* expression patterns between larval and adult stages are suggestive of distinct biological roles played by Crz at different life stages.

All of the DLP neurons were also labeled by anti-Crz. We routinely observed 1-2 large and strongly stained somata, and 4-5 small and weakly stained ones (Fig. 2-5D, E). As noted previously, some of the DLP neurons likely come from persisting larval DL neurons and additional adult-specific DLP neurons could arise from dormant neuroblasts during pupal development. Consistent with this notion, immunostaining of developing pupal CNSs showed that adult-like *Crz*-expressing neurons were established in pupae, which have developed for *ca*. 48 hours after pupariation (circle in Fig. 2-6D). The number of the DL neurons begins to increase at *ca.* 24 hours after puparium formation (APF), at which an additional group of 1-3 *Crz*-neurons are very faintly stained in the region proximal to DL neurons (white arrowhead in Fig. 2-6A, n=4), thereby defining developmental time frame for the adult-specific *Crz*-neurons. During the next 6 hours of pupal development (30 hours APF), *Crz*-expressing neurons are evident in 6-8 cells per hemisphere (Fig. 2-6B, n=6), and immunoreactive signal intensities reach maximum at 36 hours APF (Fig. 2-6C, n=5). The adult-like neurite patterns are detectable at 48 hours APF (Fig. 2-6D, n=2).

Neurite patterns emanating from DLP neurons are comparable to those from larval DL neurons (Fig. 2-5E *vs.* 2-5B). The initial medial projections give rise to two main neurite pathways. One continues medially and then projects ventrally to the subesophageal ganglia (SOG) via the median bundle. The other runs ventrally to the

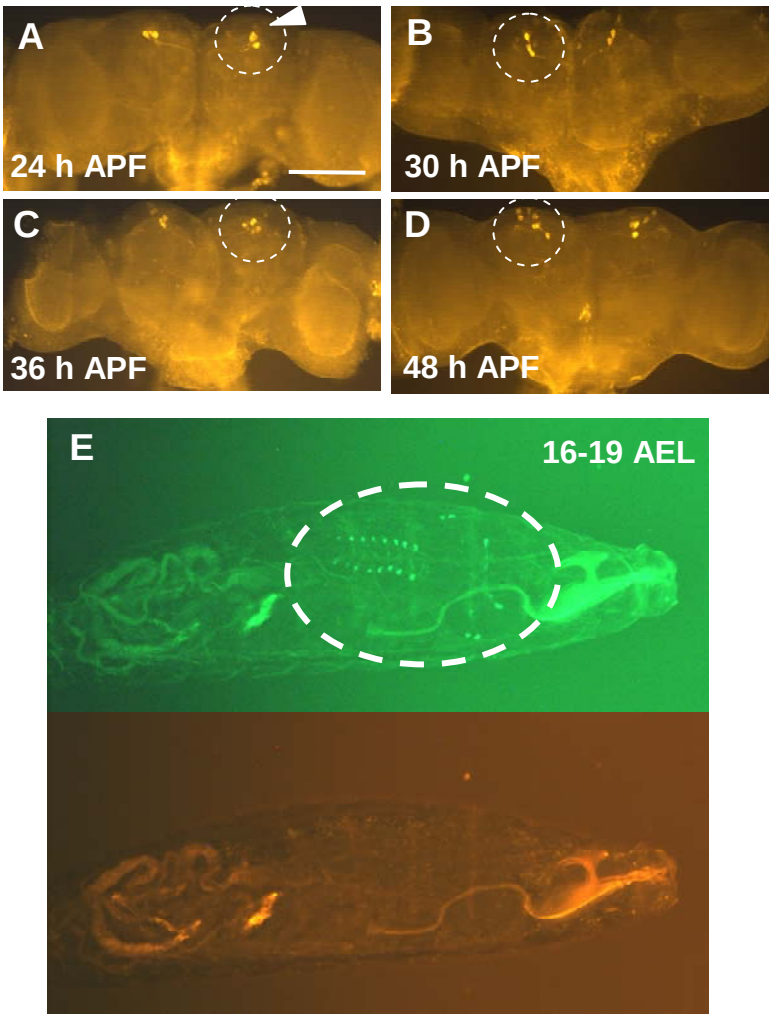

Figure 2-6. Crz expression in pupal CNS and embryo. **(A-D)** Crz-IR neurons in brain at 24-48 hours after puparium formation (APF). (A) 24 hours APF (B) 30 hours APF (C) 36 hours APF (D) 48 hours APF. Representative protocerebral Crz neurons are marked by white dotted circles and very faint additional neurons are marked by an arrowhead. **(E)** *Crz-gal4*-driven GFP expression at 16-19 hours after egg laying (AEL). GFP signals (top) are marked by a dotted circle. The same specimen was imaged through TRITC channel to detect auto-fluorescence (bottom, orange). Crz expression is not detectable in bottom panel.

esophagus foramen; this process is most likely to be the posterior lateral tract (PLT) that had been described for other cyclorrhaphous fly species (*cf.* Shiga, 2003). Since the larval DL neurons terminate at the CC, we assume that adult DLP neurons also send projections to the CC in adult. To test this, a CC-specific driver *Akh-gal4* (Lee and Park, 2004) was crossed to a UAS-*lacZ*. The brain and CC in adult progeny were then double-labeled with anti-β-GAL and anti-CAP, which would detect CC cells and *Crz*-neuronal processes, respectively. The data clearly show that axonal projections from *Crz*-neurons indeed innervate the adult CC (n=8, Fig. 2-7A-C). Therefore, consensus targets for both DL and DLP neurons further support our previous hypothesis that larval DL neurons are progenitors of a subset of adult DLP neurons. In addition to these neurite pathways, we observed extensive adult-specific arborizations of DLP neurons within the ipsilateral superior protocerebrum (arrowhead in Fig. 2-5D). Such diverse projection patterns overall suggest that DLP neurons play roles as neurosecretory cells as well as interneurons. Similar Crz-immunoreactive patterns were observed in *D. virilis* adults (not shown; n>5).

Crz expression in developing embryos

We also examined the Crz expression at the embryo stage to determine whether Crz neurons are in the process of the proliferation, or already accomplish differentiation by forming neuronal circuitry. For analyzing embryonic Crz expression, a *Crz-gal4* (see materials and methods in Chapter 3) was crossed to *UAS-mCD8-GFP*, and embryos at late stage (16-19 hours after egg laying (AEL)) were collected. *Crz-gal4*-driven GFP

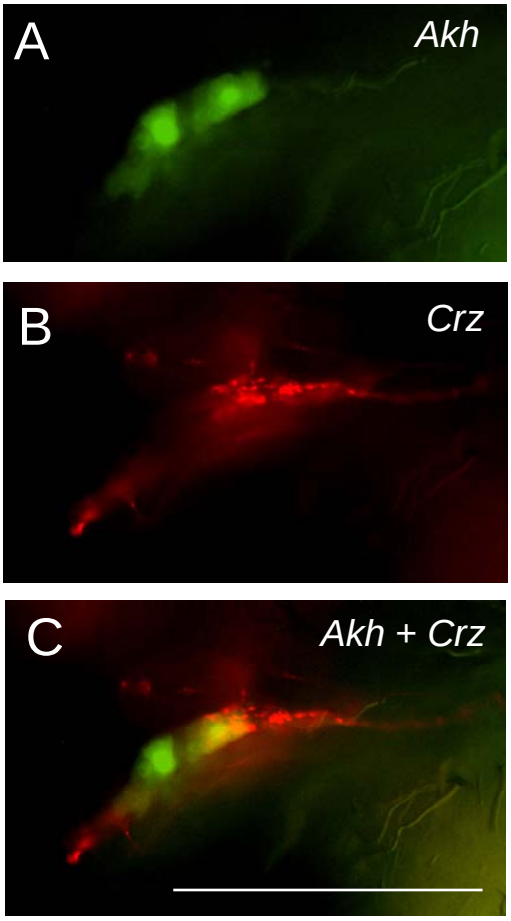

Figure 2-7. Double labeling for AKH and Crz expression in the adult corpora cardiaca (CC). The adult progeny CC obtained from [Akh-gal4 x UAS-lacZ] was labeled by anti-β-GAL and anti-Crz. (A) Akh-producing CC cells are labeled with anti-β-GAL (cf. Lee and Park, 2004) (B) Crz nerve terminal labeled by anti-CAP. (C) Composite image of A and B, showing a potential innervation of CC by Crz neurons in adults. Scale bar: 100 μm.

signals in embryos showed Crz expression that is comparable to that of 3rd instar larval stage (Fig. 2-6E). This result indicates that Crz neurons are already formed before molting to the 1st instar larva, and also suggests existence of Crz function during early larval stage.

Unusual features of *Crz* expression

In addition to the DLP neurons in *D. melanogaster* adult CNSs, *in situ* hybridization revealed numerous *Crz* mRNA producing cells widely distributed on the anterior surface of the medulla optic lobes (Fig. 2-4E, F). These signals unlikely resulted from a hybridization of our antisense RNA probe with nonspecific targets, since control experiments using sense probe did not produce any such signals in CNSs (n=13, data not shown). Moreover, *Crz* promoter-driven GFP expression was also observed in this structure (see p. 77), validating that cells in the medulla optic lobes produce genuine *Crz* transcripts.

Interestingly, hybridization signals in the optic lobes (OL) varied in young adults (less than 2 days after eclosion), in which they were detected in 6 specimens out of 14 tissues processed. In contrast, tissues from older adults (12 days old after eclosion) produced OL signals in all specimens examined (n=10), implying that age-related factors are involved in the activation of *Crz* transcription in this structure.

In contrast to the *in situ* hybridization results, *Dm-Crz* mRNA producing OL cells were not detectable with anti-Crz (Fig. 2-5D). One possibility for this is that prepro-Crz is processed differentially, resulting in the storage of the CAP peptides (instead of Crz) exclusively in the OL cells. If this were the case, CAP-specific antibodies would likely

label the OL cells. We tested this hypothesis by employing polyclonal antibodies raised against CAP region only (anti-CAP, see Materials and Methods). Double immunolabeling of *D. melanogaster* larval CNSs for Crz and CAP resulted in identical staining patterns, verifying the specificity of anti-CAP to the CRZ precursors (Fig. 2-8A-C). In adult brains, anti-CAP labeled all of Crz-immunoreactive DLP neurons, whereas neither antibody detected the OL cells (Fig. 2-8D-F). The results negated our hypothesis of differential processing of the Crz precursor in the OL cells. The lack of detectable peptide products in this vision-related structure could be due to either rapid turnover of peptides or translational silencing of *Dm-Crz* mRNA.

To examine the characteristics of *Crz* promoter-driven cells in optic lobes, adult brains obtained from *UAS-mCD-GFP*;;*Crz-gal4* were labeled with anti-ELAV neuronal maker (Robinow and White, 1991). Crz promoter-driven GFP-labeled cells located at the surface of the medulla overlap with ELAV-IRy whereas those present inside the medulla do not, suggesting that the former group is neurons and the latter is non-neuronal cells. (Fig. 2-9D, E).

OL-specific *Crz* expression was not observed in other fly species examined, regardless of age or sex (*e.g.*, *D. virilis* shown in Fig. 2-4G). The lack of such expression in *D. simulans* in particular is somewhat surprising, given that this species is closely related to *D. melanogaster*, sharing overall 96% homology of genomic sequences (Ranz et al., 2003). Recent microarray data, however, show that ca. 50% of coding sequences examined differ in their expression levels between the two species (Ranz et al., 2003), supporting the difference in OL-specific *Crz* expression.

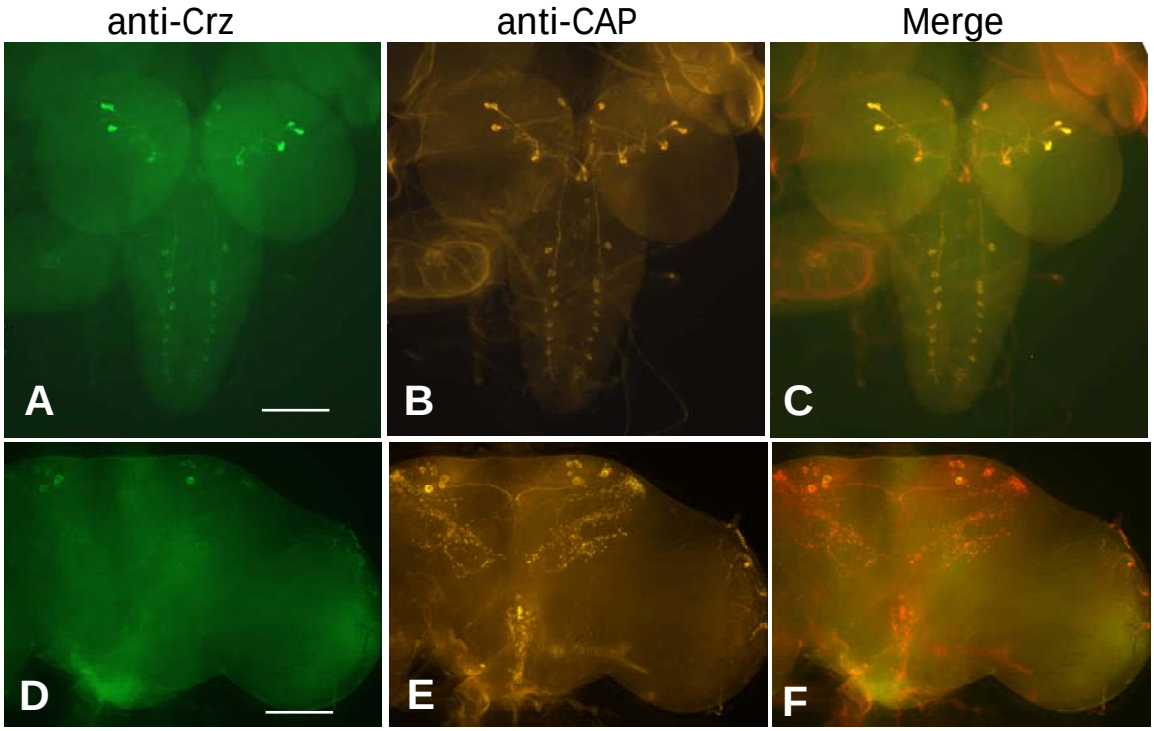

Figure 2-8. Double immuno-labeling for Crz and CAP in the CNS. (A-C) larva. (D-F) adult. (A, D) Crz-immunoreactive signals in green. (B, E) CAP-immunoreactive signals in orange. The two kinds of signals are merged within panels C and F. Signals elicited by both antibodies occur within the same neurons. However, neither antibody labeled any optic lobe cells (*cf.* Fig. 2-4F). Scale bar: 100 μm.

Figure 2-9. *Crz* promoter-active cells in the adult Optic Lobe (OL). The adult brains obtained from double transgenic line *UAS-mCD8-GFP;; Crz-gal4*^{T2a} were processed for GFP staining (n>10). (A-C) Left OL of the same specimen. B and C are blow-out of the square in A. (A) A low resolution image of anterior view of the OL. GFP-labeled *Crz* promoter-active cells are detected globally in the anterior side of the medulla of OL. (B) Neuron-like *Crz* promoter active cells (arrowhead) in OL. These cells have the morphology similar to neurons which has a cell body and axonal projections. A focal plane was set on the surface of the anterior of OL. A cluster of cells are represented by a white arrowhead. (C) The other group of *Crz* promoter-active cells (arrows) that reside in a different focal plane inside OL. (D, E) Adult brains from *UAS-mCD8-GFP;;Crz-gal4*^{T2a} were processed for IHC using neuronal marker anti-ELAV. Different focal planes of a right optic lobe of the same specimen were taken. (D) ELAV-IRys (red) are detected in nuclei of *Crz* promoter-active cells (yellow, enclosed by brackets) located superficially in the anterior of the medulla of OL, indicating that these cells are neurons. (E) ELAV-IRys are not detected in *Crz* promoter-active cells (green, enclosed by brackets) located inside the medulla, suggesting these cells are non-neuronal cells. Scale bar: in A, 100 μm, in B, 25 μm for B, C, in D, 25 μm for D, E.

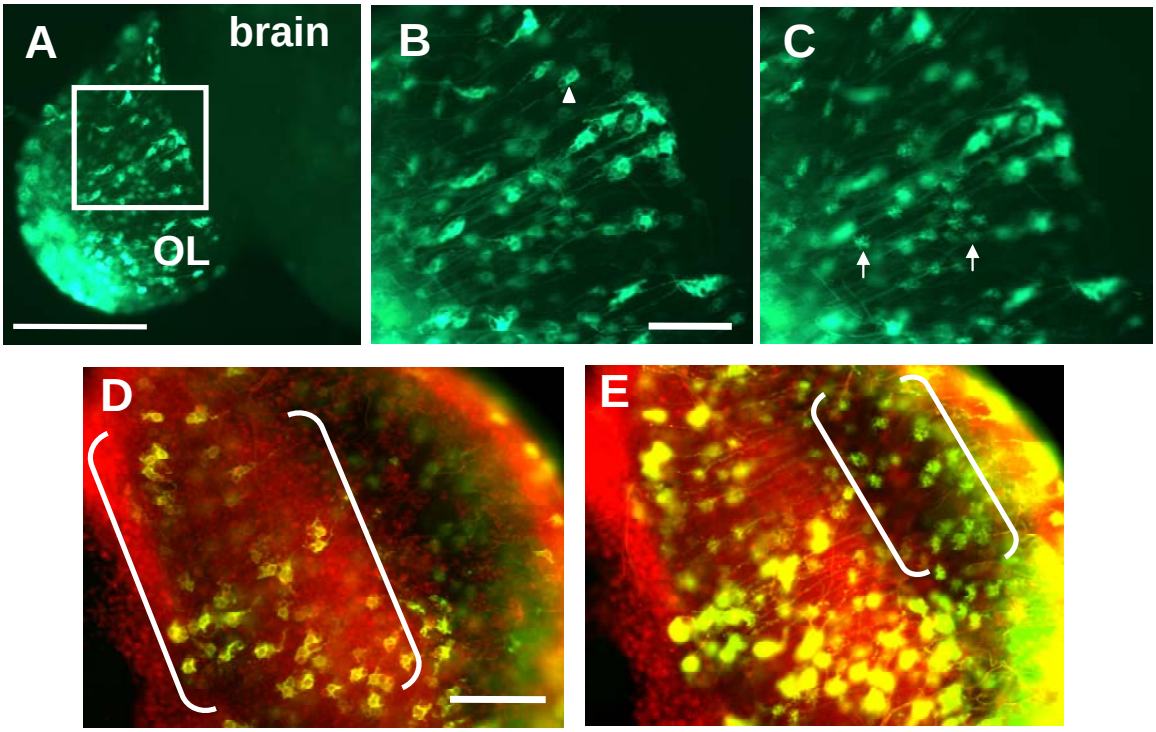

Figure 2-9.

Cell-specific transcriptional regulation of the *Dm-Crz* gene by clock factors

A microarray screening showed that *Crz* expression was up-regulated in extracts of an arrhythmic *Clock*^{Jrk} (*Clk*^{Jrk}) mutant heads, indicating that *Crz* transcription is negatively regulated by the CLK transcription factor (McDonald and Rosbash, 2001). This finding raised questions as to whether such up-regulation is due to elevated *Crz* transcription in the native neurons or ectopic expression in *Clk*^{Jrk} flies. To address this question, we performed whole-mount *in situ* hybridizations in *Clk*^{Jrk} homozygous mutant CNSs. Our results showed that neither staining intensities nor the number of *Crz* neurons changed in *Clk*^{Jrk} larval CNSs (Fig. 2-10B vs. A). However, in *Clk*^{Jrk} adults, in addition to normal DLP neurons (open arrowheads in Fig. 2-10E), we consistently detected two pairs of ectopic *Crz*-expressing cells in anterior brain region; one pair of cells is located just dorsal to the antennal glomeruli and the other in the tritocerebrum (black arrowheads in Fig. 2-10E). *In situ* hybridization signals in these ectopic cells were relatively weaker than those in DLP neurons. Intriguingly, two pairs of ectopic *Crz* cells were also detected in adult brains of another arrhythmic *cycle*^{02} (*cyc*^{02}) mutant (black arrowheads in Fig. 2-10F). Judging from similar anatomical locations, the ectopic cells in *cyc*^{02} are likely to be identical to those detected in the *Clk*^{Jrk} mutant (Fig. 2-10F *vs.* E), although signal intensities in *cyc*^{02} were relatively weaker than those in *Clk*^{Jrk}. Neither *Clk*^{Jrk} nor *cyc*^{02} mutation affected *Crz* expression in both larval CNSs and adult DLP cells (Fig. 2-10).

The heterodimeric CLK:CYC complex is known to be a functional unit that activates transcription of target genes--notably *period* (*per*) and *timeless* (*tim*), whose

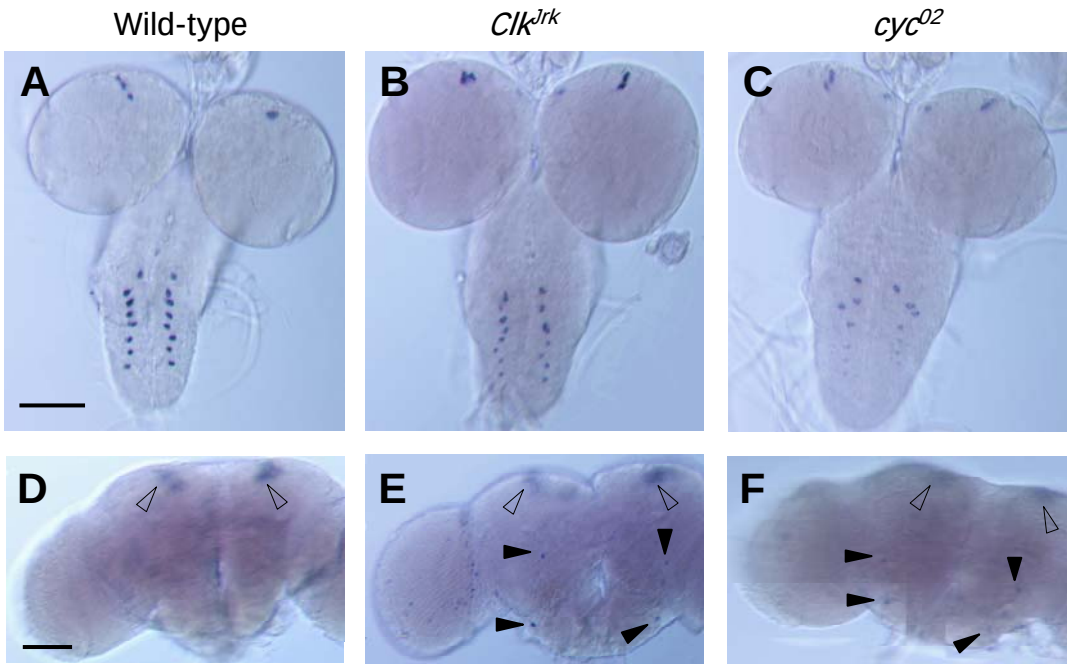

Figure 2-10. *Dm-Crz* mRNA expression in the CNSs of clock mutants. **(A-C)** Larval CNSs. (A) wild-type. (B) Clk^{Jrk} (n=6). (C) cyc^{02} (n=6) mutant. **(D-F)** Anterior view of adult brains. Two pairs of ectopic *Crz*-expressing cells in both clock mutant brains are indicated by solid arrowheads (n=16 for Clk^{Jrk}, and n=4 for cyc^{02}). DLP neurons (open arrowheads) are out of focus here. Scale bar: 100 μm.

expressions are severely reduced in *Clk*^{Jrk} and *cyc*^{0} mutants (reviewed by Stanewsky, 2002). In this context, our foregoing results suggest that CLK and CYC proteins cooperatively suppress *Crz* transcription only in the ectopic cells just described. Although CLK:CYC could act as a direct repressor for *Crz* expression, it would also be possible that ectopic *Crz* expression in *Clk*^{Jrk} and *cyc*^{02} mutants results indirectly from the reduction of *per* and *tim* expression in the same genetic backgrounds. However, ectopic *Crz* expression sites were not detected in *per*^{01} and *tim*^{01} mutants (not shown; at least 5 CNSs were examined for each mutant), suggesting that cell-specific negative regulation of *Crz* expression by CLK:CYC is independent of PER or TIM.

It is well documented that the CLK:CYC heterodimer activates downstream target genes through direct binding to its cognate E-box sequence (CTCGTG) in target promoters (*e.g.*, Hao et al., 1999). Although molecular mechanisms underlying negative regulation by CLK:CYC are unknown, it is conceivable that such regulation is also mediated by the direct binding of CLK:CYC to the E-box. Manual scanning of 5'-upstream regulatory region of the *Crz* gene, however, did not detect any consensus E-box, indicating an indirect regulation of *Crz* by CLK:CYC, as is the case for the *Pdf* gene (Park et al., 2000).

Anatomical relationship between Crz and Pdf neurons

In the course of analyzing *Crz* expression, we noticed that somata of Crz neurons in adult brains (*i.e.*, DLP neurons, Fig. 2-4D, E) could be in the vicinity of nerve terminals stemming from small ventro-lateral neurons (s-LNv), which express *per*, *tim*, and *Pdf* (reviewed by Stanewsky, 2002). To assess the anatomical relationship between

these peptidergic neurons, wild-type adult brains of *D. melanogaster* were doubly labeled by anti-Crz and anti-PDF. As shown in figure 2-11A, DLP cell bodies are indeed positioned near *Pdf*-nerve terminals. In order to obtain better views of such relationship, we performed double labeling in which *Pdf*-neurons were marked by *Pdf* promoter-driven mCD8-*GFP* expression, whereas *Crz*-neurons were labeled by anti-CAP. Despite subtle variability among brain specimens, overall results clearly show that *Pdf* axon terminals are intimately associated with neurites originating from DLP somata (Figs. 2-11B, C, n=13), suggesting potential neuronal interactions between these two kinds of neurochemically differentiated cells. However, the question as to whether DLP neuronal activities are postsynaptically modulated by *Pdf* neuronal inputs remains elusive. In this regard, it would be interesting to determine whether PDF receptor is expressed in the Crz neurons (Hyun et al., 2005).

V. Discussion

Crz expression in other insect groups

In this report, we show that Crz-immunoreactivities are restricted to 24 neurons in the larval CNS (8 in the brain and 16 in the ventral nerve cord) and 12-16 neurons in the pars lateralis of the adult brain in *Drosophila*. Such *Crz* expression patterns are comparable to Crz-like immunoreactive patterns reported for the blow fly *Phormia terraenovae* (Cantera et al., 1994), suggesting similar *Crz* gene's functions among distantly related fly species. By comparison, in the wax moth *Galleria mellonella*, *Crz* mRNAs are localized in a cluster of four lateral neurosecretory cells in each protocerebral

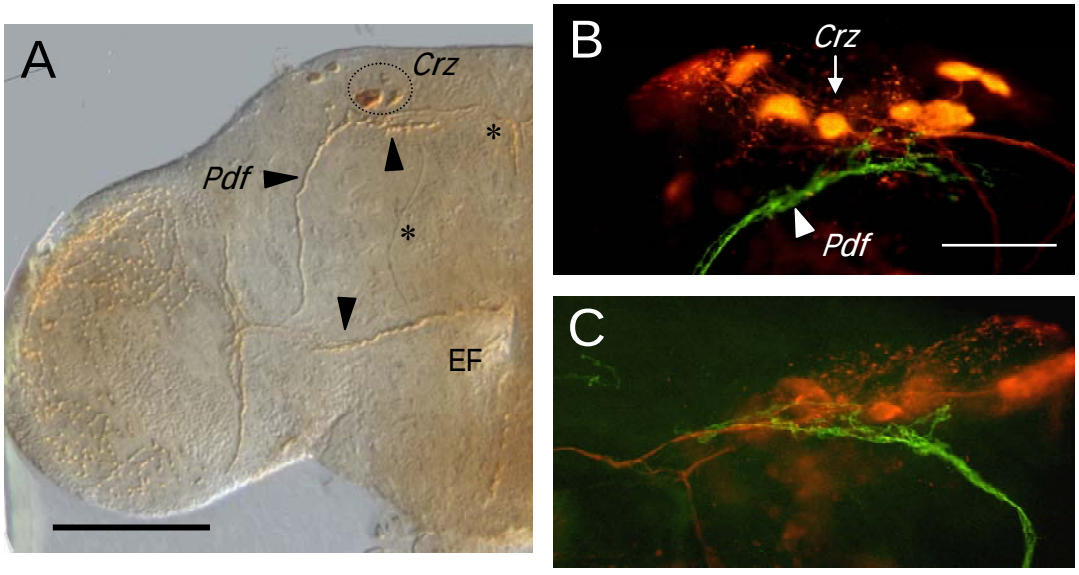

Figure 2-11. Anatomical relationship between *Pdf*- and *Crz*-neurons in the adult brain. **(A)** Colorimetric immunostaining of the adult brain mediated by simultaneous application of anti-Crz and anti-Pdf (n=5). A subset of Crz neuronal cell bodies (circle) is located in the vicinity of Pdf-nerve terminals (black arrowhead) within the dorso-posterior protocerebrum. Crz-immunoreactive axons are indicated by stars. Scale bar: 100 µm. **(B, C)** Double-labeling of *Pdf*- and *Crz*-neurons in adult progeny obtained from [*Pdf-gal4* x *UAS-mCD8-GFP*] cross. *GFP*-reported *Pdf* axon terminals are shown in green, and anti-CAP-mediated immunofluorescent *Crz* neurons are shown in red. Images were acquired at the same focal plane. This type of neuroanatomical association suggests that these two peptidergic neurons might form a functional neural network. Scale bar: 40 µm.

hemisphere, but none in the ventral ganglia (Hansen et al., 2001). Similar pattern of Crz neurons is also observed in the honey bee *Apis mellifera* (Verleyen et al., 2006). In the American cockroach (Dictyoptera), there are *ca*. 10 Crz-like immunoreactive lateral neurosecretory cells in the protocerebrum, whose fibers project to the ipsilateral corpora cardiaca (Veenstra and Davis, 1993). Additional Crz-like immunoreactive cells are detected in the thoracic and abdominal neuromeres, at the base of the optic lobes, in the deuto- and tritocerebrum and subesophageal ganglion. Whether these immunosignals are specific to Crz are unknown, in part because *in situ Crz* mRNA localization was not performed in parallel for this insect.

The presence of Crz-like immunoreactive neurons has also been observed in other major insect orders, including Zygentoma, Hymenoptera, Lepidoptera, and Hemiptera, except for the order of Coleoptera (Tanaka 2000b; Roller et al., 2003). Although Crz-like immunoreactive patterns are more-or-less variable among different insect groups, a subset of Crz-like immunoreactive neurons is consistently found in the pars lateralis of the protocerebrum (Roller et al., 2003). Since the retrocerebral complex (CC+CA) is a consensus target for these lateral neurosecretory cells, we speculate that they are likely to be homologous to larval DL and adult DLP neurons in *Drosophila*.

Putative Corazonin functions in *Drosophila*

Although *Crz* gene functions in *Drosophila* remain elusive, multiple roles played by this gene could be inferred from its expression patterns (*cf*. Nässel, 2002). First, Crz-immunoreactive terminals at the neurohemal releasing sites indicate that Crz acts as a neurohormone. Such neurohormonal function was reported in the moth, *Manduca sexta*

in which Crz is released into the hemolymph just before the onset of ecdysis motor program and induces the release of eclosion triggering hormone from the Inka cells, which in turn stimulates ecdysis behavior (Kim et al., 2004). Second, Crz is also likely to play a role as a neuromodulator or neurotransmitter that influences downstream neuronal activities, since Crz-immunoreactive axons also terminate within the CNS. Third, *Crz* expression in the VNC and dorso-medial brain, which are found to occur only in larval stages, suggests that Crz produced from these neurons mediates distinct functions in juveniles.

Crz neurons could be associated with the biological clock as a putative target of pacemaking neurons. It was previously shown that *Pdf* expressing s-LNv's is essential for normal circadian locomotor activity rhythms (Renn et al., 1999). The s-LNv cells project dorsally to the superior protocerebrum, and it has been postulated that PDF peptides released from these nerve terminals act locally in order to deliver circadian messages to this brain region (Helfrich-Förster, 1998; Park et al., 2000; Williams et al., 2001; Ping et al., 2003). Interestingly, our data suggest that Crz-expressing DLP neurons are downstream of the PDF-sLNv neurons, thus possibly forming a neural circuitry controlling biological clock function. If so, then, Crz neurons may receive neuronal input from the PDF-sLNv neurons, thus performing functions associated with certain aspects of the biological clock.

Crz or Crz-containing DLP neurons may have a function related to photoperiodic time measurement. Shiga et al. (2003) reported that surgical ablation of Crz-like immunoreactive neurosecretory cells in *M. sexta* suppressed pupal diapause under short-day conditions (*e.g.*, 10-h light:14-h dark). From these data, the authors proposed that

Crz-immunoreactive neurons might be a component of the photoperiodic clock that measures lengths of day (or night). In *D. melanogaster*, female ovarian diapause is also regulated by the lengths of photophase (or scotophase) (Saunders et al., 1989). Based on these studies, it is tempting to propose that *Crz*-expressing DLP neurons in *Drosophila* may be an element of the photoperiodic clock that monitors seasonal changes of photoperiodism, thereby contributing to seasonal adjustment of various physiological processes.

Chapter Three

Programmed Cell Death Mechanisms of Crz-Expressing Neurons in Drosophila melanogaster

*This chapter was modified from Choi et al., 2006 and additional results were also supplemented.

Youn-Jeong Choi, Gyunghee Lee, Jae H. Park. (2006). Programmed Cell Death Mechanisms of Identifiable Peptidergic Neurons in *Drosophila melanogaster*. *Development* 133:2223-2232.

In this paper I cooperated to discover the idea searching for papers, generated most data, wrote a draft, co-worked to edit the manuscript, and worked for publishing.

I. Abstract

The molecular basis of programmed cell death (PCD) of neurons during early metamorphic development of the central nervous system (CNS) in *Drosophila melanogaster* is largely unknown, in part due to the lack of appropriate model systems. Here we provide evidence showing that a group of neurons (vCrz) that express the neuropeptide *Corazonin* (*Crz*) gene in the ventral nerve cord of the larval CNS undergo programmed death within 6 hours after the onset of metamorphosis. The death was prevented by targeted expression of caspase inhibitor *p35*, suggesting that these larval neurons are eliminated via a caspase-dependent pathway. Genetic and transgenic

disruptions of ecdysone signal transduction involving ecdysone receptor-B (EcR-B) isoforms suppressed vCrz death, whereas transgenic re-introduction of either EcR-B1- or B2-isoform into the *EcR-B*-null mutant resumed normal death. Expression of *reaper* in vCrz neurons and suppression of vCrz cell death in a *reaper*-null mutant suggest that *reaper* functions are required for the death, while no apparent role was found for *hid* or *grim* as a death promoter. Our data further suggest that *diap1* does not play roles as a central regulator of the PCD of vCrz neurons. Significant delay of vCrz cell death was observed in mutants lacking *dronc* or *dark* functions, indicating that formation of an apoptosome is necessary, but not sufficient, for timely execution of the death. These results suggest that activated ecdysone signaling determines precise developmental timing of the neuronal degeneration during early metamorphosis, and that subsequent *reaper*-mediated caspase activation occurs through a novel DIAP1-independent pathway.

II. Introduction

In holometabolous insects that develop through complete metamorphosis, significant behavioral changes are observed from juveniles to adults. For instance, *Drosophila* larvae display simple behaviors including feeding, crawling, and defensive thrashing, whereas adult flies lead more complicated life styles such as foraging, flying, mating, and aggression in order to survive and fulfill successful reproduction. This type of behavioral transition is accompanied by substantial reorganization of the nervous system, which establishes adult-specific neural circuitry, thereby accommodating new life styles (Truman et al., 1993; Levine et al., 1995; Consoulas et al., 2000; Tissot and Stocker, 2000). During metamorphosis, larval neurons face mainly two different fates: remodeling or programmed

cell death (PCD). The former is a recycling process of persistent neurons and is characterized primarily by significant modifications in synaptic architectures, resulting from withdrawal of larval-specific connections, followed by reconnection with new targets (*e.g.,* Kraft et al., 1998; Lee et al., 2000b). By comparison, other neurons are scheduled to die via developmentally regulated genetic programs, since their functions are no longer required for ensuing life stages.

Several studies have implicated ecdysone as a central endocrine regulator that initiates genetic programs orchestrating overall reorganization processes of the insect nervous system during metamorphosis (Truman et al., 1993). For instance, genetic analyses have shown that ecdysone receptor activities are essential for cell-autonomous remodeling of mushroom body γ-neurons and SCP-immunoreactive (IR) neurosecretory cells (Schubiger et al., 1998, 2003; Lee et al., 2000b). In addition to the remodeling, ecdysone has been shown to cause apoptosis of obsolete larval neurons. In a moth, identified motoneurons innervating larval proleg muscles are degenerated in response to a prepupal ecdysone surge (Weeks, 2003, and references therein). Treatment of isolated motoneurons with ecdysone *in vitro* also causes the death, suggesting that ecdysone directly induces a cell-autonomous death program (Streichert et al., 1997).

Although the underlying molecular mechanisms for post-embryonic neuronal PCD are largely unknown, extensive genetic studies have identified key molecular players that either enhance or suppress PCD occurring in developing *Drosophila* embryos and compound eyes (reviewed in Cashio et al., 2005; Kornbluth and White, 2005). Apoptotic death is a direct consequence of massive destruction of cellular components mediated by specialized proteolytic enzymes, caspases (reviewed in Salvesen and Abrams, 2004). In

living cells, the caspases are inactivated and/or degraded by the action of *Drosophila* inhibitor of apoptotic protein 1 (DIAP1) through forming a complex with caspases (Meier et al., 2000; Muro et al., 2002; Wilson et al., 2002). When cells are challenged with death stimuli, death activators (collectively referred to as RHG) encoded by *reaper* (*rpr*), *head involution defective* (*hid*) and *grim* which are defined by deficiency *Df(3L)H99* (White et al., 1994; Grether et al., 1995; Chen et al., 1996), bind to DIAP1, liberating caspases from the DIAP1-caspase complexes, resulting in the activation of caspases (Wang et al., 1999b; Goyal et al., 2000). Physical interactions between RHG proteins and DIAP1 are also known to downregulate DIAP1 levels via ubiquitin-mediated self-degradation of DIAP1, which further ensures an irreversible death pathway (Ryoo et al., 2002; Yoo et al., 2002). Products of two additional pro-apoptotic genes, *sickle* and *jafrac2*, are also implicated as DIAP1 antagonists (Christich et al., 2002; Srinivasula et al., 2002; Tenev et al., 2002; Wing et al., 2002).

Fundamental molecular cell death mechanisms just described appear to be conserved in the tissues that require ecdysone for their death at a precise developmental stage. Larval salivary glands are degenerated in response to an ecdysone stimulus during metamorphosis in which ecdysone activates transcription of *rpr* and *hid* directly, or indirectly via ecdysone-responsive transcription factors such as *Broad Complex* (*BR-C*), *E74* and *E93* (Jiang et al., 2000; Lee et al., 2002b). Premature destruction of these tissues throughout larval growth is prevented by DIAP1, until ecdysone-induced RPR or HID proteins overcome the inhibitory action of DIAP1 (Yin and Thummel, 2004).

During the prepupal stage, a number of unwanted larval neurons are removed from the CNS in *Drosophila*. Neuronal degeneration is particularly prominent in the abdominal

ganglion, leading to significant shrinkage of this neuropil (Truman, 1990; Truman et al., 1993). Although ecdysone is an important developmental cue for the PCD of certain motoneurons in a moth (Weeks, 2003), ecdysone functions in the PCD of obsolete larval interneurons in the CNS are largely unexplored. Here we show that peptidergic neurons expressing *Corazonin* (*Crz*) in the ventral nerve cord (vCrz) are programmed to die during early metamorphosis in *Drosophila*. Our data further suggest that activated ecdysone signaling induces *rpr* expression, and subsequent activation of caspases does not involve *diap1* functions.

III. Materials and methods

Drosophila strains and genetic manipulations

Canton-S was used as a wild-type. For visualization of Crz-neurons, a *Crz-gal4* driver (see below) was crossed to a *UAS-lacZ* or *UAS-mCD8-GFP* reporter, which respectively produces GAL4-inducible β-galactosidase or membrane-targeted green fluorescence protein (GFP) (Phelps and Brand, 1998; Lee and Luo, 1999).

Double homozygous lines carrying both *Crz-gal4* and *UAS-lacZ* (or *UAS-mCD8-GFP*) transgenes were generated by genetic crosses. These flies were crossed to the following *UAS* responders to produce various types of transgenic manipulations; *UAS-EcR-A*, *UAS-EcR-B1*, and *UAS-EcR-B2* to overexpress specific Ecdysone Receptor (EcR) isoforms (Lee et al., 2000b); *UAS-EcR-B1*^{F645A} and *UAS-EcR-B1*^{W650A} to express dominant negative (DN) forms of the EcR-B1 (Cherbas et al., 2003, Fig. 3-1); *UAS-diap1* (Hay et al., 1995) to produce inhibitors of apoptosis; *symUAS-diap1*^{RNAi} to knockdown

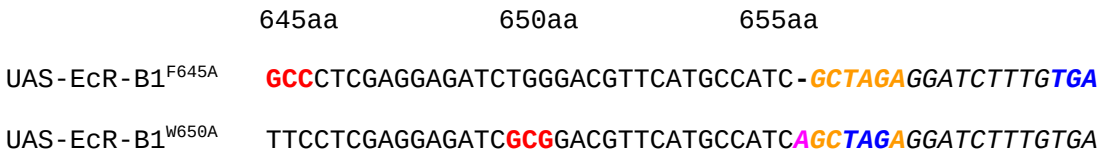

Figure 3-1. Sequence analysis of *EcR-B1* dominant negative mutants. Each construct was generated from the template *EcR-B1* cDNA which is truncated after 655 amino acid (aa) position (EcR-B1Δ655, Cherbas et al., 2003). The truncated EcR-B1 behaves similarly as its wild type. The codon (TTC) encoding phenylalanine at 645 aa is replaced by alanine codon (GCC in red) in *UAS-EcR-B1*^{F645A} construct, and the codon (TGG) encoding tryptophan at 650 aa is replaced by alanine codon (GCG in red) in *UAS-EcR-B1*^{W650A} construct. Letters in Italic is UAS vector. Six-base sequences in orange are the restriction enzyme sites for cloning and the predicted stop codons are presented in blue. The base A in pink from *UAS-EcR-B1*^{W650A} construct is not present in the original *EcR-B1* sequence.

diap1 mRNA (Huh et al., 2004) ; *UAS-cyt-c-d* and *UAS-cyt-c-p* to express cytochrome c (Arama et al., 2006); *UAS-Buffy* to express anti-apoptotic Bcl-2 family protein (Quinn et al., 2003). In some experiments, a double homozygous *Crz-gal4*, *UAS-p35* line was used for inhibition of caspases (Hay et al., 1995). Two *dco* (*discs overgrown*) alleles, dco^{3} and dco^{18}, were used to determine ecdysone effect on vCrz PCD (Sehnal and Bryant, 1993). ap^{4} (*apterous*) mutant was used for analyzing Juvenile Hormone effect on vCrz PCD (Altaratz et al., 1991).

For *EcR-B*-null mutant, $EcR^{31}/CyO, y^{+}$ was crossed to $EcR^{99}/CyO, y^{+}$, from which F1 larvae lacking y^{+} marker (EcR^{31}/EcR^{99}) were collected and dissected after completion of apolysis as described (Schubiger et al., 1998, 2003). To rescue the *EcR-B* mutation, *y w*; EcR^{31}/CyO, y^{+}; *UAS-EcR-B1* (or *B2*) were mated with *y w*; EcR^{99}/CyO, y^{+}; *Crz-gal4* to obtain EcR^{31}/EcR^{99}; *UAS-EcR-B1* (or *B2*)/*Crz-gal4*. The *EcR-A*-null (EcR^{112}/EcR^{M554fs}) and *EcR-B1*-null (EcR^{Q50st}/EcR^{31}) mutants were produced as described previously (Bender et al., 1997; Carney et al., 2004).

The following deficiencies were used to generate *rpr*- and *hid*-null mutations; *Df(3L)XR38*, *Df(3L)H99*, and *Df(3L)X14* (for short, *XR38*, *H99*, and *X14*, respectively). Homozygous deletion of the *rpr* locus was obtained by combining *H99* with *XR38* in trans as described (Peterson et al., 2002). Flies lacking *hid* functions were produced by transallelic combination of *H99* (or *X14*) with hid^{05014} allele (Grether et al., 1995). Although most of the *hid* mutants are embryonic lethal, a few escapers enabled us to assess vCrz neuronal death in these mutants (Peterson et al., 2002).

Null mutations of caspase-encoding *dronc* gene were obtained by transallelic combinations of $dronc^{I24}$ (or $dronc^{I29}$) with $dronc^{51}$ (Chew et al., 2004, Xu et al., 2005).

Two *thread* (*th*, a.k.a. *diap1*) alleles, th^4 (loss-of-function) and th^{SL} (gain-of-function), were used in some experiments (Lisi et al., 2000). $dark^{CD4}$ was used as a *Drosophila Apaf-1-related killer* (*dark*) mutation, $dcp\text{-}1^{prev1}$ as a *Drosophila* caspase-1 (*dcp-1)*-null mutation, and $dredd^{B118}$ and $dredd^{L23}$ as a *dredd* mutation. The mutant alleles in this study are summarized in Table 3-1.

Transgenic lines

To construct *P*-element containing *Crz* promoter fused to the *gal4* coding sequence (hereafter referred to as *Crz-gal4*), a genomic region upstream of the *Crz* gene (-1155 to +78 relative to the transcription start site +1, Choi et al., 2005) was amplified by PCR, and subcloned into pBluescript at the *Sma* I site, from which an *Xba* I-*EcoR* I fragment was inserted into pPTGAL vector (Fig. 3-2A, Sharma et al., 2002). For *rpr-gal4* construct, previously defined 1.3-kb *rpr* upstream sequence (Jiang et al., 2000) was inserted into pPTGAL at *Bgl* II/*EcoR* I sites.

For RNAi constructs of *rpr*, *hid*, and *grim*, first each partial cDNA was cloned in pBS-SK (Stratagene) and then transferred to symUAST-w vector (Huh et al., 2004) which will produce a double-stranded RNA of each gene. To generate a *rpr* RNAi construct, a *rpr* cDNA sequence (+55 to +509, +1: transcription start site) was amplified from a *rpr* full length cDNA (Yin and Thummel, 2004) and cloned between *Xho* I and *Pst* I sites of pBS-SK. A *rpr* cDNA was then excised with *Xho* I and *Not* I and inserted to symUAST-w, and the resulting plasmid was re-excised with *Eco*R I to remove an unnecessary part. For a *hid* RNAi, a *hid* cDNA fragment (+311 to +1166, +: transcription start site) was amplified by PCR from a *hid* full length cDNA (Yin and

Table 3-1. Mutant alleles used in this experiment

locus	allele	type of mutation	type of lesion	references
EcR	EcR^{112}	amorphic (A isoform)	deletion by P element mobilization	Carney et al., 2004
	EcR^{M554fs}	amorphic (A, B1, B2)	point mutation, M554 frame shift	Bender et al., 1997
	EcR^{Q50st}	amorphic (B1)	point mutation, Q50 stop codon	Bender et al., 1997
	EcR^{31}	amorphic (B1, B2)	deletion by P element mobilization	Schubiger et al., 1998
	EcR^{99}	amorphic (B1, B2)	deletion by P element mobilization	Schubiger et al., 1998
BR-C	$2Bc^{1}$	amorphic	mutation by EMS in 2B5	Belyaeva et al., 1980
	br^{5}	amorphic	mutation by EMS in 2B5	Belyaeva et al., 1980
	rbp^{5}	hypomorphic	mutation by EMS in 2B5	Belyaeva et al., 1980
dco	dco^{3}	ND	mutation by EMS in 84B-E	Jursnich et al., 1990
	dco^{18}	hypomorphic	mutation by EMS in 84B-E	Jursnich et al., 1990
apterous	ap^{4}	hypomorphic	spontaneous	Ringo et al., 1991
Cell	*XR38*	deletion (*rpr*, *sickle*)	deletion in 75C1,2	Peterson et al., 2002
death	*H99*	deletion (*hid*, *grim*, *rpr*)	deletion in 75C1,2	White et al., 1994
	X14	deletion (*hid*)	deletion in 75C1,2	White et al., 1994
	hid^{05014}	amorphic	P element insertion	Grether et al., 1995
diap1	*Df(3L)brm11*	deletion	deletion in 71F-72D	Brizuela et al., 1994
	th^{4}	amorphic	point mutation, H283Y	Lisi et al., 2000
	th^{SL}	hypermorphic	point mutation, V85M	Lisi et al., 2000
dronc	$dronc^{51}$	amorphic	deletion by P element mobilization	Chew et al., 2004
	$dronc^{I24}$	amorphic	point mutation, W28 stop codon	Xu et al., 2005
	$dronc^{I29}$	amorphic	point mutation, Q53 stop codon	Xu et al., 2005
dark	$dark^{CD4}$	hypomorphic	P element mobilization	Rodriguez et al., 1999
dcp-1	$dcp\text{-}1^{prev1}$	amorphic	deletion by P element mobilization	Laundrie et al., 2003
dredd	$dredd^{B118}$	amorphic	point mutation, R127 stop codon	Leulier et al., 2000
	$dredd^{L23}$	amorphic	point mutation, W458R	Leulier et al., 2000
cyt-c-p	$cyt\text{-}c\text{-}p^{l(2)K13905}$	strong hypomorphic	P element insertion	Arama et al., 2006
cyt-c-d	$cyt\text{-}c\text{-}d^{Z2\text{-}1091}$	amorphic	point mutation, W62 stop codon	Arama et al., 2006
	$cyt\text{-}c\text{-}d^{bln1}$	amorphic	P element insertion	Arama et al., 2006

ND; not determined.

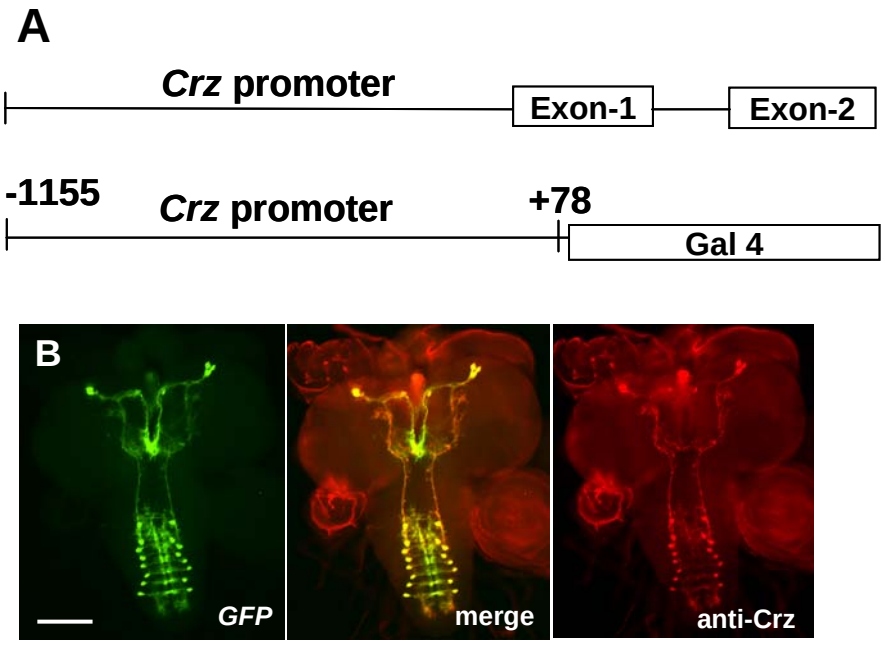

Figure 3-2. Characterization of *Crz-gal4*. **(A)** Schematic illustration of *Crz* promoter region used for *Crz-gal4* line. **(B)** Co-localization (center) of *Crz-gal4*-induced *GFP* expression (left) in Crz-IR neurons (right). Scale bar: 100 μm

Thummel, 2004) and inserted between *Eco*R I and *Sal* I of pBS-SK. A *Eco*R I/*Sal* I fragment was then excised and inserted between *Eco*R I and *Xho* I sites of symUAST-w. For generation of *grim* RNAi, a *grim* cDNA fragment (+2 to +850, +: transcription start site) was amplified by PCR from a nonintronic genomic DNA and inserted between *Xho* I and *Sal* I sites of pBS-SK. A *grim* cDNA was excised with *Xho* I and *Eco*R I and inserted to symUAST-w. The recombinant symUAST-w vector was mixed with pUChsπΔ2-3 helper plasmid (Laski et al., 1986) and injected into the *y w* or w^{1118} embryos for germ-line transformation (Rubin and Spradling, 1982). *Crz-gal4* (S2b, T2a) and *rpr-gal4* (III) lines were used in this study. RNAi lines which are inserted in II and III chromosomes were characterized here.

X-gal histochemistry and immunohistochemistry (IHC)

To detect β-galactosidase expression, dissected CNSs were fixed in 0.2% glutaraldehyde in PBS for 5 minutes at room temperature, washed in PBS three times for 5 minutes each, and then incubated at 37°C overnight in the buffer (10 mM Sodium-phosphate (pH 7.4), 0.15M NaCl, 1 mM $MgCl_2$, 5 mM K·Ferro-CN, 5 mM K·Ferri-CN, 0.1% Triton X-100) containing X-gal (5-bromo-4-chloro-3-indolyl-β-D-galactoside in Dimethylformamide) with the final concentration of 1 mg/ml. The tissues were rinsed in PBS briefly, dehydrated in ethanol, and mounted in glycerol (e.g., Park et al., 2000).

Whole-mount Crz-IHC was performed as described in Chapter 2. The anti-Crz was previously referred to as anti-CAP, which was raised against Crz-Associated Peptide within the precursor (Fig. 2-1). To co-localize EcR-immunoreactivity (IRy) in Crz-neurons, rabbit anti-Crz at 1:500 dilution, and mouse monoclonal anti-EcR-A (15G1a) or

anti-EcR-B1 (AD4.4) at 1:100 dilution (Talbot et al., 1993) were simultaneously applied to the CNSs. The primary antibodies were detected by FITC- or TRITC-conjugated secondary antibodies (Jackson ImmunoResearch) at 1:200 dilution. The specimens were then cleared in 60% glycerol and mounted in Vectashield medium (Vector Laboratory). Fluorescent signals were acquired by Leica TCS confocal microscopy or Olympus BX61 connected with CC-12 camera.

TUNEL (Terminal deoxynucleotidyl transferase-mediated dUTP Nick-End Labeling) assay

TUNEL was performed to detect DNA fragmentation in doomed vCrz neurons using a commercial kit (Deadend^{TM} Fluorometric TUNEL system, Promega). CNSs were fixed in 4% paraformaldehyde in PBS for 30 minutes at room temperature, washed in PBS containing 1% Triton X-100, and then incubated in a reaction containing fluorescein-12-dUTP and terminal deoxynucleotidyl transferase at 37°C for 1 hour. Following termination of the reaction by washing tissues with 2X SSC, the tissues were subjected to Crz-IHC. Both TUNEL- and Crz-immunoreactive (IR) signals were visualized by epi-fluorescence.

Double labeling by *in situ* hybridization (ISH) and IHC

Chromogenic ISH of *Crz* mRNA was performed using digoxigenin (Dig)-labeled cRNA probe as described previously in Chapter 2. Fluorescent ISH using TSA (Tyramide signal amplification) system was employed to detect *rpr* transcripts within Crz neurons (e.g., Zaidi et al., 2000). For this, CNS tissues were first hybridized with dig-

labeled *rpr* cRNA probe, and then the tissues were incubated with anti-Crz (1:150,000) at 4°C overnight. Such an extreme dilution of antibody is necessary since it has been known that immunoreactive signals interefere with *in situ* labeling (Draizen et al., 1999). After rinsing, FITC-conjugated secondary antibody was added to the tissues for 2 hours to obtain Crz-IRy. During the final 30 minutes of the incubation period, horseradish peroxidase-conjugated anti-Dig was added to the incubation. Finally, Cy3-labeled tyramide substrate was added to produce ISH signals as recommended (Renaissance TSA Fluorescence Systems, Perkin Elmer).

20-hydroxyecdysone (20-HE) treatment

To determine ecdysone effect on vCrz PCD, ecdysone feeding assay as well as ecdysone treatment to *in vitro* organ culture were performed. To feed ecdysone to larvae, instant fly food (Carolina Biological Supply Co.) was made with 20-hydroxyecdysone (HE) (Sigma) at a final concentration of 60 μg/ml in 1% ethanol. The progeny (*UAS-EcR-B1/UAS-lacZ:pCrz-gal4/+*) eggs were transfered to instant food containing 20-HE and incubated at 25°C until dissection.

For CNS culture, the mid 3rd instar larval CNS (*Crz-gal4* / *UAS-mCD8-GFP*) was dissected in Schneider's medium (Sigma) and transfered to a 24-well plate containing 500 μl of Schneider's medium with insulin (50 μg/ml), gentamycin sulfate (2 mg/ml), amphotericin (30 μg/ml), and 20-HE (1μg/ml) as modified from Datta (1999) and Emery et al. (1997). Subsequently the plate was placed in a billups-rothenberg modulator incubator chamber, and then 20 psi of O_2 was flushed into a chamber for 2 minutes. The chamber was sealed and kept at 25°C for 2 days. Since *in vivo* system it takes

approximately two days to develop from mid 3rd instar larvae to 12 hours after puparium formation (APF) when vCrz PCD is completed, 2 day incubation was chosen. For whole organ culture, whole organs of wandering larvae were obtained by peeling off the larval cuticle, transferred to the same medium as above, except for a higher dose of 20-HE (3 μg/ml), and incubated at 25°C for 20 hours. Since it takes approximately 20 hours to develop from wandering larvae to 12 hours APF *in vivo* system, 20-hour incubation was chosen. The fluorescent signals were visualized through a fluorescence stereomicroscope (Leica MZ16FA).

Juvenile hormone (JH) application

To investigate the effect of JH, we applied JH to the wild-type animals in two different ways. First, methoprene (Chemservice co.), which is a synthetic JH agonist, was topically applied to wandering larvae and white prepupae as described in Dubrovsky et al. (2000). Methoprene liquid is diluted at a final concentration of 150 μg/μl in acetone (Sigma). 0.2 μl of methoprene stock was topically applied to each animal. Only acetone was also applied to animals as a control. CNSs were dissected at the time when normally vCrz PCD is completed and processed to immunohistochemistry with anti-CAP. The other way is that animals were fed with food containing methoprene. Methoprene stock was made in 95% ethanol and was diluted in food medium at a final concentration of 1.07 mg/ml (Restifo and Wilson, 1998). Only ethanol was added to the medium for a control. Wild-type 1st instar larvae were collected with a layer of food and transferred to methoprene-treated food. To eliminate over-crowding, 40 larvae were transferred to a vial. The animals were incubated at 25°C until they reached at 12 hours APF.

IV.Results

Programmed death of vCrz neurons

Spatial *Crz* expression patterns change significantly during metamorphosis as previously described in Chapter 2. In third-instar larval CNSs, *Crz* gene products are detected in three pairs of DL neurons and in a pair of DM neurons in the brain, and eight pairs of symmetrically positioned neurons (vCrz) in the ventral nerve cord (VNC) (Fig. 3-3 A, C). In the CNSs taken from pupae aged for ~36 hours APF, *Crz* transcripts are found in 6-8 cells per hemi-brain (Fig. 3-3B), but none in the VNC. When IHC was performed at an earlier stage (12-24 hours APF), protocerebral Crz-IR patterns remain unchanged from their larval patterns (arrowheads in Fig. 3-3D), while no vCrz neuron are visible (arrow in Fig. 3-3D). These temporal expression data suggest that adult-like protocerebral Crz-neurons have been established between 24-36 hours APF, while vCrz expression disappeared within 12-24 hours APF.

The loss of vCrz expression could be due to programmed death of these neurons. We tested this possibility by transgenic rescue of cell death using the *gal4/UAS* system (Phelph and Brand, 1998). As a preliminary step, we tested fidelity of the *Crz-gal4* driver. As shown in Fig. 3-2B, *Crz-gal4*-driven GFP signals are completely overlapped with Crz-IRy in third-instar larval CNS. *LacZ*-reporter expression also faithfully recapitulates endogenous *Crz* expression in early pupal stages (Fig. 3-4), suggesting that

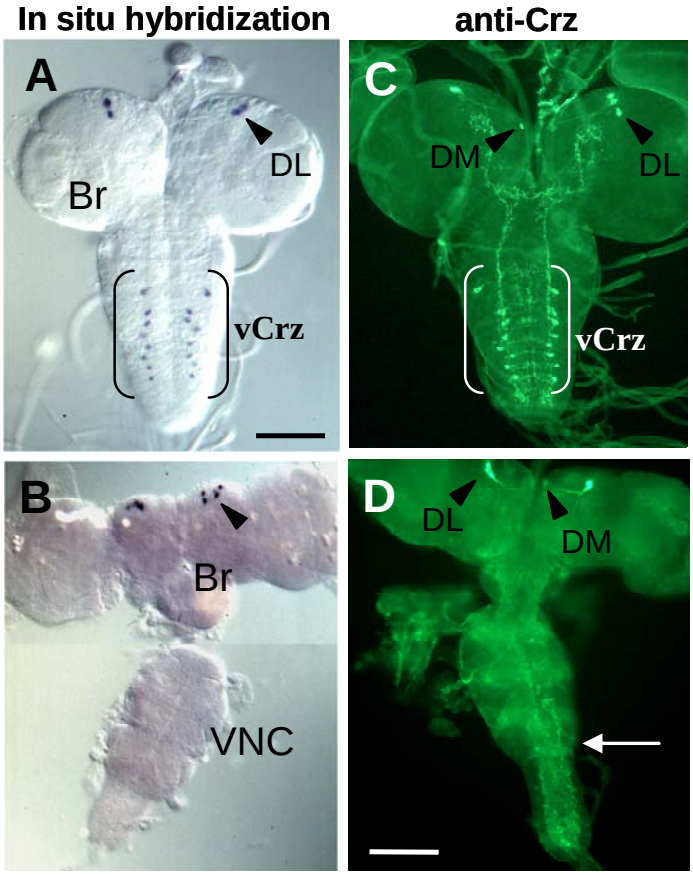

Figure 3-3. *Crz* expression in the CNS during metamorphosis. **(A, B)** ISH of *Crz* mRNA. (A) Third-instar larval CNS, showing three pairs of DL-neuron in the brain (Br), and eight pairs of vCrz neurons (brackets). (B) Pupal CNS at approximately 36 hours APF. The number of neurons in the brain (arrowhead) is found to be 6-8 per lobe, whereas none of vCrz neurons are detectable. **(C, D)** Crz-IR neurons in third-instar larval CNS (C), or pupal CNS at 12-24 hours APF (D). Consistent with the ISH results, no Crz-IR neurons are detectable in the VNC of the pupal CNS (arrow). At least five specimens were processed for each panel. Scale bars: 100 μm.

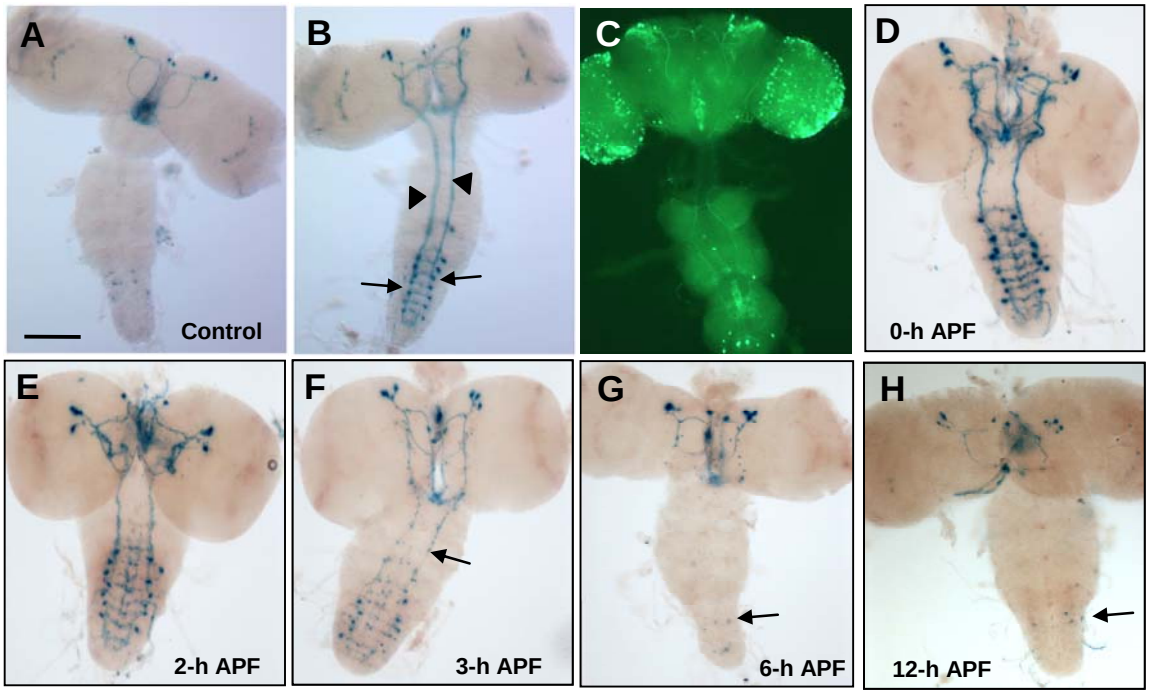

Figure 3-4. Rescue of vCrz-cell death by transgenic expression of *p35*. **(A)** Control 1-day old pupa (*UAS-lacZ*/+; *Crz-gal4*/+). **(B)** One-day-old pupa expressing *p35* in Crz neurons (*UAS-lacZ*/+; *Crz-gal4*, *UAS-p35*/+). Persistent vCrz neuronal somata and ascending projections are designated by arrows and arrowheads, respectively. **(C)** Two-day-old adult CNS expressing *p35* in Crz neurons (*mCD8-GFP*/+;;*Crz-gal4*, *UAS-p35*/+). A few vCrz neurons still survive after eclosion. **(D-H)** Progressive removal of *lacZ*-marked vCrz neurons (*UAS-lacZ*/+; *Crz-gal4*/+) during metamorphosis. White prepupae were aged at 25°C for durations designated in each panel, and then processed for X-gal staining. (D) White prepupa (n=5). (E) 2 hours APF (n=6). (F) 3 hours APF (n=4). Arrow points to discontinued projection. (G) 6 hours APF (n=9). Faint dots (arrow) most likely come from residual β-galactosidase activity (not from live cells). (H) 12 hours APF (n=5). Residual X-gal staining products indicated by an arrow occasionally linger up until 24 hours APF. Scale bar: 100 μm.

the 1.2-kb upstream sequence contains *cis*-elements necessary for appropriate control of spatial and developmental *Crz* expression.

Using *Crz-gal4* driver, we induced expression of a caspase inhibitor, *p35* (Hay et al., 1995), to test whether *p35* can prevent cell death, thereby maintaining *Crz* expression in pupal VNC. Thus, a *Crz-gal4*, *UAS-p35* double homozygous strain was crossed to the *UAS-lacZ*, and then the progeny were processed for X-gal histochemistry. Remarkably, all vCrz neurons marked by *lacZ* expression are persistently present at 24 hours APF (Fig. 3-4B vs. A). At even 2-day-old adult stage (Fig. 3-4C), partial sets of vCrz neurons are still detectable and undergo significant remodeling during development. These data strongly support that the loss of vCrz expression during pupal development is due to caspase-dependent cell death, not due to transcriptional silencing of the *Crz* gene.

Developmental timing of vCrz neuronal death

To determine the developmental clock of the vCrz neuronal death, *lacZ*-reported *Crz* expression was examined in various prepupal stages. Elimination of vCrz neurons occurs progressively over a 2~6-hour period after pupariation (Fig. 3-4D-H). At 2 hours APF, 1-2 cells are undetectable (Fig. 3-4E), suggesting that execution of the death has begun in some cells at around this stage. At 3 hours APF, *ca.* 40% of the neurons are lost in a random fashion, and staining in the projections is fainter and discontinuous, leaving broken line-like appearance (arrow in Fig. 3-4F). This perhaps reflects phagocytic elimination of non-functional cellular components possibly by glial cells (e.g., Sonnenfeld and Jacobs, 1995; Watts et al., 2004). At 6 hours APF, most X-gal signals are undetectable, except for a few faint dots (arrow in Fig. 3-4G). This type of signals,

which most likely reflects residual β-galactosidase activity, was seen in some tissues taken even after 12 hours APF (arrow in Fig. 3-4H).

Suppression of cell death by *p35* suggests that vCrz neurons die through the activation of caspases. Another hallmark of the apoptosis is degradation of genomic DNA into nucleosomal units, which is catalyzed by a caspase-activated DNase (Wyllie, 1980; Enari et al., 1998). To determine whether such a biochemical event occurs in doomed vCrz neurons, we performed TUNEL to detect fragmented DNAs (Prochazkova et al., 2003). Since our foregoing data imply that pro-apoptotic machinery comes into play almost immediately after pupariation (Fig. 3-4), 0-3-hour-old prepupal CNSs were processed for TUNEL, followed by Crz-IHC. As a result, TUNEL signals are detected in ~4% of total vCrz neurons examined (Fig. 3-5). Lack of the signals in other vCrz neurons may be due to unsynchronized onset of the death or inefficient labeling reaction for whole-mounted tissues. Nevertheless, these findings together with the caspase-dependent cell death suggest that vCrz neuronal death occurs in an apoptotic fashion; however, precise determination of the type of cell death (apoptotic vs. autophagic) requires electron microscopic identification of specific cytological markers (Baehrecke, 2003).

Ecdysone signaling initiates the death program in vCrz neurons

Since the beginning of vCrz death is approximately coincident with a surge of ecdysone at pupariation (Riddiford, 1993; Truman et al., 1994), and the ecdysone is a key endocrine signal orchestrating overall metamorphic reformation of the CNS in insects including *Drosophila* (Weeks, 2003), ecdysone could be a developmental cue, activating

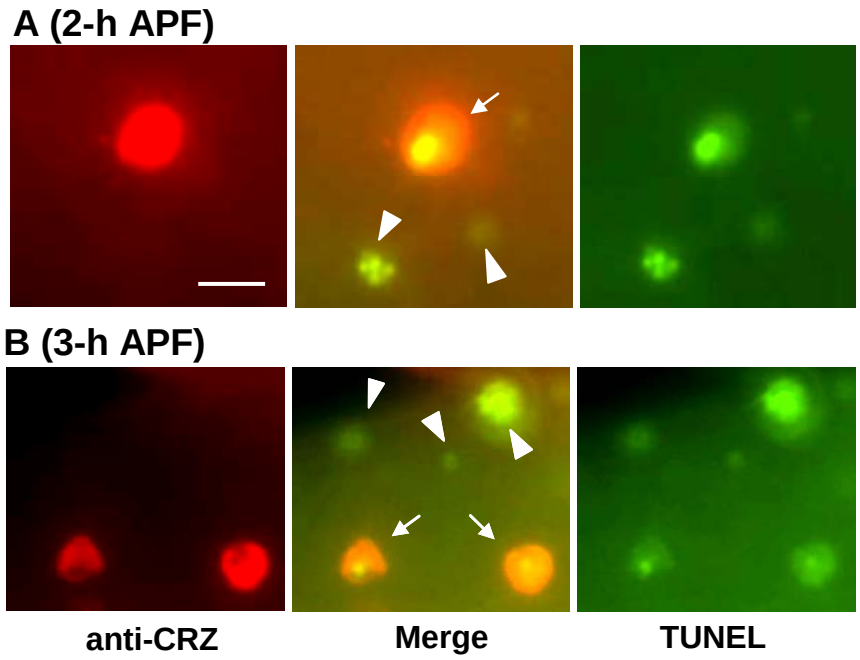

Figure 3-5. DNA fragmentation in vCrz neurons. Wild-type prepupal CNSs at 2 hours APF **(A)** or 3 hours APF **(B)** were subjected to TUNEL assay (right), followed by Crz-IHC (left). These images were merged to show superimposition of the two signals (center). TUNEL-positive vCrz neurons are indicated by arrows and TUNEL signals in non-vCrz cells by arrowheads. Scale bar: 10 μm.

genetic death program in doomed vCrz neurons. It is well documented that the ecdysone signal is transduced by a heterodimeric receptor complex consisting of EcR and ultraspiracle (reviewed in King-Jones and Thummel, 2005). The EcR-encoding gene produces three isoforms (A, B1, and B2) via usage of different promoters and alternative splicing, which share common C-terminal ligand and DNA binding domains but variable N-termini (Talbot et al., 1993).

Recently, Cherbas et al. (2003) developed two dominant-negative (DN) forms of EcR-B1 ($B1^{F645A}$ and $B1^{W650A}$) lacking transcriptional activator functions, but still retaining DNA binding ability (Fig. 3-1). Ectopic expression of these mutant variants effectively blocked ecdysone-led physiological processes, perhaps via competitively inhibiting wild-type receptor functions (Cherbas et al., 2003). This prompted us to test whether ectopic EcR-$B1^{DN}$ expression interferes with normal vCrz cell death. For this, progeny from [*UAS-lacZ*; *Crz-gal4* x *UAS-EcR-B1*^{F645A} (or *UAS-EcR-B1*^{W650A})] were subjected to X-gal histochemistry. Intriguingly, all of the vCrz neurons are detectable at 12 hours APF (Fig. 3-6B, C vs. A), showing that both EcR-$B1^{DN}$s are (equally) capable of blocking vCrz PCD. The results strongly support our hypothesis that EcR-mediated signaling plays a decisive role in the initiation of the death pathway within vCrz neurons.

EcR-B isoforms are major players for vCrz PCD

Distinct temporal expression profiles of each EcR-isoform have suggested that each isoform exhibits developmental stage-specific functions for adult CNS formation during metamorphosis (Truman et al., 1994). For instance, EcR-B-isoforms are involved

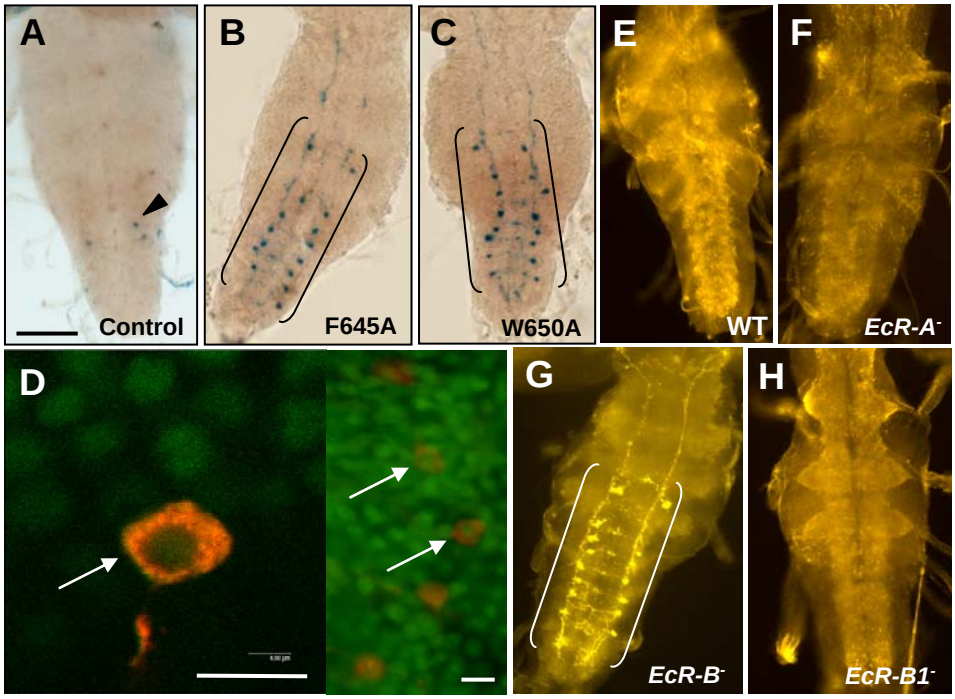

Figure 3-6. Inhibition of vCrz cell death by targeted expression of *EcR-B1* dominant negative forms. CNSs were dissected at 12 hours APF and processed for X-gal staining. **(A)** Control (*UAS-lacZ/+*; *Crz-gal4/+*). An arrowhead indicates the staining from residual β-galactosidase activity. **(B)** *UAS-lacZ/+*; *Crz-gal4/UAS-EcR-B1*^{F645A} (n=4). **(C)** *UAS-lacZ/+*; *Crz-gal4/UAS-EcR-B1*^{W650A} (n=4). Live vCrz neurons are shown within the brackets. **(D, left)** A confocal image showing nuclear EcR-B1-IRy (green) in a vCrz neuron (orange, arrow) at white prepupal stage of wild-type. **(D, right)** An independent specimen showing two vCrz neurons containing EcR-B1-IRy (arrows). **(E-H)** Crz-IRy in various *EcR* mutants at 12-17 hours APF. (E) Wild-type. (F) *EcR-A* mutant (*EcRM*^{554fs}/*EcR*^{112}). (G) *EcR-B* mutant (*EcR*^{31}/*EcR*^{99}) after completion of apolysis. Survived vCrz neurons are shown in the brackets. (H) *EcR-B1* mutant (*EcR*^{31}/*EcR*^{Q50st}). Scale bars: (A) 50 μm, (D) 10 μm.

in modifications of certain larval neurons during early metamorphosis (Lee et al., 2000b; Schubiger et al., 2003). To determine which types of EcR are involved in vCrz cell death, we examined isoform-specific immunoreactivity in vCrz neurons except for the EcR-B2 due to lack of an available antibody. Consistent with a previous report (Truman et al., 1994), widespread EcR-B1-IRy was observed in white prepupal CNS (Fig. 3-6D), whereas EcR-A-IRy was almost undetectable (data not shown). Furthermore, EcR-B1-IRy was evident in the nuclei of vCrz neurons (Fig. 3-6D), supporting a role of the EcR-B1 as a signal transducer for the PCD of vCrz.

To gain more insight into isoform-specific functions, we examined Crz-IRy in various *EcR* loss-of-function mutants. In animals heterozygous for the *EcR*-null mutant allele (EcR^{M554fs}) lacking one copy of all EcR-isoforms (Bender et al., 1997), Crz-IHC results indicated normal cell death, suggesting that a half dose of the EcR is sufficient for mediating vCrz cell death (data not shown, n>5). Consistent with the absence of EcR-A-IRy, an *EcR-A*-null mutation (EcR^{112}/EcR^{M554fs}) did not affect normal vCrz-PCD (Fig. 3-6F *vs.* E). Therefore, we conclude that EcR-A isoform is not a signal transducer for this type of cellular event.

As documented previously, animals carrying a null mutation for both EcR-B1 and EcR-B2 were generated by a trans-heterozygous combination of EcR^{31} and EcR^{99} alleles (Schubiger et al., 1998). Although most of mutant animals are developmentally arrested during the course of larval growth, a few escapers develop into prepupae (Schubiger et al., 2003), thereby permitting us to assess vCrz cell death in this genetic background. Remarkably, Crz-IHC revealed ~12 vCrz-neurons at stages when vCrz neurons were normally absent (Figs 3-6G, 3-7A vs. 3-6E), suggesting that the death pathway in the

Figure 3-7. Rescue of *EcR-B* mutant phenotype by transgenic expression of *EcR-B1* or *EcR-B2*-isoform. (A) *EcR-B* mutant control (EcR^{31}/EcR^{99}). (B) EcR^{31}/EcR^{99}; *UAS-EcR-B1*/*Crz-gal4*. (C) EcR^{31}/EcR^{99}; *UAS-EcR-B2*/*Crz-gal4*. The histograms indicate percentages of the CNSs showing no cell death (open bar), partial (gray bar), or complete death (black bar). As described in the text, the CNSs were grouped into 'E' (Early), 'I' (Intermediate), or 'L' (Late), depending on their developmental status. Numbers of tissues examined in each category are noted on the right of each bar (N), and mean numbers of vCrz neurons (± s.d.) are in parentheses. The CNSs belonging to the 'E' group were not found in the EcR-B2 rescue group. Representative images taken from the 'I' group are shown in the left. Scale bar: 100 μm.

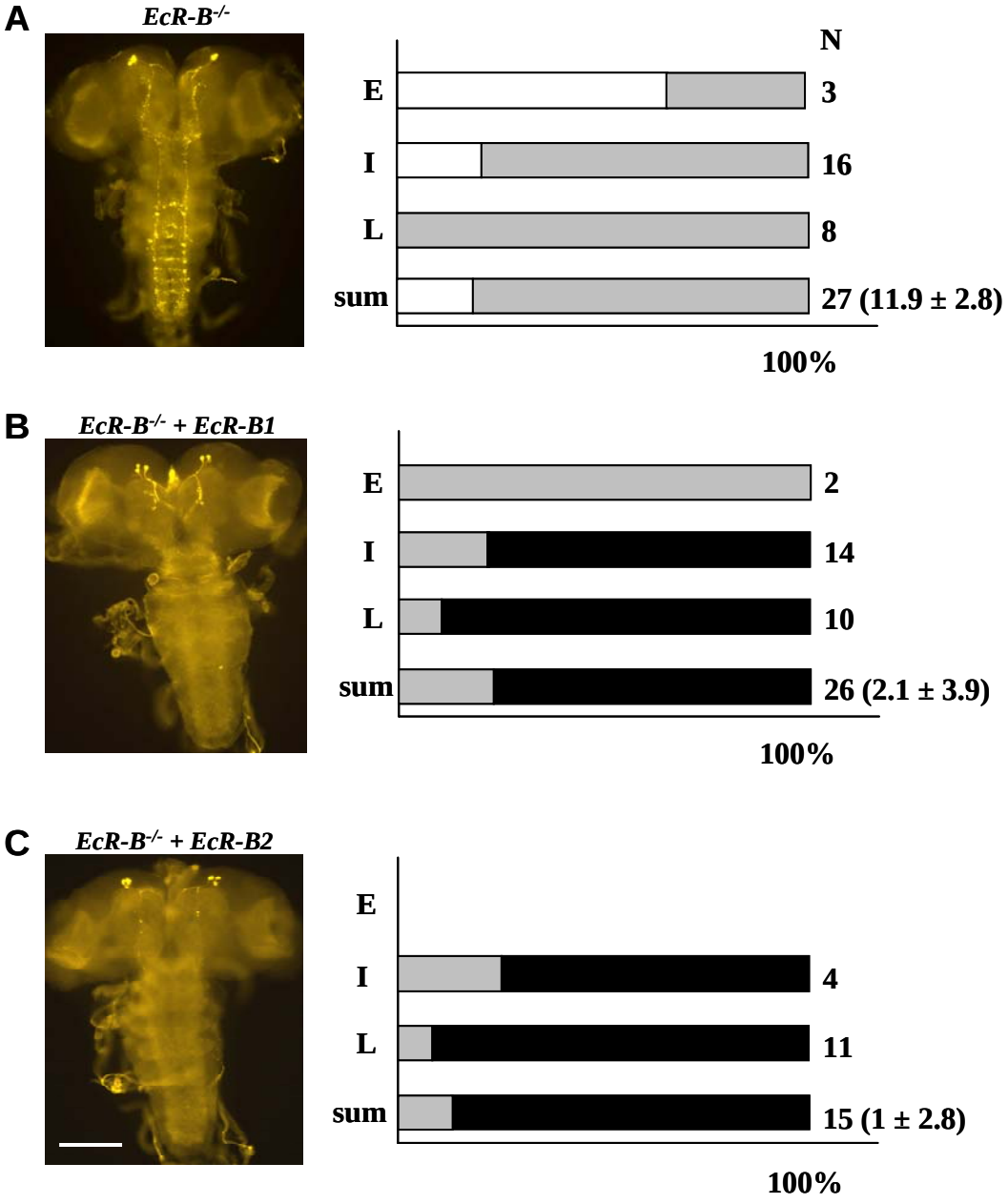
A
EcR-B-/-
N
E
3
I
16
L
8
sum
27 (11.9 ± 2.8)
100%
B
EcR-B-/- + EcR-B1
E
2
I
14
L
10
sum
26 (2.1 ± 3.9)
100%
C
EcR-B-/- + EcR-B2
E
I
4
L
11
sum
15 (1 ± 2.8)
100%

Figure 3-7.

majority of vCrz neurons is unable to proceed in the absence of EcR-B receptors. Therefore, our histological and genetic evidence together demonstrates that EcR-B-isoforms play significant roles for vCrz cell death.

Both EcR-B1 and EcR-B2 are involved in vCrz PCD

We further determined whether both EcR-B1 and EcR-B2 are required or either of them is sufficient for vCrz PCD. To test this, an EcR-B1-specific mutant (EcR^{Q50st}/EcR^{31}) was examined for Crz-IRy (Bender et al., 1997). Surprisingly, complete lack of EcR-B1 showed no deficit in vCrz PCD (Fig. 3-6H). This result may suggest that only EcR-B2 is necessary for the death. Alternatively, EcR-B1 and EcR-B2 may have redundant functions, so that either isoform alone is sufficient for normal PCD.

To address this issue, it would be necessary to analyze *EcR-B2* specific mutants. Since such mutants are unavailable, we employed transgenic rescue of the *EcR-B* mutant. For this attempt, we generated *y w*; EcR^{31}/CyO, y^{+}; *UAS-EcR-B1* (or *EcR-B2*) and *y w*; EcR^{99}/CyO, y^{+}; *Crz-gal4* strains. These lines were crossed with each other and F1-larvae carrying *y* marker (i.e., EcR^{31}/EcR^{99}; *Crz-gal4/UAS-EcR-B1* (or *B2*)) were collected and dissected after complete apolysis (separation of the old cuticle from the underlying epidermis) for Crz-IHC. Since individual CNS morphology was variable depending on their developmental progress, the CNSs were classified as 'Early', 'Intermediate', or 'Late' phenotypes (*cf*. Schubiger et al., 2003). In the 'Early' group, CNSs retain white prepupa-like morphology in which the optic lobes are not yet extended and subesophageal ganglia are broadly attached to the VNC. In the 'Late' group, optic lobes

are highly developed, and areas between the subesophageal ganglia and VNC begin to constrict; this is nearly equivalent to wild-type at 12 hours APF (Truman et al., 1993). In the 'Intermediate' group, CNSs show various levels of development between 'Early' and 'Late' groups.

Crz-IHC revealed significant differences between *EcR-B* mutant and transgene-rescued lines. Complete lack of PCD was seen in 18% of the *EcR-B* mutant CNSs, and partial cell death in the remaining 82% of specimens. Overall, 75% of vCrz neurons did not undergo PCD in the *EcR-B* mutant (Fig. 3-7A). In contrast, expression of *EcR-B1* or *EcR-B2* in the mutant restored complete cell death in 73% or 87% of tissues, respectively, while 4-11 neurons were detectable in the remaining specimen (Fig. 3-7B, C). These data suggest that either EcR-B1 or EcR-B2 alone is capable of mediating PCD of vCrz neurons, and support the idea that EcR-B1 and EcR-B2 have redundant functions for this purpose.

Ecdysone effect on vCrz PCD

To determine ecdysone function for vCrz PCD, we applied the active form of ecdysteroid, 20-HE, to larvae to see whether 20-HE accelerates vCrz PCD. To enhance the susceptibility to 20-HE, we used flies over-producing *EcR-B1* in the Crz neurons, instead of wild type. Thus, a *Crz-gal4*, UAS-*lacZ* was crossed with *UAS-EcR-B1*, and 1st instar larval progenies were fed with food containing 20-HE and collected at different developmental stages (3rd instar larva, 2 hours APF, and 8 hours APF), and then the dissected CNSs were processed for X-gal histochemistry. *Crz* promoter-driven β-gal

expressions revealed no effect of 20-HE on vCrz PCD (data not shown), suggesting no direct effect of ecdysone on vCrz PCD.

It is possible that ecdysone administered through feeding may not reach CNS *in vivo* system. To treat the CNS directly with 20-HE, we cultured the CNS dissected from mid 3rd instar larvae (*UAS-mCD8-GFP/+;;Crz-gal4/+*) in the medium supplemented with 20-HE, and then GFP signals were examined at 2 days after addition of 20-HE to the medium. The CNSs showed little change in Crz expression pattern as well as intensity, indicating that *in vitro* ecdysone treatment did not trigger vCrz PCD. The failure of vCrz PCD in this CNS culture may result from brain injury perhaps created by dissection, or it may be due to developmental arrest of isolated CNS in the culture condition. Thus, to avoid these obstacles, we cultured whole organs of wandering 3rd instar larvae of *Crz-gal4*/*UAS-mCD8-GFP* in the medium containing higher dosage of 20-HE than in CNS-only culture, and GFP signals were visualized after 20-hour incubation. *Crz* promoter-driven GFP expression did not show any sign of vCrz PCD, suggesting that 20-HE is unable to cause cell death in this system. However, we do not know whether our *in vitro* culture condition mimics *in vivo* system because we did not have a positive control. For example, since the salivary gland degeneration has been known to be triggered by ecdysone (Dorstyn et al., 1999), the salivary gland culture should show premature degeneration in our condition. However, we did not test salivary gland cell death yet. As an alternative way to treat with ecdysone, it might be necessary that the medium with 20-HE is replaced with ecdysone-free medium to mimic the natural surge of ecdysone titer during pupation. It will be interesting to see if such an artificial ecdysone peak induces vCrz PCD.

To determine the effect of ecdysone genetically, we employed *dco* (*discs overgrown*) mutants which feature disc overgrowth and prolonged life period during larval stage. In this mutant, the overall ecdysteroid titer was reduced, and the surge that is normally observed at pupariation was not detectable. It is not known yet why *dco* mutation reduces the level of ecdysteroid (Sehnal and Bryant, 1993). Using this mutant we determined whether lack of ecdysone peak suppresses vCrz PCD. Since the animal possessing the heteroallelic combination of two *dco* alleles, dco^{3} and dco^{18}, can survive up to pupal apolysis (Jursnich et al., 1990; Sehnal and Bryant, 1993), we tested vCrz PCD in these mutants. As a result, *Crz*-IR cells in dco^{3}/dco^{18} mutant were undetectable at 6 hours APF (n=4, Fig. 3-8A), suggesting *dco* mutation does not affect the cell death. Or it is possible that low level of ecdysone in *dco* mutants is sufficient to cause vCrz PCD.

Ectopic expression of ecdysone receptor isoforms

vCrz PCD does not occur during larval-larval molting. It is possible that a low level of EcR expression might not be sufficient to induce certain developmental process triggered by ecdysone. Thus we hypothesized that precocious induction of a high level of EcR-B1 and EcR-B2 may cause premature vCrz cell death. To test this, we attempted to express each EcR isoform in Crz neurons using the Gal4/UAS system. A *UAS-mCD8-GFP*;; *Crz-gal4* ^{T2a} was crossed with UAS-EcR-A, UAS-EcR-B1, or UAS-EcR-B2 (or wild-type as control), and the CNSs from the progeny at 1-2 hours APF were examined for GFP signals. Quite contrary to this prediction, none of the EcR isoforms did affect *Crz* expression, suggesting that ectopic EcR expression does not cause premature cell death (Fig 3-9B-D).

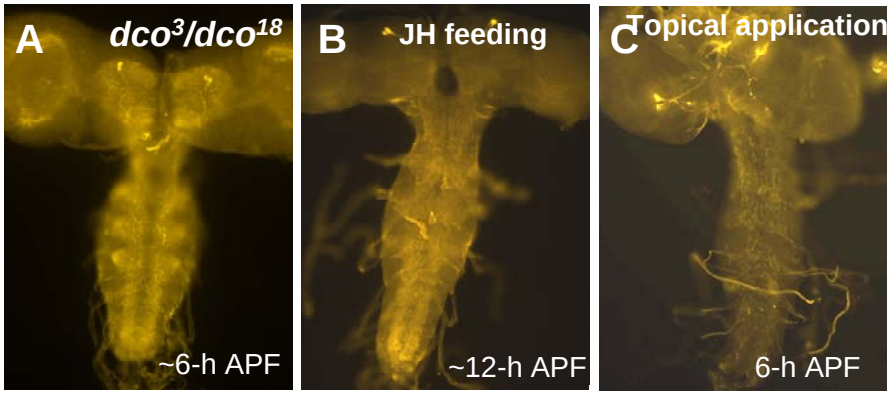

Figure 3-8. Ecdysone and Juvenile Hormone (JH) effects on vCrz PCD. **(A)** Crz-IHC of *dco*^{3}/*dco*^{18} at ~6 hours APF. No Crz-IR cells in VNC suggests that *dco* mutation does not affect the cell death. **(B, C)** JH effect. (B) CS 1st instar larvae were fed with methoprene (Met) and collected after head eversion. Crz-IRys were not detected in VNC, suggesting JH feeding does not affect vCrz PCD. (C) CS white prepupa were topically applied with Met, and Crz-IRys of dissected CNSs at 6 hours APF were not detectable in VNC, suggesting no role of JH for vCrz PCD.

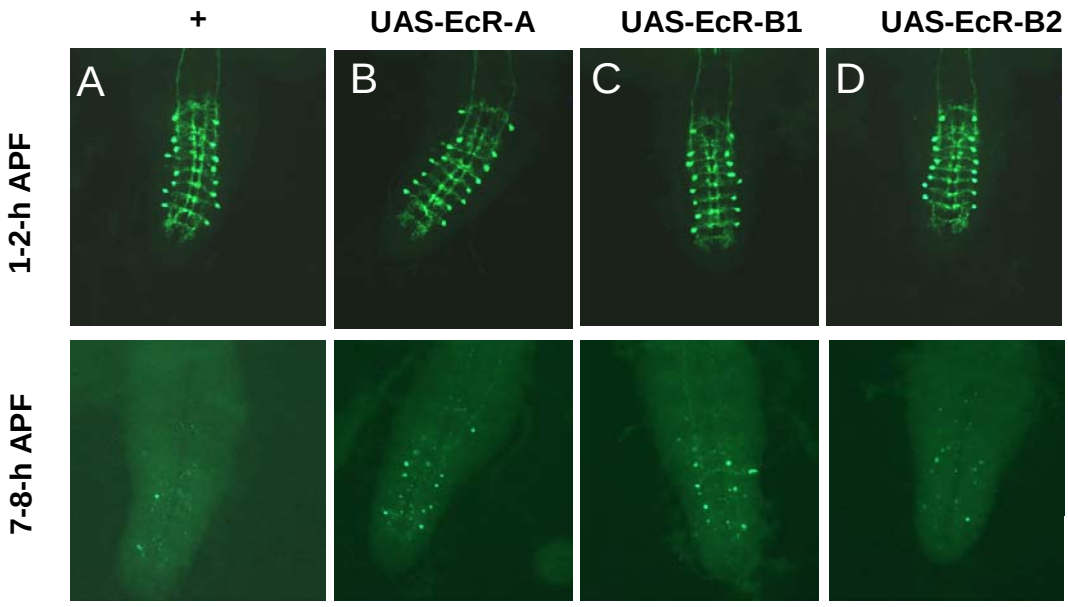

Figure 3-9. Ectopic expression of different EcR isoforms in vCrz neurons. (Top) VNC at 1-2 hours APF. (Bottom) VNC at 7-8 hours APF. **(A)** *UAS-mCD8-GFP*/+;;*Crz-gal4*/+ **(B)** *UAS-mCD8-GFP*/+;*Crz-gal4*/*UAS-EcR-A* **(C)** *UAS-mCD8-GFP*/+;; *Crz-gal4*/*UAS-EcR-B1* **(D)** *UAS-mCD8-GFP*/+; *UAS-EcR-B2*/+; *Crz-gal4*/+.

To determine if vCrz PCD is affected by the induced level of EcR isoforms at later developmental stages, the progeny at 7-8 hours APF were collected and processed for GFP visualization. Interestingly, ectopic expression of the A and B1 forms delayed vCrz PCD. The ectopic EcR-A^{III} expression resulted in survival of 4.8 (± 2.5) vCrz neurons at 8 hours APF (n=5, Fig.3-9B), while $B1^{II}$ expression induced survival of 7.2 (± 0.8) vCrz neurons at 7 hours APF (n=5, Fig. 3-9C). B2 expression did not show any effect at 7 hours APF (n=4, Fig. 3-9D). It has been known that EcR-A and EcR-B1 have an inhibitory impact on the expression of the other (Schubiger et al., 2003). High level of EcR-A suppresses EcR-B1 expression in wing discs at the time when wing discs possess high level of endogenous EcR-B1. In contrast, high level of EcR-B1 or B2 reduces EcR-A expression in the same discs at the time when discs express high level of endogenous EcR-A. If this is the case in vCrz neurons, delay of vCrz PCD by EcR-A overexpression is can be explained; ectopic expression of EcR-A might inhibit EcR-B1 expression, thus prevent or delay vCrz PCD. However, it is quite unexpected that EcR-B1 expression delayed vCrz PCD. So far, the molecular basis underlying this protection is not known yet.

We also used EcR-B1 overexpression line (*Crz-gal4/+, UAS-lacZ/UAS-EcR-B1*) for the aforementioned ecdysone feeding assay (see p. 113) and the data showed that vCrz PCD was not affected by EcR-B1 overexpression at 8 hours APF. It is interesting why the same EcR-B1 overexpression cause different consequences: delay of vCrz PCD vs. no effect. Only difference between two experiments is the usage of different types of UAS lines: *UAS-lacZ* and *UAS-mCD8-GFP*. Perhaps GFP staining is more sensitive to

detect vCrz neurons rather than X-gal staining. However, more examinations will be necessary to determine the effect of overexpressed EcR-B1 for vCrz PCD.

Juvenile Hormone (JH) effect on v*Crz* PCD

In most insects, application of JH to early final instar larvae prevents metamorphosis (Riddiford, 1993) and it has been postulated that JH prevents metamorphosis by modulating ecdysteroid actions (Riddiford, 1993). For example, in the presence of the ecdysone peak, high level of JH induces larval-larval molting whereas low level of JH induces larval-pupal metamorphosis. Therefore, we hypothesized that maintenance of high JH level during the larval-pupal transformation may prevent vCrz PCD. To test this, 1st instar larvae of wild type were fed with food supplemented with the synthetic JH, methoprene (Met) and were incubated at 25°C until they reached the head eversion stage, approximately 12 hours APF. Crz-IHC showed all vCrz neurons were not detectable, suggesting that JH feeding does not have an effect on vCrz PCD (Fig 3-8B). To comfirm the effectiveness of Met, we observed the developmental process of Met-fed progeny. As reported previously, Met-fed pupae were not able to eclose, verifying that Met is an effective reagent. As an alternative way, Met was topically applied to each wild-type white prepupa, and the resulting pupae were incubated for 6 hours and then collected. Crz-IHC revealed that all vCrz neurons were not detectable, suggesting no role of JH for vCrz PCD (Fig. 3-8C). To give longer exposure time of the juveniles to Met and thus maximize the JH effect, Met was also topically applied at an earlier stage (wandering larva) and the animals were incubated until 12-16 hours APF. Crz-IHC

showed the absence of vCrz IRys at this time point (n=6), confirming no effect of JH on vCrz PCD.

To further examine JH effect *in vivo*, we observed Crz expression in ap^4 (*apterous*) mutant. ap^4 mutants are female sterile and have a dramatically reduced JH level (Altaratz et al., 1991). JH production from the corpora allatum is much reduced in sterile adult females, and the ring glands of wandering larvae have been known to produce JH at almost 50% of the normal rate. How the ap^4 mutation causes the reduction in JH level is not known yet. We reasoned that the reduced level of JH in this mutant may be unable to antagonize ecdysone function and thus induce premature vCrz PCD. In contrast to this prediction, Crz-IHC of wandering larvae of ap^4 mutants revealed no sign of vCrz PCD, suggesting little effect of ap^4 mutation.

Downstream apoptotic pathways of EcR signaling:

We are further interested in the mechanisms by which activated EcR signaling is transduced to activate downstream apoptotic pathways for the vCrz PCD.

***Reaper* (*rpr*) is a proapoptotic executor of vCrz-PCD**

Pro-apoptotic genes, *rpr, hid,* and *grim*, defined by the *H99* deletion, are well-known death activators in *Drosophila* (White et al, 1994). Since *rpr* and *hid* have been shown to promote ecdysone-mediated PCD of the salivary glands and midgut (Yin and Thummel, 2004), we hypothesized that either or both of these genes are apoptotic inducers for the vCrz PCD.

The PCD of vCrz neurons was unaffected by heterozygous *H99* deletion, suggesting that one copy of the wild-type *rpr*, *hid*, and *grim* alleles is sufficient for inducing vCrz-cell death (Fig. 3-10A). Heterozygosity for *XR38* deletion, which removes *rpr* as well as *sickle* (Peterson et al., 2002; Wing et al., 2002), also did not affect normal PCD (Fig. 3-10B). Intriguingly, however, *ca.* 7 pairs of vCrz neurons survived in a *rpr*-null mutant (*XR38/H99*) (Fig. 3-10C, n>5). A similar result was obtained by *Crz-gal4*-mediated *GFP* expression in the same mutant background (*UAS-mCD8-GFP/+; pCrz-gal4/+; XR38/H99*, n=3, Fig.3-10D). These data strongly support a crucial role that *rpr* plays in the destruction of vCrz neurons.

In contrast, PCD of the vCrz neurons in mutants lacking *hid* functions (*X14*/*hid*^{05014} and *H99/hid*^{05014}, Grether et al., 1995; Peterson et al., 2002) occurred normally (Fig. 3-10E), suggesting that *hid* is not a death promoter for vCrz neurons. Due to a lack of specific mutants, possible roles for *grim* were not tested. However, since *grim* ISH signals were hardly detectable in larval as well as early prepupal vCrz neurons in wild-type (data not shown), we suggest that *grim* might not be involved in vCrz PCD.

To determine cell-autonomous roles of *rpr*, we investigated whether *rpr* is expressed in vCrz neurons by ISH. To validate our *rpr* cRNA probe, ISH was first performed on the CNSs taken from the progeny of [*Crz-gal4*, *UAS-p35* x *UAS-rpr*] cross. In this genetic context, *rpr* transcripts are overproduced in Crz neurons but *rpr*-induced death is suppressed by co-expression of the *p35*. As a result, we detected faint but distinct *rpr*-ISH signals seemingly in the vCrz neurons in the third-instar larva (arrowheads in Fig. 3-11A). Except for these cells, ISH signals were nearly blank in the

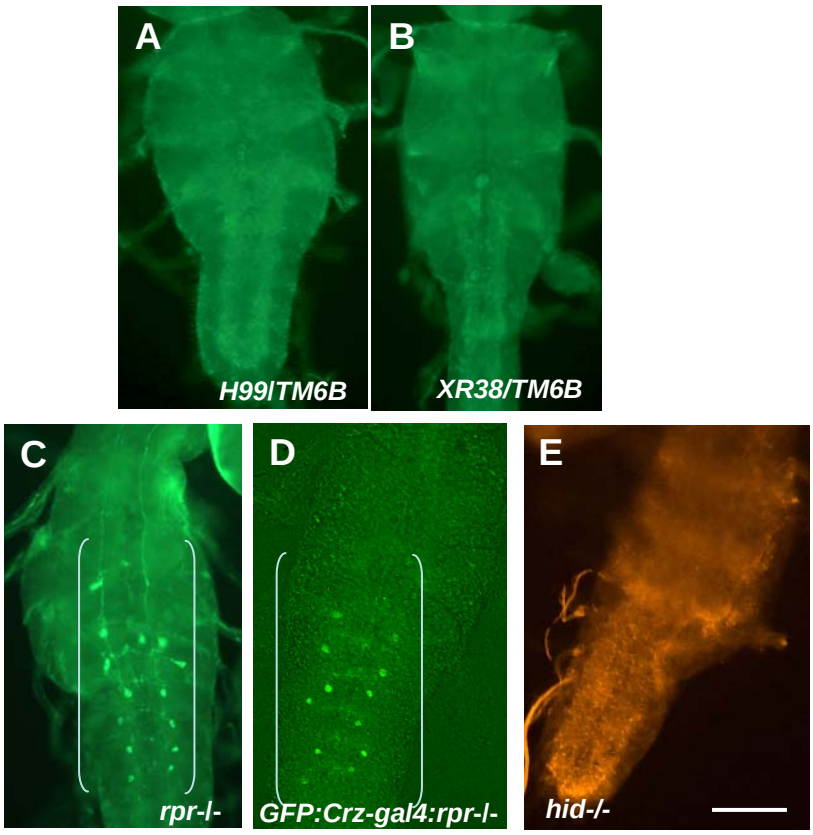

Figure 3-10. The role of *rpr* and *hid* in vCrz PCD. Crz-IRy in **(A)** *H99*/*TM6B*, **(B)** *XR38*/*TM6B*, *rpr*-null mutants **(C)** *XR38/H99*, **(D)** *UAS-mCD8-GFP/+;Crz-gal4/+; XR38/H99* at 12-16 hours APF, and **(E)** *hid* loss-of-function mutant (*X14*/*hid*^{05014}) at 8 hours APF. Note that *ca.* 14 vCrz neurons are still detectable in *rpr* mutants (brackets in C and D). Scale bars: 50 μm.

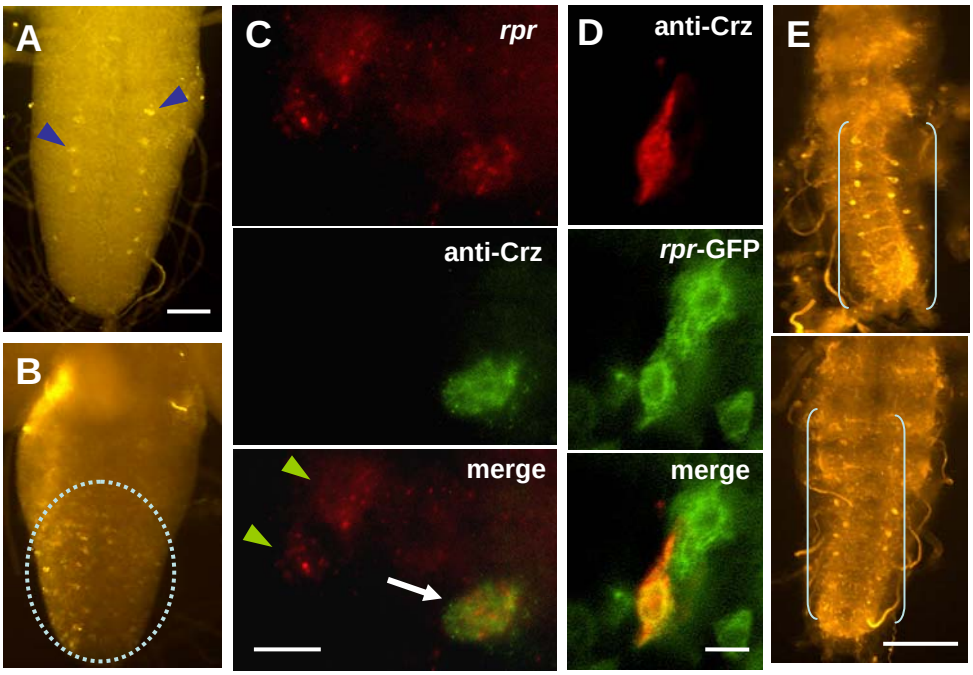

Figure 3-11. The role of *rpr* in vCrz PCD. **(A, B)** *Rpr*-ISH of the CNSs dissected from (A) third-instar larva (*Crz-gal4*, *UAS-p35*/*UAS-rpr*), or (B) wild-type prepupa at 1.5 hours APF. The hybridization signals are designated by arrowheads, or in circle, respectively. **(C)** Double labeling of wild-type CNS with *rpr*-ISH probe (top) and anti-Crz (middle) at 1.5 hours APF. Merge of the two images (bottom) shows co-localization of *rpr* mRNA in a vCrz neuron (arrow). Expression of *rpr* in non-vCrz neurons is indicated by arrowheads. **(D)** *Rpr* promoter activity in vCrz neurons at 1 hour APF. Crz-IRy (top), *rpr-gal4*-driven GFP expression (middle), and merge of the two (bottom). A vCrz neuron positive for both GFP and Crz-IRy appears in yellow color (arrow). **(E)** *Rpr-gal4*-mediated *p35* expression (*rpr-gal4/UAS-p35*) suppresses the death of ~10 vCrz neurons (brackets) at 7-9 hours APF. Two different specimens are shown here. Scale bars: in A, 50 μm for A, B; in C, D, 10 μm; in I, 50 μm.

entire larval CNS, suggesting that *rpr* is transcriptionally silent in most cells of this tissue at this stage. Having validated the *rpr* cRNA probe, we extended ISH to wild-type prepupal CNS. At 1.5 hours APF, numerous *rpr*-ISH signals were revealed particularly in the abdominal ganglionic region (circle in Fig. 3-11B), while the sense probe did not produce any signals (data not shown). Together these results suggest that *rpr* becomes transcriptionally active soon after pupariation, thereby inducing death of numerous obsolete larval neurons in this CNS region.

We applied *rpr*-ISH and Crz-IHC simultaneously to see if endogenous *rpr* mRNAs are also expressed in vCrz neurons prior to death. At 1.5 hours APF, *rpr*-ISH signals were detectable in ~10% of vCrz neurons (17 out of 177) examined (Fig. 3-11C). Unsynchronized or transient expression of *rpr* may explain such a minor proportion of *rpr*-positive vCrz neurons.To detect *rpr* expression in a more sensitive manner, we generated *rpr-gal4* transgenic flies. Previously, the 1.3-kb *rpr* upstream sequence was shown to contain an ecdysone response element (EcRE) and to be sufficient for ecdysone-dependent *rpr* expression in salivary glands (Jiang et al., 2000). When F1-progeny from [*rpr-gal4* x *UAS-mCD8-GFP*] cross was processed for Crz-IHC, 17 out of 80 vCrz neurons (21%) produced GFP signals at 1 hour APF (Fig. 3-11D). To further corroborate this result, *p35* expression was induced by *rpr-gal4*. We reasoned that if *rpr* is expressed in vCrz neurons, then *rpr-gal4*-induced *p35* would prevent vCrz PCD (*cf.* Fig. 3-4B). Remarkably, Crz-IHC revealed *ca.* 10 neurons even at 7-9 hours APF (Fig. 3-11E). Incomplete rescue of the death by *p35* is somewhat similar to the results from *rpr*-null mutation (*cf*. Fig. 3-10C). These overall data support the model in which EcR-B-induced *rpr* expression is a primary cause for vCrz PCD.

Characterization of RNAi constructs

Targeted inactivation of cell death genes was performed by generating UAS-RNAi constructs of three cell death genes *rpr*, *grim*, and *hid.* To examine the effect of lack of each cell death gene for vCrz PCD, we crossed each UAS-RNAi with a *UAS-mCD8-GFP*;;*Crz-gal4*. *Crz* promoter-driven *GFP* expression of all RNAi progenies at 7 hours APF showed cell death of vCrz neurons, indicating that targeted knock-down of each cell death gene did not prevent vCrz PCD (Table 3-2). Of interest, this rpr^{RNAi} result is contradictory to the result of *rpr*-null mutants at pupal stage (Table 3-2B vs. Fig. 3-10C). This result may result from low level of rpr^{RNAi} expression. Alternatively, rpr^{RNAi} might not have effectiveness and specificity to *rpr* gene itself.

To confirm the validity of UAS-RNAi, we also tested salivary gland cell death using RNAi lines. We expressed *UAS-*hid^{RNAi} and *UAS-*rpr^{RNAi} in the salivary glands by crossing with *34B-gal4; UAS-GFP*. However, expression of each of these RNAis did not prevent salivary gland degeneration (Table 3-2). No role of *UAS-*hid^{RNAi} for salivary gland cell death in our study is also contradictory to the result of *hs*-(heat shock promoter) hid^{RNAi} examined for salivary gland cell death in Yin and Thummel (2005). These authors found that *hs-hid RNAi* inhibits salivary gland PCD.

To further validate UAS-RNAi lines, we expressed each RNAi in the defective eyes caused by the expression of cell death genes and examined the recovery rate of the eye defect. For hid^{RNAi} analysis, a *GMR-hid, GMR-gal4*/*CyO, y+* was crossed with transgenic lines bearing single or two copies of *UAS-*hid^{RNAi}, and then eye morphology of

Table 3-2. Characterization of cell death gene RNAi constructs

A. *hid*^{RNAi}	vCrz	Salivary gland	Eye
	UAS-mCD8-GFP;;Crz-gal4	34B-gal4;UAS-GFP	GMR-gal4,GMR-hid/CyO,y+
Cross w/	UAS-hid^{RNAi}-2B (II) UAS-hid^{RNAi}-3B (II) UAS-hid^{RNAi}-4F (II) UAS-hid^{RNAi}-5B (II)	UAS-hid^{RNAi}-2B	UAS-hid^{RNAi} 5A;1B UAS-hid^{RNAi} 5B;1B UAS-hid^{RNAi} 5B;2A UAS-hid^{RNAi} 6A;1A UAS-hid^{RNAi} 6A;1B UAS-hid^{RNAi} 6A;2A UAS-hid^{RNAi} 7A;5C UAS-hid^{RNAi} 8A;2A UAS-hid^{RNAi} 9B;2A UAS-hid^{RNAi} 7A
Result	No effect at 7-h APF	No effect at 24-h APF	Recover eye defect

B. *rpr*^{RNAi}	vCrz	Salivary gland	Eye
	UAS-mCD8-GFP;;Crz-gal4	34B-gal4; UAS-GFP	GMR-gal4, GMR-rpr
Cross w/	UAS-rpr^{RNAi}-1A UAS-rpr^{RNAi}-5B	UAS-rpr^{RNAi}-1A UAS-rpr^{RNAi}-7C	UAS-rpr^{RNAi}-1A UAS-rpr^{RNAi}-5B UAS-rpr^{RNAi}-1C UAS-rpr^{RNAi}-5A UAS-rpr^{RNAi}-1A;7A* UAS-rpr^{RNAi}-1F;1C UAS-rpr^{RNAi}-1F;4B UAS-rpr^{RNAi}-1A;7B UAS-rpr^{RNAi}-1F;7B UAS-rpr^{RNAi}-1A;5A* UAS-rpr^{RNAi}-5B;5A* UAS-rpr^{RNAi}-1A;4B
Result	No effect at 7-h APF	No effect at 24-h APF	Rescue eye defect

C. *grim*^{RNAi}	vCrz	Salivary gland	Eye
	UAS-mCD8-GFP;;Crz-gal4	34B-gal4; UAS-GFP	GMR-gal4, GMR-grim
Cross w/	UAS-grim^{RNAi}-2A UAS-grim^{RNAi}-4B UAS-grim^{RNAi}-6A UAS-grim^{RNAi}-7B	not determined	UAS-grim^{RNAi} -3 UAS-grim^{RNAi}-11A UAS-grim^{RNAi}-1B UAS-grim^{RNAi}-6A UAS-grim^{RNAi}-4C;9 UAS-grim^{RNAi}-6A;3 UAS-grim^{RNAi}-1B;11A UAS-grim^{RNAi}-1B;3 UAS-grim^{RNAi}-2A;3 UAS-grim^{RNAi}-6A;11A UAS-grim^{RNAi}-7B;11A
Result	No effect at 7-h APF	not determined	Rescue eye defect

* indicates full recovery of the eye defect caused by *rpr* expression

the progeny was scored. Due to eye-specific *hid* expression by eye-specific promoter, GMR (glass multiple repeat), compound eyes are severely degenerated in the *GMR-gal4*, *GMR-hid*/*CyO, y+* parents (Fig. 3-12A). Remarkably, however, eye-specific expression of *hid* RNAi significantly resuced *hid*-mediated PCD of the eyes (Fig. 3-12C, D vs. A). Two copies of hid^{RNAi} recovered the eye defect more strongly than one copy. This result confirms the effectiveness of *UAS-*hid^{RNAi} lines at least in the eye. To validate *UAS-*rpr^{RNAi}, a *GMR-gal4;;GMR-rpr* was crossed with transgenic lines bearing one or two copies of *UAS-*rpr^{RNAi} and the eye morphology was examined. Like *UAS-*hid^{RNAi}, the expression of *UAS-*rpr^{RNAi} recovered the eye defect caused by *GMR-rpr* (Fig. 3-12D) in a dose dependent manner (Fig. 3-12 E-G). Likewise, in case of *UAS-*$grim^{RNAi}$, the eye defect caused by *GMR-grim* (Fig. 3-12 H) was fully rescued by the expression of all *UAS-*$grim^{RNAi}$ lines regardless of copy number (Fig. 3-12 I-K and Table 3-2C). These findings suggest that all three RNAi lines are effective in the eye.

Next, to confirm the specificity of RNAi lines, each UAS-RNAi line was crossed to transgenic lines bearing *GMR-gal4:GMR-hid,* or *GMR-gal4:GMR-rpr*, or *GMR-gal4:GMR-grim,* and then the progeny was examined for the eye morphology. Interestingly, hid^{RNAi} rescued the eye defects caused by all three genes *rpr*, *grim*, or *hid* (Fig. 3-13B, F, J). In contrast, $grim^{RNAi}$ expression rescued the eye defect caused by only *grim* (Fig. 3-13C, G, K). rpr^{RNAi} rescued the defect caused by *grim* and *rpr* (Fig. 3-13D, H, L). These results suggest that $grim^{RNAi}$ has highest specificity. The rescue of eye defects caused by all three genes by hid^{RNAi} does not seem to result from the sequence homology among *rpr*, *hid*, and *grim* because hid^{RNAi} could rescue the eye effect

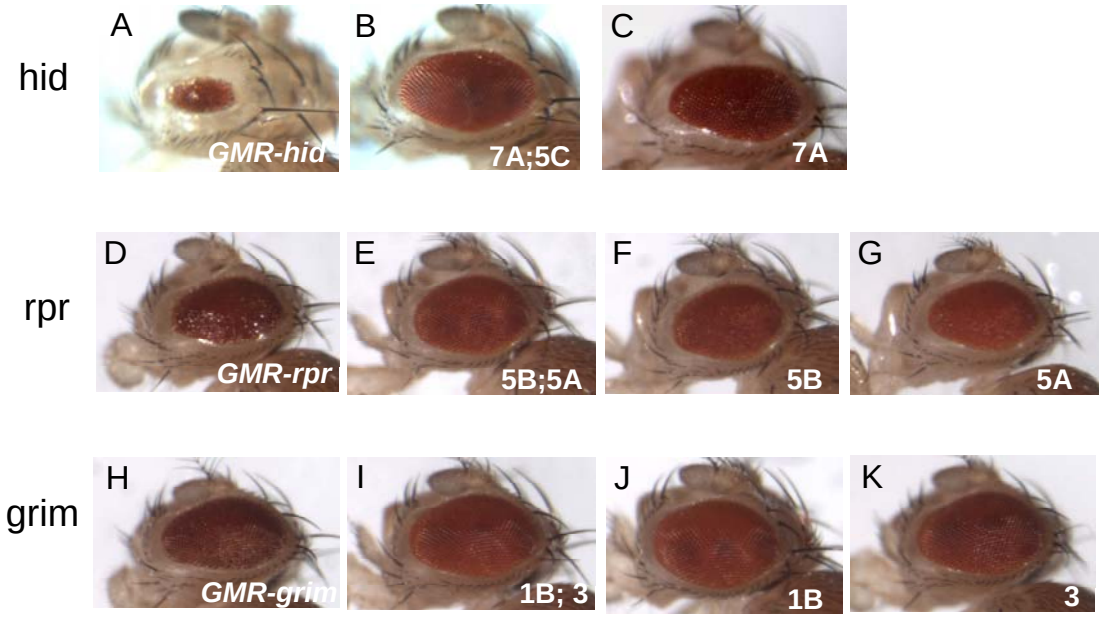

Figure 3-12. Effect of RNA interference (RNAi) in the eyes. **(A-C)** The eye defect caused by *GMR-hid* (A) was fully recovered by the expression of two copies (B) of *hid*^{RNAi}, but not fully but significantly recovered by one copy (C). **(D-G)** The eye defect caused by *GMR-rpr* (D) was recovered fully by two copies (E) of *rpr*^{RNAi}, but not fully but significantly by single copy (F, G). **(H-K)** The eye defect caused by *GMR-grim* (H) was recovered fully by one (J, K) or two copies (I) of *grim*^{RNAi}. Genetic backgrounds are as follows. (A) *GMR-hid, GMR-gal4/+,* (B) *GMR-hid, GMR-gal4 /UAS-hid*^{RNAi} *7A; UAS-hid*^{RNAi} *5C/+*, (C) *GMR-hid, GMR-gal4/UAS-hid*^{RNAi} *7A,* (D) *GMR-gal4/+;;GMR-rpr/+*, (E) *GMR-gal4/+;UAS-rpr*^{RNAi} *5B/+; GMR-rpr/UAS-rpr*^{RNAi} *5A,* (F) *GMR-gal4/+;UAS-rpr*^{RNAi} *5B/+;GMR-rpr/+*, (G) *GMR-gal4/+;;GMR-rpr/UAS-rpr*^{RNAi} *5A*, (H) *GMR-gal4/+;GMR-grim/+*, (I) *GMR-gal4/+; GMR-grim/UAS-grim*^{RNAi} *1B*; *UAS-grim*^{RNAi} *3/+*, (J) *GMR-gal4/+; GMR-grim/ UAS-grim*^{RNAi} *1B,* (K) *GMR-gal4/+; GMR-grim/+;UAS-grim*^{RNAi} *3/+*.

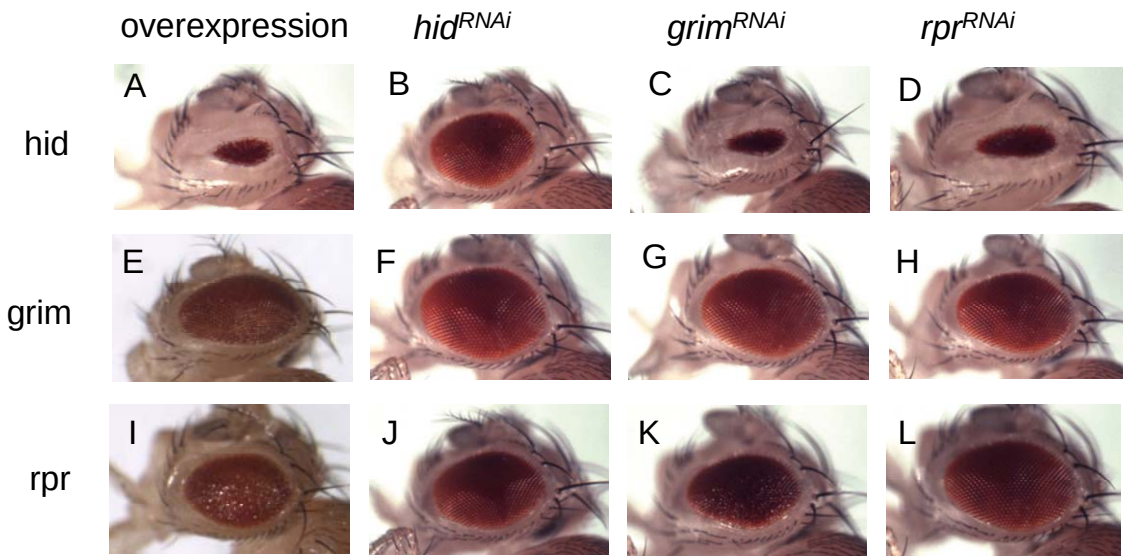

Figure 3-13. *In vivo* RNAi targeting of cell death activators. To validate the efficiency and specificity of UAS-RNAi, we used transgenic lines overexpressing cell death genes in the eye. **(A-D)** A *hid* overexpressing line (*GMR-gal4, GMR-hid*/CyO, y+) was crossed to (A) w^{1118} (B)*UAS-hid*^{RNAi} (C) *UAS-grim*^{RNAi} and (D) *UAS-rpr*^{RNAi}. Only *hid*^{RNAi} expression (B) rescued the eye defect caused by *hid* overexpression (A). **(E-H)** A *grim* overexpression line (*GMR-gal4; GMR-grim*) was crossed as above. Eye defects caused by *grim* overexpression (E) were rescued by all three RNAi expressions (F-H). **(I-L)** A *rpr* overexpressing line (*GMR-gal4;;GMR-rpr*) was crossed as above. The eye defect caused by *rpr* overexpression (I) was rescued by *hid*^{RNAi} (J) and *rpr*^{RNAi} (L) but not by *grim*^{RNAi} (K). We used RNAi transgenic lines bearing two copies of each RNAi construct. For example, *hid*^{RNAi}: *UAS-hid*^{RNAi} 7A;5C, *grim*^{RNAi}: *UAS-grim*^{RNAi} 1B;3, *rpr*^{RNAi}: *UAS-rpr*^{RNAi} 5B;5A.

caused by *grim* expression, however, conversely, $grim^{RNAi}$ could not rescue the eye defect caused by *hid* expression. Further studies are necessary to determine the molecular bases underlying this result.

Since all three RNAi transgenes effectively rescued the eye defect caused by corresponding gene as seen in Fig. 3-12, these RNAi expression by eye-specific promoter (*GMR)-gal4* seems to be productive. Since RNAi expression in vCrz and salivary gland seems to be low compared to the eye, it will be necessary to test again with higher dosages of UAS RNAi. In addition, the usage of the strongest phenotypic alleles of UAS RNAi transgenic line is necessary because many transgenic lines of the same RNAi construct have different level of effectiveness.

Diap1 is not required for survival of vCrz neurons

Although vCrz cell death is most likely to be a cellular response to an ecdysone surge occurring at pupariation, this event does not occur prematurely during ecdysone-led larval-to-larval moltings (Riddiford, 1993). This could be due to anti-apoptotic factors that counteract the pro-apoptotic machinery in larval vCrz-neurons. The best candidate for this role is *diap1*, whose anti-apoptotic activity comes from the inhibition of caspase activity (reviewed in Bergmann et al., 2003). If *diap1* is important for the survival of vCrz-neurons during larval growth, then the larval vCrz neurons would contain high levels of DIAP1. Our IHC, however, did not detect any DIAP1-IRy within larval vCrz-neurons of wild-type (data not shown, n=12). Despite this, since undetectable levels of DIAP1 still could be sufficient for this role, we attempted to knockdown *diap1* transcript

levels via RNA interference (RNAi). For this, progeny from [*symUAS-diap1*^{RNAi} x *UAS-mCD8-GFP*; *Crz-gal4*] cross was examined for GFP signals. Such a transgenic manipulation was intended to produce double-stranded RNAs from complementary RNAs symmetrically transcribed from the *diap1* cDNA, which then mediate degradation of *diap1* mRNA specifically in Crz-neurons (Giordano et al., 2002; Huh et al., 2004). Our data showed that GFP expression at 1 hour APF in *diap1*^{RNAi} was essentially the same as that in wild-type (Fig. 3-14B *vs.* A), indicating that *diap1*-knockdown did not cause premature cell death. Similar results were obtained when two copies of the *Crz-gal4* transgene were employed to increase *diap1*^{RNAi} dosage or by heat-shock-induced *diap1*^{RNAi} (data not shown; *cf.* Yin and Thummel, 2004).

Since the negative results could be due to the lack of effective *diap1*^{RNAi}, we checked the validity of *symUAS-diap1*^{RNAi} in salivary gland PCD. In doing so, the *34B-gal4*; *UAS-GFP* (salivary gland-specific driver, Yin and Thummel, 2004) was crossed to the *symUAS-diap1*^{RNAi}, and then GFP signals were examined in white prepupa. In contrast to intense signals seen in the control salivary glands, such signals were significantly reduced by *diap1*^{RNAi} expression, reflecting premature death of this tissue (Fig. 3-14C). This is consistent with a previous report employing *heat shock-diap1*^{RNAi} (Yin and Thummel, 2004), thus validating *symUAS-diap1*^{RNAi}.

Genetic reduction of *diap1* levels in half also did not accelerate death of vCrz neurons, as mutants heterozygous for *th*^{4} or *Df(3L)brm11* alleles showed normally scheduled death of vCrz-neurons (data not shown), although these alleles dominantly exacerbate *rpr*-induced death of photoreceptor cells (e.g., Lisi et al., 2000). These overall

Figure 3-14. Lack of role for *diap1* in the vCrz PCD. **(A)** Control (*UAS-mCD8-GFP/+;;Crz-gal4/+*). **(B)** Targeted expression of the *diap1*^{RNAi} in Crz neurons (*UAS-mCD8-GFP/+*; *symUAS-diap1*^{RNAi}*/+*; *Crz-gal4/+*) (*cf*. Huh et al., 2004). Intact GFP signals (vCrz) at 1 hour APF suggest that knockdown of endogenous *diap1* does not cause premature cell death. **(C)** Effect of *diap1*^{RNAi} on premature death of the salivary glands. The *symUAS-diap1*^{RNAi} or *y w* (control) was crossed to the *34B-gal4*; *UAS-GFP*, and then white prepupal progeny were examined for GFP. In the control, intense GFP signals are seen in a pair of the salivary glands (left, arrow), whereas the signals are significantly weakened by *diap1*^{RNAi} (right, arrow). **(D)** Crz-IRy in homozygous *th*^{SL} at 6.5 hours APF. **(E)** X-gal histochemistry of UAS-*lacZ/+*; *Crz-gal4*/*UAS-diap1* at 6 hours APF. Both genetic and transgenic *diap1* gain-of-functions do not prevent vCrz death. **(F)** Rescue of the salivary gland degeneration by *diap1*. In a control pupa (*34B-gal4*/+; *UAS-GFP*/+, n=5) at 18 hours APF, faint GFP signals (left, arrow) reflect the PCD of this tissue. In contrast, strong GFP signals (right, arrow) are maintained by *diap1* expression (*34B-gal4*/+; *UAS-GFP*/*UAS-diap1*, n=8). Scale bars: in A, 100 μm for A, B, D-F.

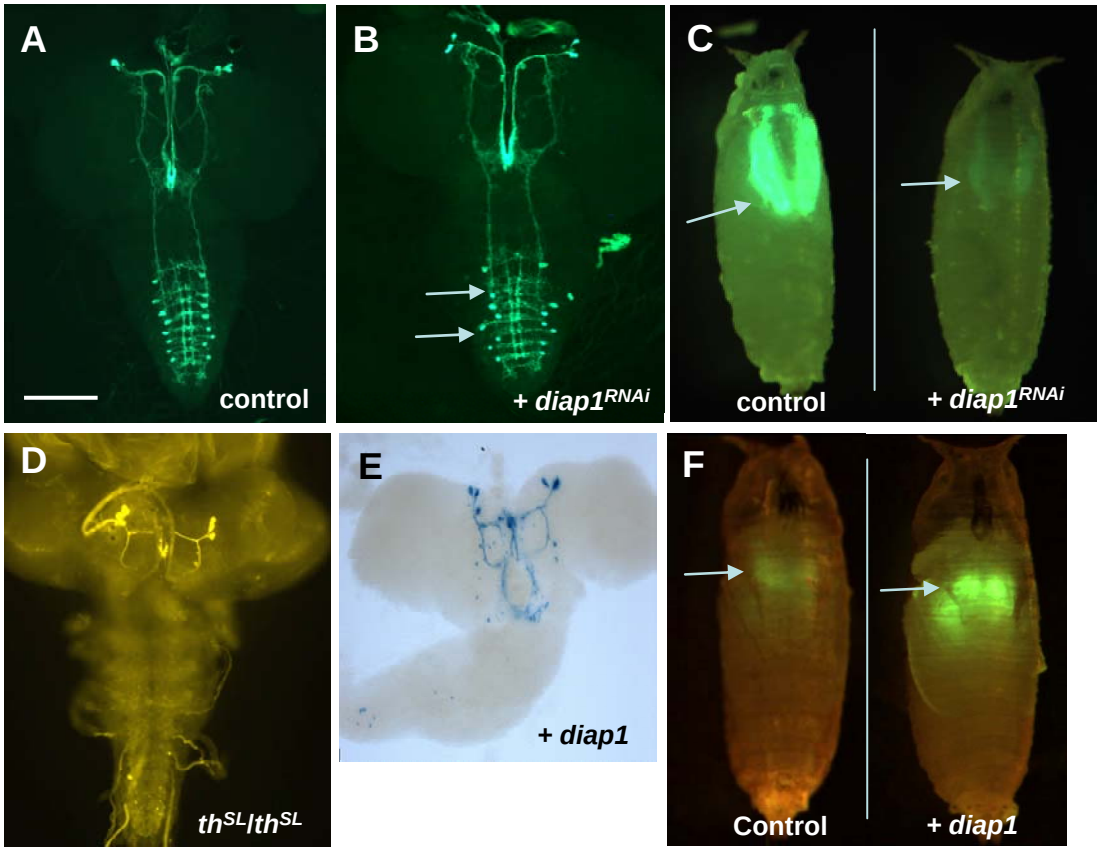
A
control
B
+ diap1RNAi
C
control
+ diap1RNAi
D
thSL/thSL
E
+ diap1
F
Control
+ diap1

Figure 3-14.

results support that RPR-mediated caspase activation does not involve RPR's role as a DIAP1-antagonist.

Since RPR's pro-apoptotic action can be nullified by DIAP1 (e.g., Lisi et al., 2000), we tested whether gain-of-*diap1* functions can suppress vCrz PCD. This was accomplished in two ways; one is th^{SL} allele that was shown to suppress *rpr*-induced photoreceptor cell death (Lisi et al., 2000). The other is from transgenic *diap1* expression in Crz-neurons (*Crz-gal4/UAS-diap1*). Neither th^{SL} nor ectopic *diap1* expression suppressed vCrz PCD (Fig. 3-14D, E). Similar results were obtained from ectopic *diap2* expression (data not shown). The negative result from ectopic *diap1* expression is unlikely due to the lack of active DIAP1, since the same transgenic construct rescued the PCD of salivary glands (Fig. 3-14F).

The failure of *diap1* expression to block the vCrz PCD could be due to insufficient amount of DIAP1 in Crz neurons. A *UAS-lacZ;Crz-gal4* was crossed to *UAS-DIAP1* and the feeding 3rd instar larval progenies were collected. Diap1-IHC of the CNSs from these young larvae showed distinct DIAP1 expression in Crz neurons. Quite surprisingly, such DIAP1-IRy was not maintained in older larvae (Fig. 3-15 A, B). This result led us to test *diap1* super-ectopic expression using genetic manipulation. Unlike one copy of each transgene, two copies of *UAS-diap1* and two copies of *Crz-gal4* transgenes were capable of delaying vCrz PCD. Crz-IHC of the CNSs obtained from *Crz-gal4* ^{S2b}; *UAS-diap1* revealed that ca. 9.6 (±4.0) vCrz cells (n=3) and 7 v*Crz* cells (n=1) survived at 12 hours APF and 16.5 hours APF, respectively (Fig. 3-15E, H). The degree and time of delayed vCrz PCD is proportionate to the number of transgenes. One copy of *Crz-gal4* and two copies of *UAS-diap1* (Fig. 3-15D, G), or two copies of *Crz-*

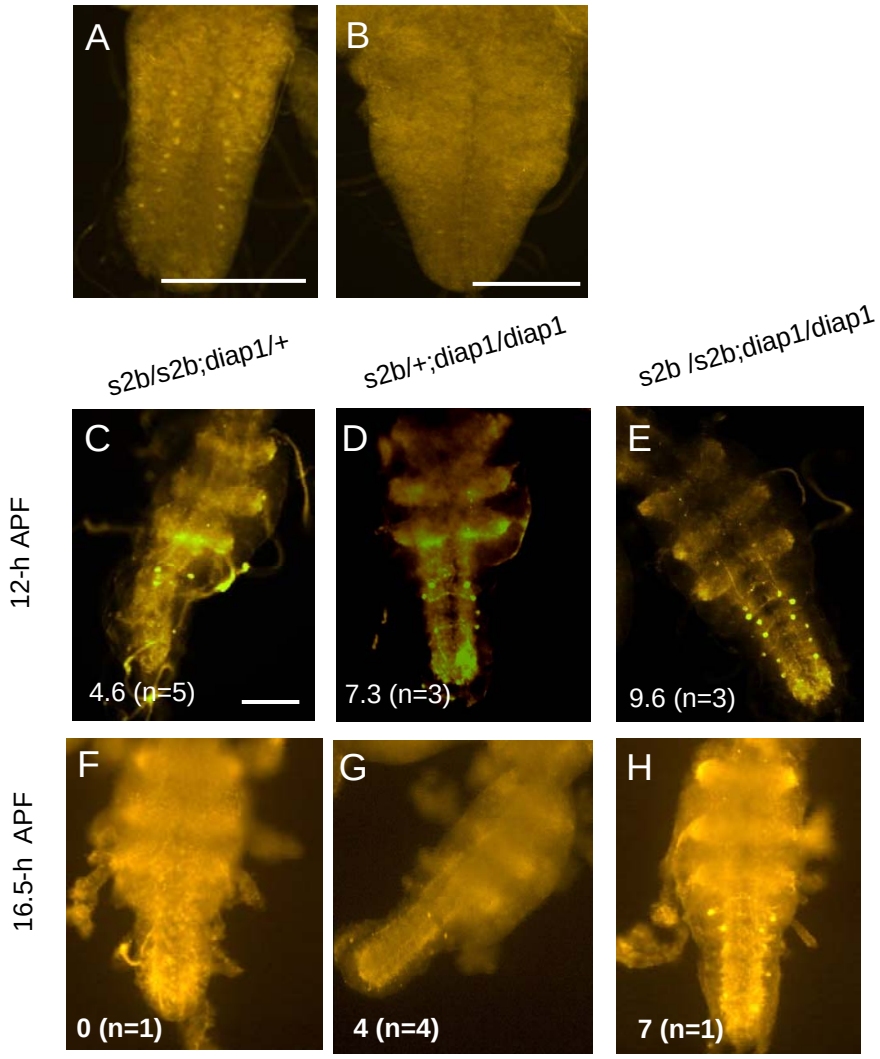

Figure 3-15. Super-ectopic DIAP1 expression in Crz neurons. **(A, B)** DIAP1-IHC of the VNCs obtained from the cross [*UAS-lacZ;Crz-gal4*^{T2a} x *UAS-diap1*] at early 3rd instar larva (A) and late 3rd instar larva (B). Significant reduction of Crz-IRy is evident in the late 3rd larval VNC. **(C-H)** Delay of vCrz PCD is dose-dependent. Crz-IRys of the VNC of **(C, F)** *Crz-gal4*^{S2b}; *UAS-diap1*/+ **(D,G)** *Crz-gal4* ^{S2b}/+;*UAS-diap1* **(E, H)** *Crz-gal4* ^{S2b};*UAS-diap1* at 12 hours APF (C-E) and 16.5 hours APF (F-H). The average number of survived neurons are noted on the left bottom and the number of examined specimen are in parentheses. Scale bar: 100 μm in A, B, 50 μm in C-H.

gal4 and one copy of *UAS-diap1* (Fig. 3-15C, F) delayed vCrz PCD more weakly than two copies of both *Crz-gal4* and *UAS-diap1*. In addition, although flies have three transgenes similarly, *Crz-gal4*^{s2b}/+;*UAS-diap1*/*UAS-diap1* delayed PCD more strongly than *Crz-gal4* ^{s2b}/ *Crz-gal4* ^{s2b};*UAS-diap1*/+ since more vCrz cells were observed at the same stage.

The effect of caspases and Drosophila *Apaf-1* on vCrz PCD

Since the apical caspase DRONC is a primary target of DIAP1 (Meier et al., 2000; Muro et al., 2002; Wilson et al., 2002), the lack of DIAP1's function may suggest that DRONC is not responsible for vCrz death. Contradictory to this prediction, vCrz-PCD was significantly delayed in *dronc* null-mutant (*dronc*^{51}/*dronc*^{I24}, Chew et al., 2004; Xu et al., 2005). *Ca.* 12 neurons still survived at 7 hours APF, while the number was reduced to ~8 at 16 hours APF (Fig. 3-16A, Table 3-3), and none at 48 hours APF (data not shown). Comparable delay of the death was observed in other *dronc*-null mutant types (*dronc*^{51}/*dronc*^{I29}, *dronc*^{I24}/*dronc*^{I24}, *dronc*^{I29}/*dronc*^{I29}) (Table 3-3), suggesting that DRONC is an important caspase that executes vCrz-cell death. However, the delay of death in the absence of DRONC indicates that activities from other caspases are also required for timely execution of vCrz PCD.

Seven caspase-encoding genes have been reported in *Drosophila* genome, namely dronc, dredd, strica, drICE, dcp-1, damm, and decay (Kumar and Doumanis, 2000), and mutants of two caspase-encoding genes except *dronc* are available: *dcp-1* and *dredd* (Laundrie et al., 2003, Leulier et al., 2000). We tested Crz-IHC in these mutants. *dcp-1* null mutation (*dcp-1*^{prev1}) is generated by imprecise *P*-element excision and creates Dcp-1

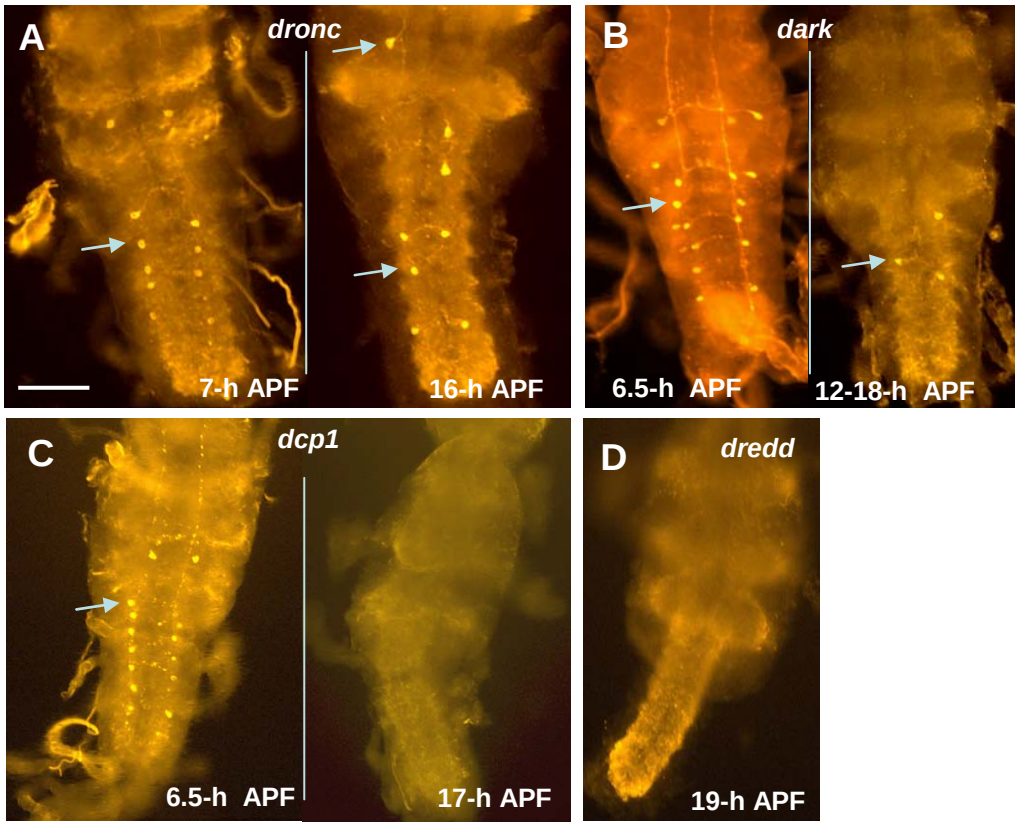

Figure 3-16. The roles of caspases in vCrz PCD. **(A-C)** Delayed PCD of vCrz neurons (A) in a *dronc*-null mutant ($dronc^{51}/dronc^{I24}$), (B) in a homozygous *dark*-null mutant ($dark^{CD4}$), or (C) in a homozygous *dcp-1*-null mutant ($dcp\text{-}1^{prev1}$). Arrows point to Crz-IR neurons that still survive at stages indicated in each panel. **(D)** Crz-IR of the VNC in a homozygous *dredd*-null mutant. Scale bars: 50 μm.

Table 3-3. Time-course development of vCrz PCD in mutants

mutant	7 h APF	16 h APF	2 days APF
dronc^{51}/*dronc*^{I24}	11 (n=4)	8 (n=3)	0 (n=2)
dronc^{51}/*dronc*^{I29}	11 (n=3)	10 (n=2)	0 (n=3)
dronc^{I24}/*dronc*^{I24}	10 (n=3)	ND	0 (n=1)
dronc^{I29}/*dronc*^{I29}	11 (n=3)	ND	ND
dark ^{CD4}	14 (n=3)	2 (n=6, 12-18.5h APF)	ND
dcp1^{prev1}	11(n=4, 6.5 h APF)	0 (n=2, 17 h APF)	ND
dredd	ND	ND	0 (n=3, 19 h APF)

Crz-IHC in mutants was observed at three different stages. The number of survived vCrz neurons was represented below each developmental stage. The times within parentheses are the exact time when animals were collected. ND; not determined.

truncated proteins although homozygotes for this allele are viable and fertile (Laundrie et al., 2003). In this mutant, vCrz PCD was delayed (Fig. 3-16C, Table 3-3). Ca. 11 vCrz cells survived at 6.5 hours APF, but none was detected at 17 hours APF. The comparison of vCrz-IRy between *dronc* and *dcp-1* mutants at 6.5-7 hours APF and at 16-17 hours APF (Table 3-3) indicates that vCrz neurons in *dcp-1*^{prev1} disappear faster than those in *dronc* mutants. These data suggest that DCP-1 resides downstream of Dronc in cell death pathway (see IV section in Chapter 5). *dredd* mutations (*dredd* ^{B118} and *dredd*^{L23}), which were generated by EMS mutagenesis, produce Dredd truncated protein (loss of function) and one amino acid substituted one, respectively. (Leulier et al., 2000). vCrz neurons disappear at 19 hours APF in both mutants (Fig. 3-16D, Table 3-3). However, it was not tested yet whether vCrz PCD is delayed or not.

Activation of DRONC may require the adaptor protein DARK, a fly homolog of vertebrate Apaf-1 (Apoptotic protease activating factor) (Rodriguez et al., 1999). If so, then lack of DARK may phenocopy *dronc*-null mutants. Remarkably, Crz-IR patterns in a homozygous *dark* mutant (*dark*^{CD4}), which is a strong hypomorphic allele (Rodriguez et al., 1999; Akdemir et al., 2006), were comparable to those of *dronc* mutants (Fig. 3-16B vs. A, Table 3-3). These data suggests that an apoptosome consisting of DRONC and DARK is an essential component for vCrz PCD.

The roles of *cyt-c* and *Buffy* in vCrz PCD

In vertebrates, the cytochrome-c (cyt-c) is an essential upstream component for the formation of apoptosome (Acehan et al., 2002). Thus it is interesting to see whether *cyt-c* is also responsible for vCrz PCD. The *Drosophila* genome possesses two *cyt-c* genes:

cyt-c-d and *cyt-c-p* (Limbach and Wu, 1985). *cyt-c-d* is required for caspase activation during spermatid differentiation, whereas *cyt-c-p* is required for respiration in the soma although both share high percentage of identity in protein primary structures and have redundant functions (Arama et al., 2003; Arama et al., 2006). To investigate if *cyt-c* is required for vCrz PCD, first we observed Crz expression in *cyt-c* loss-of-function mutants. A *UAS-mCD8-GFP*;;*Crz-gal4*^{T2a} was crossed with *cyt-c-p*$^{l(2)K13905}$/*CyO, y+* (for *cyt-c-p* mutation) and with *cyt-c-d* $^{Z2\text{-}1091}$/*CyO, y+* or *cyt-c-d*^{bln1}/*CyO, y+* (for *cyt-c-d* mutation), and then offsprings carrying the *y* marker were collected at 7 hours APF. In all of these genetic backgrounds, *Crz-gal4*-driven GFP expression showed complete death of vCrz neurons, suggesting that loss of one copy of each gene does not affect vCrz PCD (Table 3-4). To yield the progeny which deletes one copy of each gene, *cyt-c-*p$^{l(2)K13905}$/*CyO, y+* was crossed with *cyt-c-d* $^{Z2\text{-}1091}$/*CyO, y+*. The CNS of yellow progeny at 7 hours APF was dissected and Crz-IHC showed no vCrz neurons (Table 3-4), suggesting that half dosage of each gene does not affect vCrz PCD. Likewise, in a transheterozygous *cyt-c-d* mutants (*Z2-1091*/*bln*^{1}*)* which deletes *cyt-c-d* completely, Crz-IHC at 7 hours APF showed no vCrz neurons (Table 3-4), suggesting no role for the *cyt-c-d* on vCrz PCD. It is, however, possible that *cyt-c-p* may take over the missing *cyt-c-d* function since they has been found to have redundant functions. The generation of *cyt-c-d*-specific or *cyt-c-p*-specific targeted knock-down using RNA interference will be useful to determine the role of each gene for vCrz PCD.

We also investigated whether elevated expression of the *cyt-c* is able to accentuate vCrz PCD. To do this, a UAS-*mCD8-GFP*;;*Crz-gal4* was crossed with *UAS-cyt-c-p* or *UAS-cyt-c-d,* and then the progeny at 1 hour APF and 7 hours APF were

Table 3-4. Effect of *cyt-c* and *Buffy* on vCrz PCD

	cyt-c-p	*cyt-c-d*	Crz-IRys in VNC at 1 h APF	Crz-IRys in VNC at 6.5-7 h APF
Copy number	2	1	ND	None
	1	2	ND	None
	1	1	ND	None
	2	0	ND	None
	cyt-c-p overexpression		8 pairs	None
	cyt-c-d overexpression		8 pairs	None
	Buffy overexpression		ND	None

ND; not determined.

collected. Crz-IHC of these prepupae revealed normal programming of vCrz cell death, suggesting that *cyt-c* expression does not accelerate vCrz PCD (Table 3-4) and thus *cyt-c* may not be required for vCrz PCD.

If cyt-c is not involved in the formation of 'Dronc-Dark' complex, it is possible that this complex becomes activated by some other factor. The candidate for this is Bcl-2 family Buffy which has been reported as anti-apoptotic protein in *Drosophila* (Quinn et al., 2003). It is proposed that Buffy (bound to membrane or cytoplasm) binds and inhibits Dronc-Dark complexes and then releases this complex to be activated in response to death stimuli (Kornbluth and White, 2005). To determine if *Buffy* is able to block vCrz PCD, a *UAS-mCD8-GFP*;;*Crz-gal4* was crossed with *UAS-Buffy*^{II}. *Crz-gal4*-driven GFP expression of progeny CNS at 6.5 hours APF showed no vCrz neurons (Table 3-4), suggesting *Buffy* may not have a role for blocking vCrz PCD.

V. Discussion

During post-embryonic CNS development in *Drosophila*, two prominent waves of neuronal cell death have been observed mostly in the VNC: the first during prepupal stage, and the second within 24 hours after adult emergence (reviewed in Truman et al., 1993). As for the latter, a group of ~300 neurons (termed type-II) which had been characterized by high levels of EcR-A expression throughout the latter half of pupal development and a subset of neurons expressing CCAP neuropeptide in the VNC, undergo PCD in response to the fall in ecdysone levels (Robinow et al., 1993, 1997; Draizen et al., 1999). Such hormonal change triggers accumulation of *rpr* and *grim* transcripts (Robinow et al., 1997; Draizen et al., 1999); at least for CCAP-neurons, *rpr*

was verified to be a death activator (Peterson et al., 2002). It is, however, unknown as to how the fall in ecdysone levels is signaled to activate *rpr* expression and whether *rpr* promotes the death by antagonizing DIAP1 functions.

In contrast to the post-eclosion neurons just described, vCrz neurons are removed via PCD soon after the onset of metamorphosis (this study). Although we have no direct evidence for ecdysone as a death signal for this event, our data suggest that activation of EcR-B in response to a surge of ecdysone at pupariation might be a key upstream molecular event, which in turn stimulates an irreversible death pathway in which *rpr* plays a critical role. Therefore, these two comparative model systems show how ecdysone regulates the PCD of distinct neuronal groups at different developmental stages.

Interestingly, EcR-B receptors are also major signal transducers for remodeling of persistent larval neurons during early metamorphosis. For instance, SCP-IR neurons and mushroom body γ-neurons initially lose their neurites at this stage (Schubiger et al., 1998, 2003; Lee et al., 2000b). Genetic ablations of *EcR-B* prevent such processes, and the mutant phenotype is rescued by transgenic expression of EcR-B isoforms. Therefore, EcR-B-mediated signal transduction likely controls remodeling of persistent neurons as well as PCD of obsolete neurons during this critical developmental period. These observations then raise an important question as to how distinct neuronal fates (remodeling *vs.* death) are determined in response to the same hormonal stimulus and receptor types involved. Perhaps activated EcR-B in persistent neurons might silence the death pathway or turn on anti-apoptotic activities.

Apoptotic pathways downstream of activated EcR

In the case of ecdysone-triggered salivary gland and midgut degeneration, Northern blotting has shown that *rpr* and *hid* are transcriptionally induced just prior to death (Jiang et al., 1997, 2000). Such induction requires BR-C functions, since *rpr* and *hid* expression in these tissues is impaired by rbp^5 and $2Bc^2$ mutant alleles of the *BR-C* locus (Jiang et al., 2000; Lee et al., 2002a). Ecdysone also directly activates *rpr* transcription in the salivary glands via an interaction between activated EcR and its consensus binding sequence (EcRE) within 1.3-kb upstream of the *rpr* (Jiang et al., 2000). Our various findings support *rpr* as an intracellular death promoter for vCrz PCD. Although we do not have definitive evidence for direct activation of *rpr* by ecdysone, since the 1.3-kb *rpr* promoter apparently drives *p35* expression in vCrz neurons (Fig. 3-11E), we favor the hypothesis that activated EcR-B directly induces *rpr* transcription in the doomed vCrz neurons. Upregulation of *rpr*, however, does not seem to require BR-C, since we found normal vCrz PCD in the *BR-C* mutants (data not shown).

Another downstream target of the ecdysone signaling is DRONC. In vitro treatment of salivary glands and midgut with ecdysone induces *dronc* expression (Dorstyn et al., 1999), perhaps through a direct interaction between activated EcR-B1 and a consensus EcRE found in the *dronc* promoter (Cakouros et al., 2002, 2004a). Upregulation of *dronc* transcription may be important for supplying doomed cells with a sufficient amount of DRONC in order to conduct massive cellular destruction in response to death signals. Further analysis will be necessary to determine if this also occurs in doomed vCrz neurons.

Involvement of RPR and caspases in the vCrz PCD raises another fundamental question as to how RPR leads to caspase activation. According to a current model,

interactions between RPR and DIAP1 antagonize DIAP1's inhibitory action, resulting in the accumulation of free active caspases (reviewed in Bergmann et al., 2003). In contrast, we did not find any evidence for DIAP1 as a survival factor for vCrz neurons. Although other DIAP1-like proteins in *Drosophila* (DIAP2, BRUCE, and DETERIN) are possibly functional in this system, we speculate that this might not be the case. This is because failure of ectopic *diap1* expression to block vCrz PCD suggests that other DIAP family members would not be effective in inhibiting vCrz cell death, since anti-apoptotic functions of these proteins are mediated by consensus BIR domains (Bergmann et al., 2003). Thus, we propose that RPR-mediated caspase activation occurs independently of DIAP1 in vCrz neurons.

RPR perhaps mediates an assembly of the apoptosome, since both DRONC and DARK--two essential components of the apoptosome--are necessary for vCrz PCD (Fig. 3-16A, B). In vertebrate cells, the formation of the apoptosome triggered by the release of cyt-c from mitochondria is an essential step toward caspase activation (Liu et al., 1996; Cain et al., 1999). However, such molecular events are not evident in flies yet. Our study suggested that cyt-c might not be involved in vCrz PCD, thus the formation of apoptosome complexes may not need cyt-c to execute vCrz PCD.

Chapter Four

Programmed cell death of subsets of CCAP neurons in D. melanogaster

I. Abstract

Crustacean cardioactive peptide (CCAP) neuronal death occurs during adult eclosion in reponse to the fall in ecdysone levels in *Drosophila*. The results of *P35* expression in CCAP neurons suggest that CCAP neurons on the ventral side of the thoracic ganglion as well as the subesophageal region in the brain undergo programmed cell death after adult eclosion. Genetic analyses reveal that cell death activators, *reaper* (*rpr*) and *hid,* are responsible for CCAP cell death, and the initiator caspase Dronc also contributes to CCAP PCD. Although overexpression of *Drosophila* inhibitor of apoptotic protein 1 (DIAP1) prevents CCAP PCD, targeted knockdown of DIAP1 does not show any effect. CCAP PCD is not affected in *dark* mutants as well as by transgenic *cyt-c* expression, suggesting no role of apoptosomes for cell death pathway. The effector caspase *dcp-1* is not required for CCAP cell death. Overall, *rpr* and *hid*-mediated caspase Dronc activation is the main death pathway for CCAP PCD.

II. Introduction

At adult eclosion, two groups of neurons was known to undergo programmed cell death in response to the fall in ecdysone levels in *Drosophila*: Type-II neurons and CCAP neurons. The former group is composed of approximately 300 neurons in the VNC and

expresses high level of EcR-A isoform (Robinow et al., 1993). The latter is a group of peptidergic neurons which express Crustacean cardioactive peptide (CCAP) and are involved in ecdysis initiation (Draizen et al., 1999; Ewer and Reynolds, 2002; Park et al., 2003). Previous studies have shown that the doomed CCAP neurons accumulate *rpr* and *grim* transcripts which is prevented by application of 20-HE (hydroxyecdysone). Peterson et al. (2002) showed that CCAP PCD is blocked in a *rpr*-null mutant. Similarly, N4 neurons, four typical type-II neurons accumulate *rpr* and *grim* transcripts prior to death and this *rpr* accumulation is inhibited by application of ecdysone (Robinow et al., 1997). These studies thus suggested *rpr* and *grim* are important for the PCD of post-eclosion neurons in response to the decline of ecdysone titers.

Despites these results, molecular death pathways downstream of *rpr* and *grim* remained enigmatic. Here, our study shows that PCD also occurs in the subesophageal ganglion of the brain and that *rpr*- and *hid*-dependent CCAP PCD occurs via a *dronc*-activated pathway. Although *diap1* knockdown does not affect CCAP PCD, ectopic expression of *diap1* and *diap2* prevents cell death.

III. Materials and methods

Drosophila species

A *CCAP-gal4* line used here was described previously (Park et al., 2003). Double homozygous lines carrying both *CCAP-gal4* and *UAS-mCD8-GFP* (or *UAS-lacZ*) were generated by genetic crosses. These lines were crossed to the following UAS responder to manipulate transgenic products as described in Chapter 3; *UAS-p35* to prevent PCD (Hay et al., 1995); *UAS-EcR-A* to overexpress a EcR-A isoform (Carney et al., 2004);

UAS-diap1 (Hay et al., 1995) and *UAS-diap2* (Wing et al., 1998) to produce *Drosophila* inhibitor of apoptotic proteins; *sym-UAS-diap1*^{RNAi} to knockdown *diap1* levels (Huh et al., 2004); *UAS-cyt-c-p* and *UAS-cyt-c-d* to produce a component of apoptosome cytochrome c (Arama et al., 2006); *UAS-Buffy* to produce a putative anti-apoptotic protein (Quinn et al., 2003).

To examine CCAP expression in a *rpr*-null mutant, a *UAS-mCD8-GFP; H99/TM6C Tb Sb* was crossed to *CCAP-gal4*; *XR38/TM6B Tb Hu* and the progeny (*UAS-mCD8-GFP/+; CCAP-gal4/+; H99/XR38*) was subjected to GFP staining. For a *head involution defective* (*hid*)-null mutant, a *UAS-mCD8-GFP;H99/TM6C* was crossed with *CCAP-gal4;hid*^{05014}*/TM6C* and the progeny *(UAS-mCD8/GFP/+; CCAP-gal4/+;hid*^{05014}*/H99)* was obtained. Since a *EcR-A*-null mutant (*EcR*^{112}*/EcR*^{m554fs}) is lethal at adult stage, the flies heterozygous for *EcR*^{112} *allele (EcR*^{112}*/CyO, y+)* was tested for a *EcR-A* mutant. A *dronc*-null mutant was obtained by transallelic combination of *dronc*^{I24} (or *dronc*^{I29}) with *dronc*^{51} (Chew et al., 2004; Xu et al., 2005). A *dark*^{CD4} allele was used as *Drosophila Apaf-1-related killer* (*Dark*) mutation (Rodriguez et al., 1999), and a *dcp-1*^{prev1} as a *Drosophila caspase-1* (*dcp-1*)-null mutant (Laundrie et al., 2003), as previously described in Chapter 3.

Histochemistry

X-gal histochemistry, GFP staining, and immunohistochemistry (IHC) were performed as described in Chapter 3. To detect *CCAP* promoter-driven *lacZ* signal in *diap1* knockdown lines, immunohistochemistry using antibody against β-galactosidase was employed. *In situ* hybridization (ISH) was processed, as described in Chapter 3

except using CCAP cRNA probe (Park et al., 2003). All images were acquired by Olympus BX61 connected with CC-12 camera.

IV.Results

Programmed cell death (PCD) of CCAP neurons during pupa to adult transformation.

In the CNS of pharate adult (fully formed adult within the pupal case), CCAP-IR neurons are observed in three distinct grops of neurons in the VNC: 24 neurons in the dorsal region of the third thoracic/abdominal ganglion (dCCAP), 6-8 in the ventral region (vCCAP), and 4-6 in the abdominal ganglion (aCCAP) (Draizen et al., 1999). Within 24 hrs after eclosion, aCCAP-IR neurons remained intact, and most of vCCAP and dCCAP neurons were found to undergo PCD. To delve into the mechanisms of such neuronal death after eclosion, we first analyzed CCAP expression patterns in the adult CNS using the GAL4/UAS system. In addition to the aforementioned CCAP-IR neurons in the VNC, GFP-labeled CCAP neurons revealed two distinct subsets of neurons within the brain: two neurons in medial protocerebrum (mCCAP), and four pairs of neurons in the subesophageal ganglion (sCCAP) (Fig. 4-1A, B).

In the brain, two mCCAP cell bodies are dorsally located along the midline in the protocerebrum. Neuronal projections of mCCAP neurons were not examined in this study. Another set of CCAP neuron in the brain is neurons which are ventrally located in the subesophageal ganglion (sCCAP). The maximum four sCCAP cell bodies were observed in each brain hemisphere, but occasionally 2-4 cells observed. Although the neurites of sCCAP neurons seem to project up toward to esophagus foramen and down to

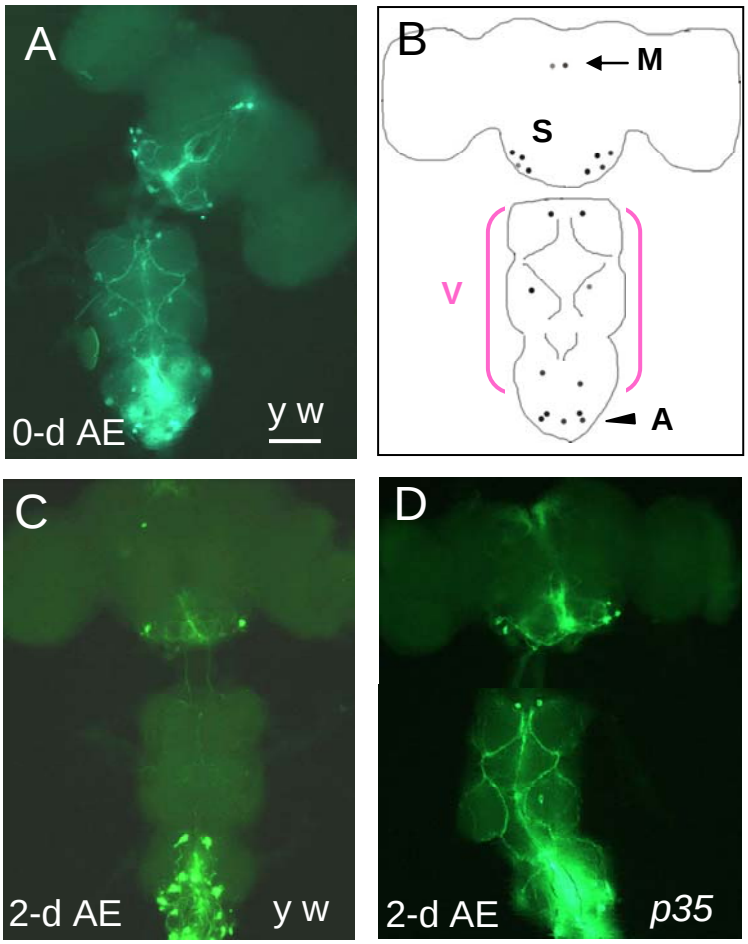

Figure 4-1. Programmed cell death of vCCAP and sCCAP neurons. *UAS-mCD8-GFP:CCAP-gal4* was crossed to (A,C) *y w* and (D) *UAS-p35*. The adult progeny CNS was observed under fluorescent microscopy. **(A, B)** CCAP expression in 0-day old CNS, (B) representative illustration of (A). The CCAP neurons located dorsally in the metathoracic neuromere (dCCAP) are omitted in B. **(C)** CCAP expression in 2-day old CNS. **(D)** *p35* expression in CCAP neurons in 2-day-old CNS. The cell death of sCCAP and vCCAP neurons was prevented by *p35*, however, mCCAP and aCCAP cells are not affected. Images in A, C are combination of all focal planes from the dorsal end to the ventral end of the CNSs whereas the image in D focuses on sCCAP neurons and vCCAP neurons. AE: After Eclosion, M: Medial protocerebrum, S: Subesophageal ganglia, A: Abdominal ganglia V: Ventral. Scale bar: 100 µm.

the ventral nerve cord, detailed examination of the anatomy was not performed. In the thoracic ganglion, 5-7 vCCAP cell bodies were observed in the ventral side and named as vCCAP neurons; Two cells are symmetrically positioned along the midline in the prothoracic neuromere, two cells symmetrically in the mesothoracic neuromere, and one to three cells in the metathoracic/abdominal neuromere. The vCCAP neurons located in metathoracic neuromere are easy to be mistakenly considered as abdominal cells or can be indistinguishable by strong dCCAP GFP signals, hence the number of vCCAP neurons we examined here is minimum 1 to maximum 3 and does not match to 4 as described in Draizen et al., (1999). A group of abdominal neurons (aCCAP) are located at the extreme posterior of the VNC, and the number of aCCAP neurons was not exactly counted. The CCAP neurons dorsally located in the metathoracic neuromere are called dCCAP neurons, and the number of dCCAP neurons was also not counted.

Previous reports suggested that vCCAP as well as dCCAP neurons are eliminated via programmed cell death soon after adult emergence while only aCCAP neurons left intact in the VNC (Draizen et al., 1999, Peterson et al., 2002). Consistent with this, CCAP promoter-driven reporter GFP signals were undetectable in the vCCAP neurons of 2-day-old CNS (Fig. 4-1C). Surprisingly, however, numerous dCCAP neurons were found to be intact. Since CCAP-IHC (Draizen et al., 1999) as well as our CCAP-ISH (See p. 159) were unable to detect dCCAP signals at this time point, it is possible that overproduction of membrane-targeted GFP may interfere with normal apoptotic pathway. We found that GFP-labeled sCCAP signals also reduce in number to approximately1.2 cells in the brain, and sCCAP neurite signals significantly reduced (Fig. 4-1C). In

contrast to these subsets of neurons, two mCCAP neurons and a group of aCCAP neurons are still detectable at 2 days after eclosion (Fig. 4-1C).

To determine PCD of vCCAP and sCCAP neurons, we ectopically expressed caspase inhibitor *p35* in CCAP neurons by crossing *CCAP-gal4;UAS-mCD8-GFP* to *UAS-p35*. In 2-day-old progeny, 4 vCCAP cells in prothoracic and mesothoracic neuromeres (The vCCAP cells in the metathoracic neuromere were not distinguishable from dCCAP neurons due to the high background of GFP-labeled dCCAP neurons, hence I focused on vCCAP neurons observed in upper two thoracic segments.) and 3-4 sCCAP neurons in each brain hemisphere remained detectable (Fig. 4-1 D vs. C). These results verify that vCCAP and sCCAP neurons undergo the programmed cell death via caspase-dependent pathways.

The role of EcR-A on CCAP PCD

Since PCD of vCCAP neurons are induced by the decline of ecdysone titers, and vCCAP neurons are EcR-A immunoreactive prior to death (Draizen et al., 1999), we hypothesized that EcR-A isoform is a signal transducer for this type of developmentally regulated cell death. Since injection of flies with 20-HE within 30 minutes of eclosion suppressed the death of vCCAP neurons, it has been postulated that active EcR-USP complex is required for protection of these neurons from premature death perhaps via suppression of proapoptotic genes (Robinow et al., 1997). It is therefore possible that reduced level of EcR-A may facilitate the PCD of vCCAP neurons, thereby inducing earlier death of vCCAP neurons. Conversely, higher levels of the EcR-A may attenuate the PCD of vCCAP neurons. To test the latter hypothesis, EcR-A isoform was

overproduced within the CCAP neurons and then GFP-reporter expression was examined in the CNS of 1-day-old adults (n=4). As a result, EcR-A expression did not suppress vCCAP and sCCAP neuronal PCD (Fig. 4-2 B vs. A), suggesting EcR-A expression does not prevent PCD in these subgroups. Interestingly, in contradiction to prediction, dCCAP PCD is accelerated. The molecular basis underlying this result is currently unknown.

In a converse experiment, we tested whether reduced EcR-A level can cause premature cell death of CCAP neurons. *EcR-A* null mutant can be obtained by combination of two alleles EcR^{112} and EcR^{M554f}; however, due to the lethality of this transallelic flies (Carney et al., 2004), we tested the flies heterozygous for only EcR^{112} allele. CCAP- ISH at 0-day-old adult revealed normal expression of vCCAP and sCCAP neurons (n=3, Fig. 4-2C). Targeted *EcR-A* ablation using RNA intereference (*UAS-EcR-A RNAi*) in CCAP neurons will give a clue of the role of EcR-A for CCAP PCD.

rpr and _hid_ are PCD activators for CCAP cell death.

Accumulation of *rpr* and *grim* transcripts in the CCAP neurons prior to the death suggests that *rpr* and *grim* are death promoters of these neurons (Draizen et al., 1999). Moreover, Peterson et al. (2002) described that Anti-CCAP staining in *rpr*-null mutant (*H99/XR38*) showed prevention of CCAP PCD. To confirm the result, we observed *CCAP*-promoter-driven GFP fluorescence in the same mutant. We crossed *UAS-mCD8-GFP; H99/TM6C* to *CCAP-gal4;XR38/TM6B*, and then Tb^{+} CNS was visualized through fluorescent microscopy. The presence of elongated VNC in *rpr*-null mutant verified the lack of *rpr* as described in Peterson et al. (2002) (Fig. 4-3A). A *rpr*-null mutant CNS showed ca. 5.5 sCCAP neurons in the brain and ca. 6.6 vCCAP neurons in the VNC at 2-

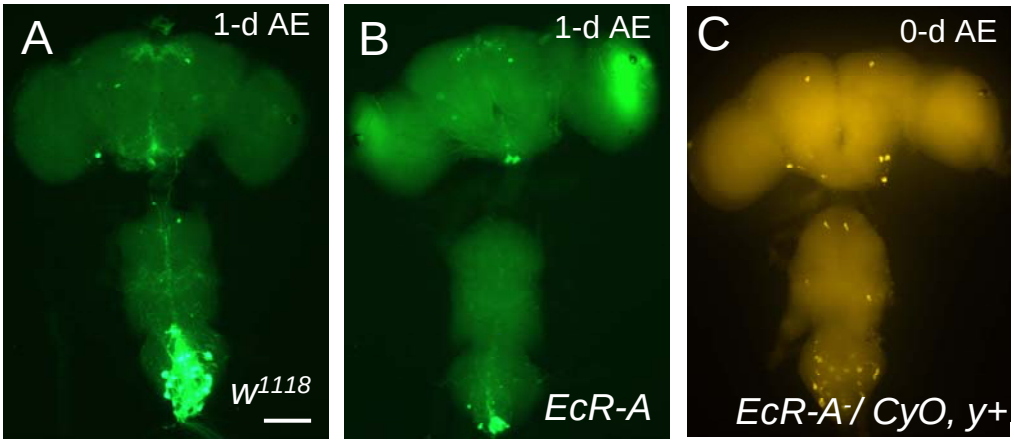

Figure 4-2. The effect of EcR-A on CCAP PCD. *UAS-mCD8-GFP:CCAP-gal4* was crossed to **(A)** w^{1118} and **(B)** *UAS-EcR-A*. The progeny CNS at 1 day after eclosion was observed under fluorescent microscopy. **(C)** CCAP-ISH of EcR^{112}*/CyO, y+* CNS at 0-day-old adult. All images are the combination of all focal planes from the dorsal end to the ventral end of the CNSs. Scale bar: 100 μm

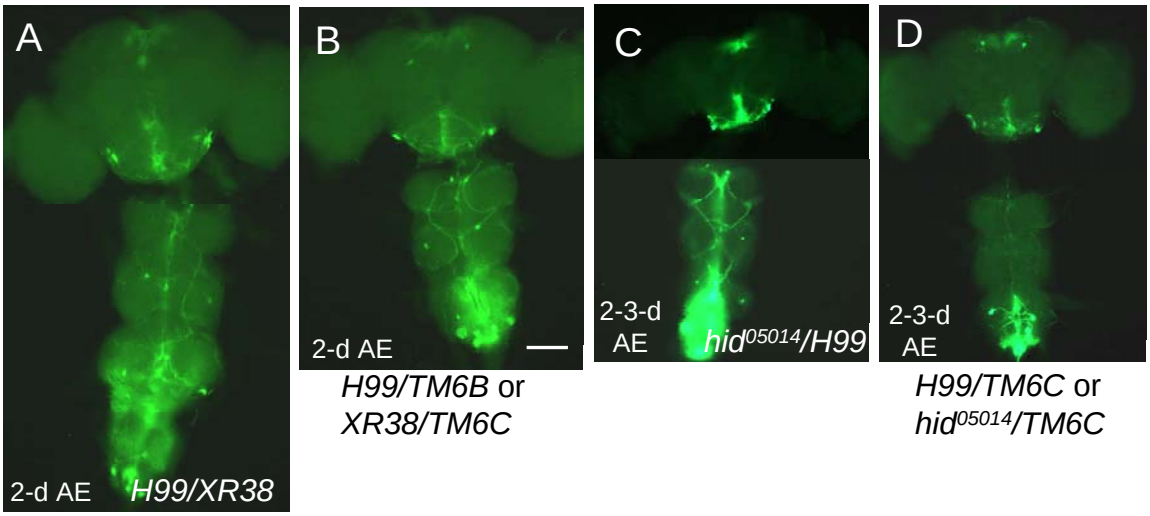

Figure 4-3. The role of *rpr* and *hid* on CCAP PCD. GFP-labeled CCAP neurons were visualized in **(A, B)** *rpr* mutants at 2-day-old adult and in **(C, D)** *hid* mutants at 2-3-day-old adult stage. (A) *UAS-mCD8-GFP*/+;*CCAP-gal4*/+; *H99/XR38* (B) *UAS-mCD8-GFP*/+; *CCAP-gal4*/+; *H99/TM6B* or *XR38/TM6C* (C) *UAS-mCD8-GFP*/+;*CCAP-gal4*/+; hid^{05014}/*H99* (D) *UAS-mCD8-GFP*/+;*CCAP-gal4*/+; hid^{05014}/ *TM6C* or *H99/TM6C.* In A and C panel, only sCCAP and vCCAP cells were focused for the images. B and D focus on all CCAP neurons. Scale bar: 100 μm.

day-old adult (n=4), indicating that sCCAP and vCCAP PCD are prevented (Fig. 4-3A). The prevention of CCAP PCD is also evident in flies heterozygous for *rpr*-null mutation. Approximately 5 sCCAP neurons in the brain and 4 vCCAP neurons in the VNC were detected in *XR38/TM6C* or *H99/TM6B* (n=4) (Fig. 4-3B). This result indicates that *rpr* plays a role for CCAP PCD.

To further define roles of *hid* for CCAP cell death, we investigated CCAP expression in a *hid* loss-of-function mutant. *UAS-mCD8-GFP; H99/TM6C* was crossed with *CCAP-gal4;hid^{05014}/TM6C* (Grether et al., 1995), and Tb^{+} progeny (*hid^{05014} /H99*) was collected as *hid*-null mutants. Ca. 6.6 sCCAP neurons and 6 vCCAP neurons were observed in a *hid* loss-of-function mutant (n=3), indicating that *hid* acts as a cell death executor for CCAP PCD (Fig. 4-3C). However, flies heterozygous for *hid* (*hid^{05014}/TM6C*) does not affect CCAP PCD (n=3) (Fig. 4-3D), suggesting that half dosage of *hid* is sufficient to cause CCAP PCD. Interestingly, types of balancer chromosomes produced opposite results since *H99/TM6C Tb Sb* does not affect CCAP PCD while *H99/TM6B Tb Hu* does (Fig. 4-3 D vs. B). Draizen et al. (1999) also analyzed vCCAP PCD in *H99/TM3 Sb* and vCCAP PCD was prevented in this mutant. Therefore, perhaps *Sb* marker in balancer *TM6C* may be involved in inhibition of *H99* effect. However, the molecular basis about this is not known yet.

Prevention of CCAP PCD by DIAP1 expression

Since *Drosophila* apoptotic protein 1 (DIAP1) is a central regulator for PCD (Hay et al., 1995), we tested whether overexpression of DIAP1 can suppress the PCD of CCAP neurons. To express DIAP1 (or DIAP2) in CCAP neurons, a double homozygous *CCAP-*

gal4, UAS-lacZ was crossed to a *UAS-Diap1* or a *UAS-Diap2* (Wing et al., 1998) and the progeny CNS was subjected to X-gal histochemistry. The wild-type 1-day-old adult CNSs show approximately 1.6 sCCAP neurons in the brain, and no vCCAP neurons in the VNC (Fig. 4-4A, D) whereas the same aged *diap1*-expressed CNSs show 5.5 sCCAP neurons and 4.6 vCCAP neurons (n=4) (Fig. 4-4B, E), and *diap2*-expressed ones show 4.6 sCCAP and 4.5 vCCAP neurons (n=5) (Fig. 4-4C, F). The data indicate that both DIAP1 and DIAP2 inhibit sCCAP and vCCAP PCD.

Since DIAP1 expression blocked CCAP PCD, we tested whether lack of DIAP1 can accelerate CCAP PCD. A *CCAP-gal4, UAS-lacZ* was crossed with *symUAS-diap1*^{RNAi}, and β-gal-IHC of the progeny CNSs was performed at pharate adults just prior to eclosion as well as 3-4.5 hours after eclosion. However, β-gal-IHC showed normal CCAP expression, suggesting that loss of DIAP1 does not affect CCAP PCD (Fig. 4-4H, I vs. G). To understand the molecular behavior of endogenous *diap1* as a role for PCD inhibitor, the super-expression of two-copies of *sym-DIAP1*^{RNAi} in CCAP neurons instead of one copy as above will be necessary.

The role of capases on CCAP PCD

Since the intiator caspase Dronc is a direct target of DIAP1, normal CCAP PCD by loss of DIAP1 suggests that Dronc also might not contribute to CCAP PCD. In contrast to the prediction, CCAP-ISH of 2-3-day-old adult CNS in *dronc*-null mutant (*dronc*^{51}/*dronc*^{I24}) revealed 4 sCCAP neurons in the brain and 6.5 vCCAP neurons in the VNC (n=2), suggesting that *dronc* function is required for CCAP PCD (Fig. 4-5C). As a control, CNSs heterozygous for *dronc* (*dronc*^{51}/ *TM6C*, *dronc*^{I24}/*TM6C*, *dronc*^{I29}/*TM6C*)

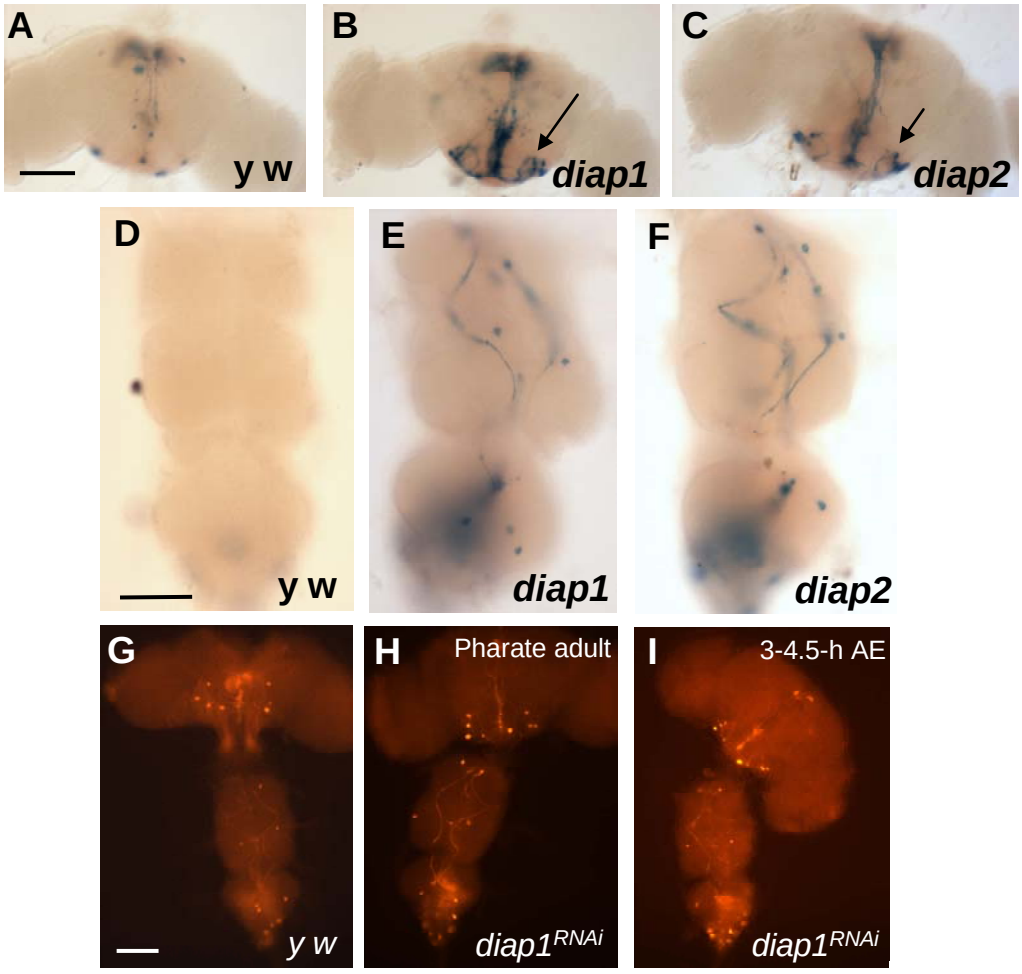

Figure 4-4. *diap1* effect on CCAP PCD. **(A-F)** X-gal histochemistry of the progeny at 1day-old adult from [*CCAP-gal4: UAS-lacZ* x (A, D) *y w* (B,E) *UAS-diap1* (C,F) *UAS-diap2*]. (A-C) brain (D-F) VNC. The *diap1* and *diap2* expression prevented the death of sCCAP neurons (arrows in B, C) and vCCAP neurons in E, F. **(G-I)** β-gal-IR cells of progeny at pharate adult (G, H) and 3-4.5 hours after eclosion (I) from the cross [*CCAP-gal4:UAS-lacZ* x (G) *y w*, (H,I) *SymUAS-DIAP1*^{RNAi}. Diap1 knockdown does not accelerate CCAP PCD. Scale bar: 100 μm.

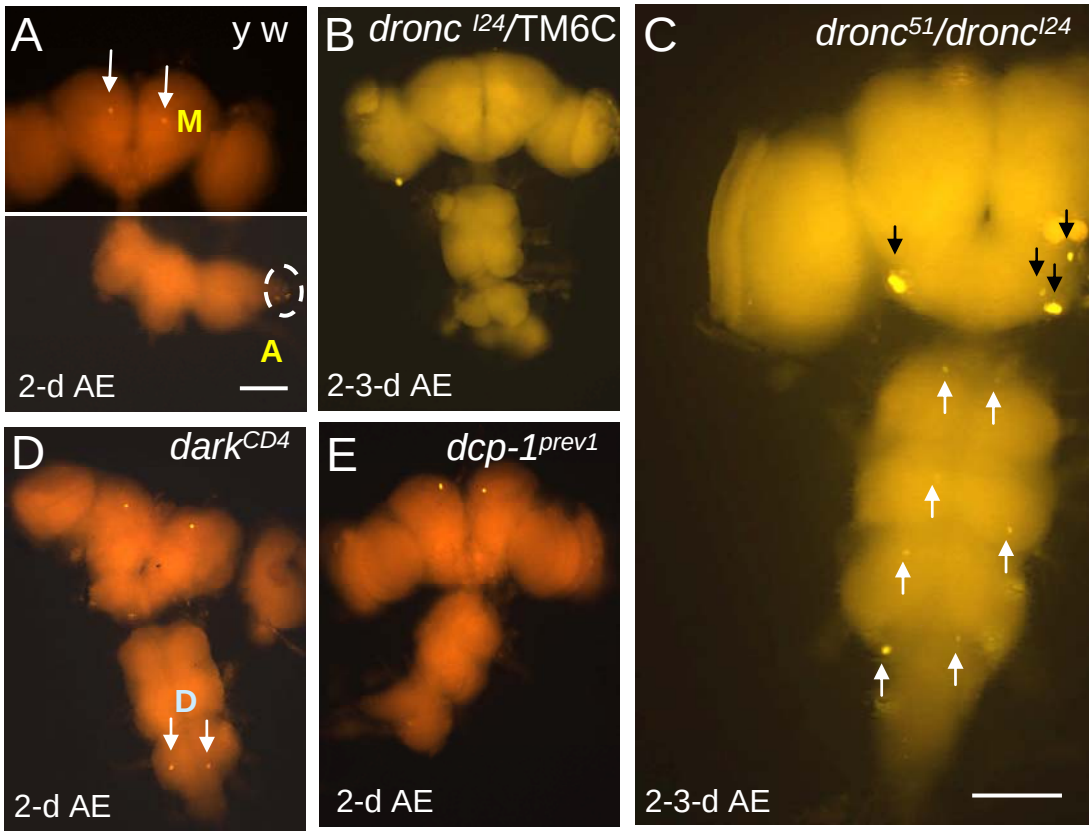

Figure 4-5. The effect of caspases and *dark* on CCAP PCD. CCAP-ISH was observed in the 2-3-day old CNSs of **(A)** *y w*, **(B)** *dronc* heterozygote, **(C)** *dronc*-null mutant, **(D)** *dark* hypomorphic homozygote, and **(E)** *dcp-1*-null mutants. (A) 2-day old *y w* CNS shows two mCCAP signals (arrows) and several aCCAP signals (dotted circle). (C) *dronc*-null mutants show 4 sCCAP signals (black arrows) and 7 vCCAP signals (white arrows). (D) *dark* mutants show two distinct dCCAP signals (arrows). (A, D, E) Pictures are generated by combining all images along the Z-axis. (B, C) Images visualize only ventral side of the CNS. M: medial protocerebrum CCAP, A: abdominal ganglia CCAP neurons, D: dorsal CCAP neurons. Scale bar:100 μm.

did not show sCCAP-and vCCAP-ISH signals at the same age as seen in *y w* control (Fig. 4-5B vs. A).

Since caspase adaptor *Dark* targets *dronc* in *Drosophila*, we examined the role of *dark*. CCAP-ISH of a *dark* hypomorphic mutant ($dark^{CD4}$) revealed no sCCAP and vCCAP signals in 2-day-old adult CNSs (n=4), suggesting that *dark* does not contribute to CCAP PCD (Fig. 4-5D). Interestingly, $dark^{CD4}$ mutants showed two dCCAP ISH signals out of 24 (n=4), suggesting a role of *dark* for dCCAP PCD in a cell-specific manner.

Since CCAP PCD is a caspase-dependent process as *p35* expression blocked the death of CCAP neurons (Fig. 4-1D), other caspases may play a role for the death. We tested the role of an effector caspase *dcp-1* for CCAP PCD. CCAP-ISH of 2-day old adult CNS in a *dcp-1*-null mutant ($dcp\text{-}1^{prev1}$) revealed no defect for PCD of sCCAP and vCCAP neurons (n=5), suggesting that *dcp-1* is not a part of CCAP PCD machinery (Fig. 4-5E).

The role of *cytochrome-c* (*cyt-c)* and *Buffy* on CCAP PCD

Since a component of apoptosome, Dronc is required for CCAP PCD, we also tested whether *cyt-c* has a role for PCD (Kornbluth and White, 2005). A *UAS-mCD8-GFP;CCAP-gal4* was crossed to *UAS-cyt-c-p* or *UAS-cyt-c-d* (Arama et al., 2006) and GFP signals in the CNS of just eclosed progeny revealed normal CCAP expression (*UAS-cyt-c-p*, n=2; *UAS-cyt-c-d*, n=4), suggesting *cyt-c-p* or *cyt-c-d* expression does not accelerate PCD (Fig. 4-6 B,C vs.A).

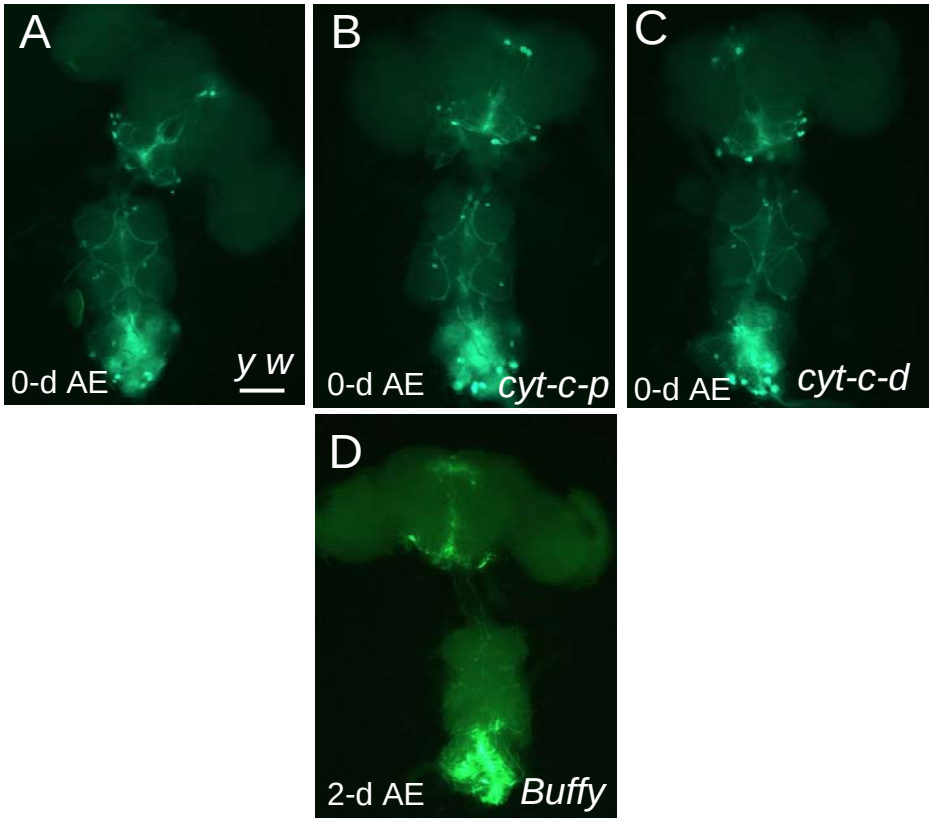

Figure 4-6. The effects of *cyt-c* and *buffy* on CCAP PCD. A *UAS-mCD8-GFP;CCAP-gal4* was crossed to **(A)** *y w*, **(B)** *UAS-cyt-c-p*, **(C)** *UAS-cyt-c-d*, **(D)** *UAS-buffy*. GFP-labeled CCAP neurons of the progeny CNSs at (A-C) 0 day and (D) 2 days after eclosion are visualized. Scale bar: 100 μm.

To test the effect of a putative anti-apoptotic protein Buffy on PCD, a *UAS-mCD8-GFP; CCAP-gal4* was crossed to *UAS-buffy* and the CNSs of 2-day-old adults were dissected. GFP signals in *Buffy*-overexpressed progeny revealed ca. 1.7 sCCAP neurons and no vCCAP neurons (n=4) while control showed 1.2 sCCAP and no vCCAP neurons (Fig. 4-6 D vs. Fig 4-1C), indicating that *buffy* overexpression does not significantly prevent sCCAP and vCCAP PCD.

V. Discussion

rpr-and *hid*-mediated Dronc activity for CCAP PCD

In response to the fall in ecdysone levels, CCAP neurons undergo cell death in *Drosophila* as well as *Manduca sexta* (Ewer et al., 1998; Draizen et al., 1999). Fly genetics made it easier to investigate the mechanism of CCAP cell death in *Drosophila* and the work in Draizen et al. (1999) was pioneering to determine neuronal death pathway. However, further examination of the mechanism of CCAP neuronal death was necessary since the PCD of this identifiable neuron can be a good model system to compare to PCD of the doomed neurons during early metamorphosis. The observation of sCCAP and vCCAP PCD in our study proved that *rpr* is a critical PCD acitivator as shown in Draizen et al. (1999). However, in contast, our study shows that *hid* is also essential for CCAP PCD. The authors of Draizen et al. (1999) examined the role of *hid* for CCAP PCD in the flies heterozygous for *hid* mutation and found no defect for CCAP PCD in these flies, concluding that *hid* may not play a role for PCD. In our study, however, we used *hid*-null mutants to analyze the role of *hid* and found that CCAP PCD was prevented.

The role of caspase Dronc for CCAP PCD was first examined here. CCAP PCD requires Dronc activity; however, Dronc activation is likely to be independent of apoptosome formation, since both *cyt-c* and *Dark* does not seem to be required for the death. It is, however, possible that residual dark activity in the hypomorphic $dark^{CD4}$ mutation (Rodriguez et al, 1999) may be sufficient for the activation of *dronc*. To determine this further, it will be necessary to test *dark*-null mutant alleles, which has been isolated recently (Mills et al., 2006). *dcp-1* is not involved in CCAP cell death, suggesting that *dcp-1* is not downstream of PCD activator *rpr* and *hid* during CCAP PCD. Taken together, CCAP neuronal death is dependent on *rp*- and *hid*-induced Dronc activities.

Diverse functions of the CCAP neurons

Crustacean cardioactive peptide (CCAP) was originally isolated from the shore crab, *Carcinus maenas* as a peptide to display heart-beat accelerating activity (Stangier et al., 1987). The main function of the neuropeptide is involved in the molting process. While molting, the new cuticle develops beneath the old one, while much of the old culticle is resorbed. The process of shedding of the remaining old cuticle is called ecdysis. CCAP is believed to be a neuropeptide that initates this ecdysis program (Ewer and Reynolds, 2002). Consistent with this, CCAP knockout flies show failure of pupal ecdysis which then causes pupal lethality in most populations (Park et al., 2003). In addition, CCAP knockout flies exhibit circardian eclosion rhythms, however, the daily distribution of eclosion events are abnormal, suggesting that CCAP plays a role in mediating circadian control of adult eclosion (Park et al., 2003).

Based on the notion that PCD occurs when the cells are harmful or no longer useful, the death of CCAP neurons after eclosion, when ecdysis processes are not needed any longer, seems to be appropriate. However, two subsets of CCAP neurons remained alive after eclosion: mCCAP and aCCAP neurons. Therefore we speculate that these two groups of neurons may not have functions associated with ecdysis behavior.

Interestingly, CCAP was found to express in a non-neuronal tissue (Sakai et al., 2004). CCAP cDNA was isolated from adult midgut of cockroach, *Periplaneta americana*. ISH and IHC using cockroach anti-CCAP revealed that CCAP is expressed in the endocrine cells in the midgut as well as in the ingluvial ganglion, which innervates the midgut muscles. The addition of CCAP to *in vitro* midgut culture elevated digestive enzyme activity and also stimulated the contraction of guts. The author suggested that CCAP is produced in the ingluvial ganglion and transported to muscle, asting as a midgut factor to stimulate gut contractions (Sakai et al., 2004). It will be interesting to see whether *Drosophila* CCAP has such a function in the midgut.

Chapter Five

Discussion

I. Summary

The primary goal of this study is to gain insights into molecular bases of Crz gene regulation and function and to identify the mechanisms of programmed neuronal cell deaths. Especially for the latter, identified neuronal PCD mechanisms can be compared to other non-neuronal cell death mechanisms, helping to generate a more defined picture of the *Drosophila* PCD machinery.

I described three aspects related to Corazonin neurons here. First is the evolutionary aspect of Crz-encoding genes and Crz expression patterns. Although *Crz* sequences evolve rapidly during the course of *Drosophila* evolution, Crz expression patterns in the CNSs are conserved, suggesting a similar biological role among different species.

The second aspect is developmental dynamics of Crz-expressing neurons. The spatial expression patterns of Crz during development correlates with its function. This is summarized as follows: (1) whole sets of Crz neurons including DL, DM and VNC neurons are already formed during embryogenesis before larval molting, suggesting that all sets of neurons might be involved in larval development or behavior. (2) Axon terminals from DL neurons project to corpora cardiaca (CC) and aorta, Crz is likely to be secreted to a circulatory system and functions as a neurohormone. (3) The function of vCrz neurons is likely to be unnecessary in adults, since vCrz neurons die within 6 hours after puparium formation. (4) Approximately 3-5 adult specific neurons are formed in

the vicinity of persisting larval DL neurons within ~2 days after puparium formation. Like larval DL neurons, adult DLP-Crz neurons also project to the CC. (5) Crz may have a function associated with biological rhythms due to Crz expression in clock neurons producing *per* (*period*) (Choi et al., 2005) and anatomical proximity of Crz neurons to the terminals of Pdf-producing clock neurons.

The third aspect is the determination of neuronal PCD mechanisms. In the course of analyzing Crz expression during development, we found that vCrz neurons undergo PCD. The observation led us to investigate the molecular PCD mechanisms using sophisticated genetic tools available for *Drosophila*. Ecdysone signaling through EcR-B isoforms is required for vCrz PCD and *rpr*-induced vCrz neuronal death also requires *dark* and caspases *dronc* and *dcp-1*. By comparison, CCAP neuronal PCD requires *rpr*, *hid*, and *dronc*. Overall, while molecular players found for the PCD of other *Drosophila* tissues are also essential in vCrz neuronal PCD, there seem to be additional mechanism(s) unique to this type of neuronal death. This is certainly an example that points to the existence of distinct death-inducing pathways, that might be specific to cell or tissue types.

II. Anti-apoptosis of vCrz neurons during larval development

For the developmentally controlled PCD, activation of PCD pathways must be precisely coordinated with overall animal's developmental process. The observation that ecdysone signaling triggers vCrz PCD raises an important question as to how these cells survive during ecdysone-led larval-to-larval molting instead of precocious death. One possibility is that ecdysone levels are not sufficiently high to induce PCD pathways in the

vCrz neurons. Alternatively, ecdysone receptor expression is too low to transduce hormonal signals to activate PCD pathways. In fact, a previous report showed that EcR expression was extremely low in the CNS of first and second instar larvae (Truman et al., 1994). Thus, we determined whether elevation of ecdysone or ecdysone receptor levels could cause premature vCrz PCD. The former is accomplished by feeding early larvae with a food containing ecdysone (Berreur et al., 1984), and the latter by ectopic expression of EcR receptors to sensitize ecdysone signaling. As a result, neither treatments caused premature vCrz PCD (Fig. 3-9).

As an alternative to the subthreshold ecdysone signaling model, high levels of juvenile hormone (JH) during larval development might counteract ecdysone-induced cell death in larvae, since an ecdysone peak concomitant with a decline of JH leads to the larval-to-pupal metamorphosis (Riddiford, 1993). If this is true, then maintenance of high JH levels during prepupal stage may prevent or at least delay PCD. In line with this, it is notable that JH is able to suppress PCD in the prothoracic glands of *Manduca sexta* (Dai and Gilbert, 1998). JH agonist, administered to *Drosophila* juveniles, has been found to induce disruption of metamorphic reorganization of the CNS and salivary gland and musculature which is the event similar to BR-C defects (Restifo and Wilson, 1998). Despite this, however, larvae administered with a JH analog (methoprene), either by feeding or topical treatment, did not affect normal progress of vCrz cell death (Fig. 3-8). Thus far, the nature of the survival factors remains elusive.

III. Comparison between vCrz and CCAP PCD

During post-embryonic development of the *Drosophila* CNS, two successive waves of cell death events play a key role in sculpturing the final adult CNS. The first one occurs mostly during prepupal development in response to ecdysone surge at the end of larval stage. The second one occurs shortly after adult eclosion, and this later neuronal cell death is a response of the decline of ecdysone titers (Riddiford, 1993; Robinow et al., 1993). The former is represented by vCrz neuronal death whereas the latter by CCAP death. How different levels of ecdysone induce cell death during two phases of metamorphosis has not been clearly understood yet. However, it is likely that differential expression of EcR isoforms correlates with stage-specific ecdysone response (Truman et al., 1994). Most larval neurons express EcR-B1 isoforms at the start of metamorphosis while at a later stage, during pupal-adult transformation, the neurons express EcR-A in the maturation process and are fated to die after adult eclosion (Robinow et al., 1993;Truman et al., 1994). How expression of EcR isoforms is temporally regulated is not known yet. We speculate that Juvenile Hormone (JH) may be a key player in regulating EcR expression since JH modifies the developmental programs triggered by the ecdysteroid (Riddiford, 1993). An alternative possibility is that since EcR-A and EcR-B isoforms are encoded by different transcription units which contain different promoters, whereas EcR B isoforms (B1 and B2) are produced from mRNAs which are transcribed by alternative splicing (Talbot et al., 1993), it is also possible that any novel factors coordinating temporal expression of EcR isoforms may involve in their specific cis-aciting regulatory regions, and thus produce each EcR isoform complying the developmental stage. Further investigation will be necessary to identify the mechanisms

of temporal EcR isoforms in reponses to ecdysone. In context with this, the comparison about the PCD mechanisms of two groups of doomed neurons in response to a rise and a fall in ecdysone level, respectively, would provide a clue to define how the expression of differential EcR isoforms triggers PCD at different development stages.

The vCrz PCD and CCAP PCD are representative models of PCD at different developmental stages. These neuronal deaths have a common pathway: *rpr*-mediated *dronc* activation (Fig. 5-1). Despite the presence of the common pathway, there are also four major differences between them. First, vCrz PCD signaling is mediated by ecdysone receptor isoforms, EcR-B1 and EcR-B2, whereas CCAP PCD is likely to be mediated by EcR-A isoform, since CCAP neurons express EcR-A but not EcR-B1 (Draizen et al., 1999). Second, *hid* and *rpr* are PCD activators for CCAP PCD, whereas only *rpr* for vCrz PCD. Third, there are different PCD phenotypes about two neuronal deaths in the *dark* hypomorphic mutant ($dark^{CD4}$). The vCrz neuronal death is delayed in $dark^{CD4}$. In contrast, CCAP PCD was unaffected by $dark^{CD4}$ mutation, suggesting that DARK might not be a component for CCAP PCD. There are several examples of *dark*-independent PCD pathways. The larval midgut PCD and death of some embryonic cells are normal in *dark*-null mutant (Akdemir et al., 2006; Mills et al., 2006). Furthermore, the caspase activity is nearly absent in the prepupal extract of *dark*-null mutants, but detected in the larval extract of the same mutants. This finding suggests that *dark*- independent caspase activation occur in some tissues or cell types at different developmental stages (Mills et al., 2006). If there is a role of *dark* for CCAP PCD, the residual level of *dark* in hypomorphic mutants may be sufficient to execute cell death. In this case, complete *dark*-null mutants should be tested for CCAP PCD to investigate *dark* function.

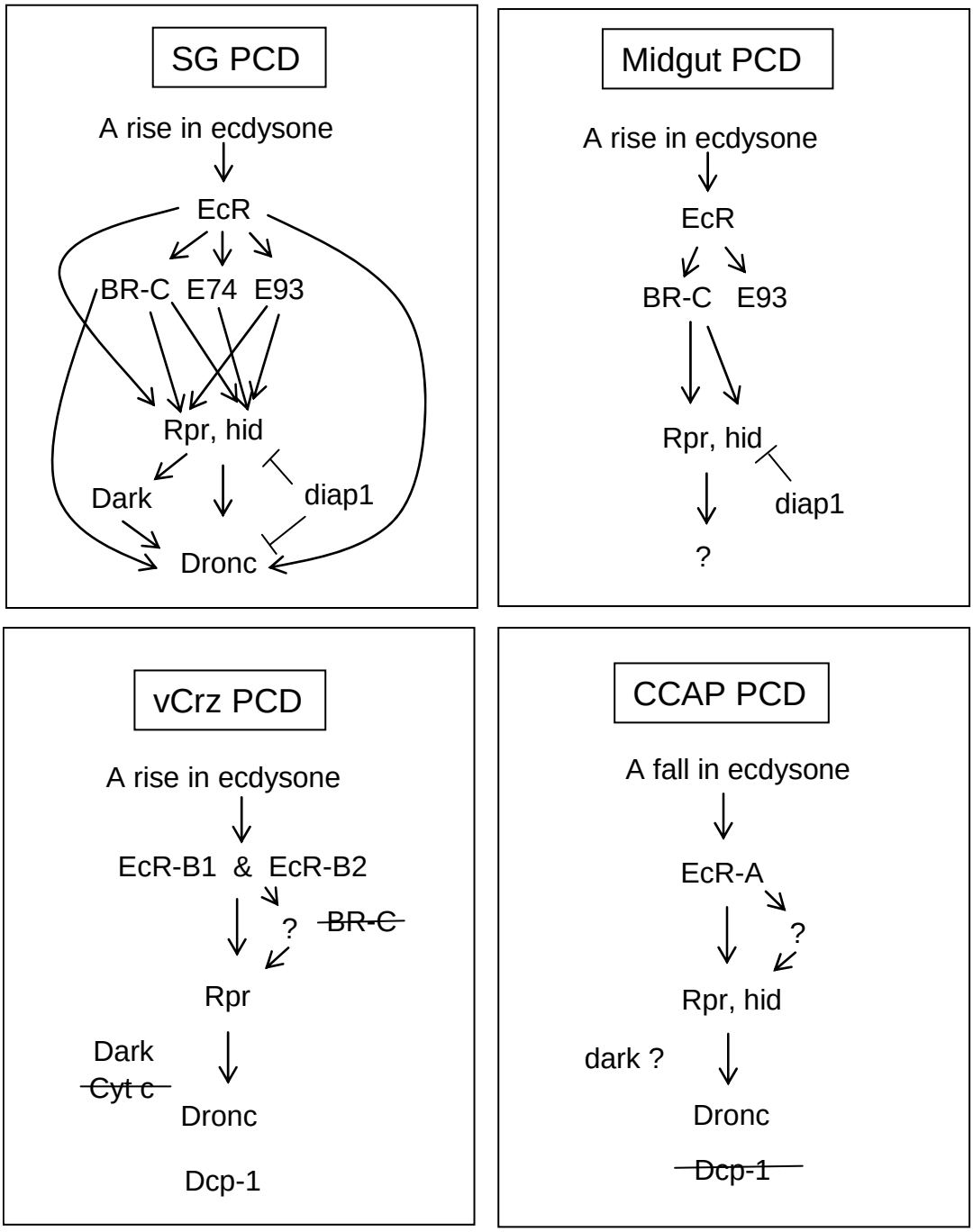

Figure 5-1. Comparison of ecdysone-induced PCD mechanisms. ? Represents components that are not defined yet. Strikethrough indicates components that are not involved in PCD.

Fourth, an effector caspase Dcp-1 is required for vCrz PCD but not for CCAP PCD, suggesting the presence of differential caspase machinery to execute PCD of different types of neurons. Since *dcp-1* was found to be dispensible for *hid*–mediated cell death in the eyes (Song et al., 2000; Leulier et al., 2006b) and CCAP PCD is caused by *hid*, perhaps lack of *dcp-1* role in CCAP PCD might be the characteristics of *hid*-mediated cell death.

IV. Upstream of the *reaper*

The proapoptotic gene, *rpr*, is essential for the PCD of vCrz neurons. Little is known, however, how *rpr* expression is induced by ecdysone signaling and how *rpr* stimulates caspase activities in vCrz PCD.

In the study of ecdysone-induced SG and midgut histolysis, activated EcR induces *rpr* transcription directly as well as indirectly (Fig. 5-1). During SG PCD, *rpr* transcription is directly activated by ecdysone via interaction between ecdysone complex and a cis-acting ecdysone response element in its promoter (Jiang et al., 2000). Alternatively, *rpr* expression is induced through activation of early genes *BR-C* or *E93,* since *rpr* transcription is reduced in these mutants (Lee et al., 2002b). For vCrz PCD, it remains to be determined whether *rpr* is induced directly or indirectly by ecdysone. We tested *Crz* expression in the *BR-C* mutants (rbp^5, $2Bc^1$, br^5), however, Crz expression was normal in those mutants, suggesting no role of *BR-C* for vCrz PCD. Thus vCrz PCD might not need *BR-C* function for *rpr* induction. Other early genes *E74* and *E93* mutants should be tested for Crz expression to determine the role of these genes. Compared to vCrz PCD, during the midgu cell death, *rpr* transcription is induced indirectly via BR-C

activation, since *rpr* expression is reduced in a *BR-C* mutant ($2Bc^2$) (Lee et al., 2002a). This is quite interesting since developmental timing of the midgut cell death is similar to that of vCrz PCD. These observations indicate that the same ecdysone peak does not necessarily induce the same genetic network of ecdysone response genes and thus the response is tissue- or cell-specific.

V. Downstream of the *rpr*

I will discuss *rpr* downstream pathways here as to how RPR leads to Dronc activation, and how Dcp-1 is activated, Dronc-independent pathway, and a *cyt-c* role in *Drosophila* cell death.

How *dronc* is activated by *rpr* signals is an important issue for defining the cell death pathways. In a conventional model, RPR antagonizes DIAP1 to unleash caspase Dronc from inactive complex with DIAP1, and then liberated Dronc becomes activated (Wang et al., 1999b; Goyal et al., 2000). The other pathway which is identified lately is Dronc activation through the interaction with Dark. Igaki et al. (2002) documented that the cell death caused by down-regulation of DIAP1 was accelerated by overexpression of *dronc* and *dark*, indicating interaction between Dronc and Dark. Furthermore, Dronc autoprocesses itself by cleaving in a Dark-dependent manner (Muro et al, 2004) and *dronc* genetically interacts with *dark* in the adult wings (Chew et al., 2004). Since our study reveals lack of Diap1 function in vCrz PCD, this result suggests that Dronc activation does not involve in the interaction with DIAP1. Instead, RPR might activate Dark which in turn forms apoptosome-like complexes with Dronc through CARD domains and induces Dronc processing.

Like Dronc, effector caspase Dcp-1 binds DIAP1 (Zachariou et al., 2003) and is tethered as an inactive form in the absence of death signal. In response to death signal, Dcp-1 is released from DIAP1 and leads to PCD. In addition, Dcp-1 needs protease function of initiator caspases like Dronc to be activated. In case of vCrz PCD, *dcp-1* is required for vCrz PCD, since *dcp-1* mutants show delayed cell death. Although the conventional model indicates that *dronc* is upstream of *dcp-1*, the comparison of vCrz PCD phenotype between *dcp-1* and *dronc* mutants suggests that these two caspases can reside not only in a hierarchy but also at a parallel level. A similar number of vCrz neurons was observed at similar developmental timing (7 hours after puparium formation) in both *dcp-1* anc *dronc* mutants (Table 3-3), suggesting they are parallel rather than in a hierarchy. However, complete death of vCrz neurons occurs earlier in *dcp-1* mutants than in *dronc* mutants (Table 3-3), suggesting for their hierarchial interaction. Interestingly, the super-expression of full length *dcp-1* is able to induce PCD in the eye (Song et al., 2000). This finding suggests that unprocessed Dcp-1 have weak autoprocessing activity and thus Dcp-1 may be activated without the help of Dronc. Altenatively, weak activity of full length Dcp-1 may result from processing by unknown factor(s). The former will be the example of the parallel model.

Third, the midgut cell death does not need *dronc* (Daish et al., 2004; Akdemir et al, 2006; Mills et al., 2006), suggesting existence of *dronc*-independent death pathway. Perhaps other initiator caspases such as Dredd or Strica may contribute to the midgut death. It is also possible that proapoptotic Bcl-2 family *debcl* might induce Dronc-independent death through unknown pathway.

To date, there is no definite evidence for the role of *cyt-c* in *Drosophila* cell death. Unlike in mammals, *Drosophila* cell culture study showed that *cyt-c* is not released from mitochondria in response to death stimuli unlike in mammals (Varkey et al., 1999; Dorstyn et al., 2002). *In vitro* study showed that *cyt-c* or any mitochondria factors are not intimately associated with the programmed cell death in *Drosophila* (Means et al., 2006). Consistent with these findings, our result showed that *cyt-c* is unlikely to be required for vCrz PCD. *cyt-c* involvement in the salivary gland and midgut degeneration was not tested yet. Since cyt c does not seem to be involved in PCD, it is conceived that the apoptosome-like complex consisting of Dronc and Dark in *Drosophila* might be a counterpart to the oligomerized complex of CED-3 and CED-4 in *C. elegans* which does not require *cyt-c*, and thus the mechanism of Dronc activation may be similar to that of *C. elegans* CED-3 activation. However, one of two *Drosophila cyt-c* genes, *cyt-c-d*, has been known to be required for caspase activation during spermatid differentiation (Arama et al., 2003; Arama et al., 2006). Perhaps this piece of genetic result suggests that cyt-c involvement in caspase activation might occur in a tissue-specific manner.

VI. Neuronal remodeling versus programmed cell death

During *Drosophila* larval-pupal metamorphosis, a wandering larval ecdysone peak triggers different neuronal fates in the nervous systems: remodeling or cell death. Larval neurons regress their neurites and later outgrow to an adult-specific form, or unnecessary neurons, such as vCrz neurons are fated to die, respectively (Levine et al., 1995; Consoulas et al., 2000). The best known examples of neurons that are respecified to perform adult-specific functions are mushroom body (MB) γ-neurons governing

olfactory learning and memory and neurosecretory cells that are immunoreactive for anti-SCP (small cardioactive peptide B) (Kraft et al., 1998; Schubiger et al., 1998). Intriguingly, EcR-B isoform-mediated ecdysone signaling regulates the remodeling process of these neurons (Lee et al., 2000b; Consoulas et al., 2002; Zheng et al., 2003; Brown et al., 2006). Since EcR-B isoform is implicated in vCrz PCD as well as remodeling process of SCP neurons and MB γ-neurons, it is intriguing why the same hormonal signal causes two different consequences. Perhaps suppression of proapoptotic functions or enhancing of prosurvival activities may occur through unknown mechanisms during the remodeling process. At least the pruning process does not seem to utilize the apoptotic machinery. For example, the pruning of MB γ-neurons is normal in neuroblast clones homozygous for Df (H99), indicating that cell death activator *rpr*, *grim*, and *hid* are not required for the pruning process (Watts et al., 2003). Moreover, *p35* expression does not affect normal MB neuronal pruning, suggesting that the pruning process is irrelevant to the caspase-dependent apoptosis pathway (Watts et al., 2003). First hypothesis for the absence of cell death during remodeling process is that the transcription of the *rpr*, *grim*, and *hid* remains off through unknown mechanisms. The other possibility is that during pupariation RHG genes may be induced by ecdysone, however, a high level of DIAP1 will inhibit the activity of RHG proteins. In this model, high level of DIAP1 should be maintained even prior to ecdysone-induced RHG activation to block the activity of RHG proteins effectively. If it is the case, knock-down of *diap1* will cause cell killing of neurons that undergo remodeling.

Literature Cited

Acehan, D., Jiang, X., Morgan, D. G., Heuser, J. E., Wang, X. and Akey, C. W. (2002). Three-dimensional structure of the apoptosome: implications for assembly, procaspase-9 binding, and activation. *Mol. Cell* **9**, 423-432.

Akdemir, F., Farkaš, R., Chen, P., Juhasz, G., Medved'ová, L., Sass, M., Wang, L., Wang, X., Chittaranjan, S., Gorshi, S. M. et al. (2006). Autophagy occurs upstream or parallel to the apoptosome during histolytic cell death. *Development* **133**, 1457-1465.

Altaratz, M., Applebaum, S. W., Richard, D. S., Gilbert, L. I. and Segal, D. (1991). Regulation of juvenile hormone synthesis in wild-type and *apterous* mutant *Drosophila*. *Mol. Cell. Endocrinol.* **81**, 205-216.

Arama, E., Agapite, J. and Steller, H. (2003). Caspase activity and a specific cytochrome c are required for sperm differentiation in *Drosophila*. *Dev. Cell* **4**, 687-697.

Arama, E., Bader, M., Srivastava, M., Bergmann, A. and Steller, H. (2006). The two *Drosophila* cytochrome c proteins can function in both respiration and caspase activation. *EMBO J.* **25**, 232-243.

Arends, M. J., Morris, R. G. and Wyllie, A. H. (1990). Apoptosis: The role of endonuclease. *Am. J. Pathol.* **136**, 593-608.

Ashkenazi, A. and Dixit, V. M. (1998). Death receptors: signaling and modulation. *Science* **281**, 1305-1308.

Baehrecke, E. H. (2002). How death shapes life during development. *Nat. Rev. Mol. Cell. Biol.* **3**, 779-787.

Baehrecke, E. H. (2003). Autophagic programmed cell death in *Drosophila*. *Cell Death Differ.* **10**, 940-945.

Baggerman, G., Cerstiaens, A. De Loof, A. and Schoofs, L. (2002). Peptidomics of the larval *Drosophila melanogaster* central nervous system. *J. Biol. Chem.* **277**, 40368-40374.

Bakhshi, A., Jensen, J. P., Goldman, P., Wright, J. J., McBride, O. W., Epstein, A. L. and Korsmeyer, S. J. (1985). Cloning the chromosomal breakpoint of t (14;18)

human lymphomas: clustering around JH on chromosome 14 and near a transcriptional unit on 18. *Cell* **41**, 899-906.

Belyaeva, E. S., Aizenzon, M. G., Semeshin, V. F., Kiss, II, Koczka, K.,Baritcheva, E. M., Gorelova, T. D., and Zhimulev, I. F. (1980). Cytogenetic analysis of the 2B3-4--2B11 region of the X-chromosome of *Drosophila melanogaster*. I. Cytology of the region and mutant complementation groups. *Chromosoma* **81**, 281-306.

Bender, M., Imam, F. B., Talbot, W. S., Ganetzky, B. and Hogness, D. S. (1997). *Drosophila* ecdysone receptor mutations reveal functional differences among receptor isoforms. *Cell* **91**, 777-788.

Bergmann, A., Yang, A. Y. and Srivastava, M. (2003). Regulators of IAP function: coming to grips with the grim reaper. *Curr. Opin. Cell Biol.* **15**, 717-724.

Berreur, P., Porcheron, P., Moriniere, M., Berreur-Bonnenfant, J., Belinski-Deutsch, S., Busson, D. and Lamour-Audit, C. (1984). Ecdysteroids during the third larval instar in *1(3)ecd-1*^{ts}, a temperature-sensitive mutant of *Drosophila melanogaster*. *Gen. Comp. Endocrinol.* **54**, 76-84.

Berry, D. L., Schwartzman, R. A. and Brown, D. D. (1998). The expression pattern of thyroid hormone response genes in the tadpole tail identifies multiple resorption programs, *Dev. Biol.* **203**, 12–23.

Bogerd, J., Kooiman, F. P., Pijnenburg, M. A. P., Hekking, L. H. P., Oudejans, R. C. H. M. and Van der Horst, D. J. (1995). Molecular cloning of three distinct cDNAs, each encoding a different adipokinetic hormone precursor, of the migratory locust, *Locusta migratoria. J. Biol. Chem.* **270**, 23038-23043.

Boise, L. H., Gonzales-Garcia, M., Postema, C. E., Ding, L., Lindsten, T., Turka, L. A., Mao, X., Nunez, G. and Thompson, C. B. (1993). Bcl-x, a bcl-2-related gene that functions as a dominant regulator of apoptotic cell death. *Cell* **74**, 597-608.

Brachmann, C. B., Jassim, O. W., Wachsmuth, B. D., Cagan, R. L. (2000). The Drosophila Bcl-2 family member dBorg-1 functions in the apoptotic response to UV-irradiation. *Curr. Biol.* **10**, 547-550.

Bradbury, A. F., Finnie, M. D. A. and Smyth, D. G. (1982). Mechanism of C-terminal amide formation by pituitary enzymes. *Nature* **298**, 686-688.

Brizuela, B. J., Elfring, L., Ballard, J., Tamkun, J. W. and Kennison, J. A. (1994). Genetic analysis of the *brahma* gene of *Drosophila melanogaster* and polytene chromosome subdivisions 72AB. *Genetics* **137**, 803-813.

Brown, D. D., Wang, Z., Furlow, J. D., Kanamori, A., Schwartzman, R. A., Remo, B. F. and Pinder, A. (1996). The thyroid hormone-induced tail resorption program during *Xenopus laevis* metamorphosis. *Proc. Natl. Acad. Sci. USA.* **93**, 1924-1929.

Brown, H. L. D., Cherbas, L., Cherbas, P. and Truman, J. W. (2006). Use of time-lapse imaging and dominant negative receptors to dissect the steroid receptor control of neuronal remodeling in *Drosophila*. *Development* **133**, 275-285.

Burset, M., Seledtsov, I. A. and Solovyev, V. V. (2001). SpliceDB: Database of canonical and non-canonical mammalian splice sites. *Nucleic Acids Res.* **29**, 255-259.

Cain, K., Brown, D. G., Langlais, C. and Cohen, G. M. (1999). Caspase activation involves the formation of the aposome, a large (~700 kDa) caspase-activating complex. *J. Biol. Chem.* **274**, 22686-22692.

Cakouros, D., Daish, T. J. and Kumar, S. (2004a). Ecdysone receptor directly binds the promoter of the *Drosophila* caspase *dronc*, regulating its expression in specific tissues. *J. Cell Biol.* **165**, 631-640.

Cakouros, D., Daish, T. J., Mills, K. and Kumar, S. (2004b). An arginine-histone methyltransferase, CARMER, coordinates ecdysone-mediated apoptosis in *Drosophila* cells. *J. Biol. Chem.* **279**, 18467-71.

Cakouros, D., Daish, T., Martin, D., Baehrecke, E. H. and Kumar, S. (2002). Ecdysone-induced expression of the caspase DRONC during hormone-dependent programmed cell death in *Drosophila* is regulated by *Broad-Complex*. *J. Cell Biol.* **157**, 985-995.

Cantera, R., Veenstra, J. A. and Nässel, D. R. (1994). Postembryonic development of corazonin-containing neurons and neurosecretory cells in the blow fly, *Phormia terraenovae*. *J. Comp. Neurol.* **350,** 559-572.

Carney, G. E., Robertson, A., Davis, M. B. and Bender, M. (2004). Creation of *EcR* isoform-specific mutations in *Drosophila melanogaster* via local P element

transposition, imprecise P element excision, and male recombination. *Mol. Genet. Genomics* **271**, 282-290.

Cashio, P., Lee, T. V. and Bergmann, A. (2005). Genetic control of programmed cell death in *Drosophila melanogaster*. *Semin. Cell Dev. Biol.* **16**, 225-235.

Chen, P., Nordstrom, W., Gish, B. and Abrams, J. M. (1996). *grim*, a novel cell death gene in *Drosophila*. *Genes Dev.* **10**, 1773-1782.

Chen, P., Rodriguez, A., Erskine, R., Thach, T. and Abrams, J. M. (1998). *Dredd*, a novel effector of the apoptosis activators *reaper, grim*, and *hid* in *Drosophila*. *Dev. Biol.* **201**, 202-216.

Cherbas, L., Hu, X., Zhimulev, I., Belyaeva, E. and Cherbas, P. (2003). EcR isoforms in *Drosophila*: testing tissue-specific requirements by targeted blockade and rescue. *Development* **130**, 271-284.

Chew, S. K., Akdemir, F., Chen, P., Lu, W.-J., Mills, K., Daish, T., Kumar, S., Rodriguez, A. and Abrams, J. M. (2004). The apical caspase *dronc* governs programmed and unprogrammed cell death in *Drosophila*. *Dev. Cell* **7**, 897-907.

Chinnaiyan, A. M., O'Rourke, K., Lane, B. R. and Dixit, V. M. (1997). Interaction of CED-4 with CED-3 and CED-9: a molecular framework for cell death. *Science* **275**, 1122-1126.

Choi, Y.-J., Lee, G. and Park, J. H. (2006). Programmed cell death mechanisms of identifiable peptidergic neurons in *Drosophila melanogaster*. *Development* **133**, 2223-2232.

Choi, Y.-J., Lee, G., Hall, J. C. and Park, J. H. (2005). Comparative analysis of *Corazonin*-encoding genes (*Crz*'s) in *Drosophila* species and functional insights into *Crz*-expressing neurons. *J. Comp. Neurol.* **482**, 372-385.

Christich, A., Kauppila, S., Chen, P., Sogame, N., Ho, S.-I., and Abrams, J. M. (2002). The damage-responsive *Drosophila* gene *sickle* encodes a novel IAP binding protein similar to but distinct from *reaper*, *grim*, and *hid*. *Curr. Biol.* **12**, 137-140.

Cleary, M. L. and Sklar, J. (1985). Nucleotide sequence of a t(14;18) chromosomal breakpoint in follicular lymphoma and demonstration of a breakpoint-cluster region

near a transcriptionally active locus on chromosome 18. *Proc. Natl. Acad. Sci. USA* **82**, 7439-7443.

Colussi, P. A., Quinn, L. M., Huang, D. C. S., Coombe, M., Read, S. H., Richardson, H. and Kumar, S. (2000). Debcl, a proapoptotic bcl-2 homologue, is a component of the *Drosophila melanogaster* cell death machinery. *J. Cell Biol.* **148**, 703-714.

Conradt, B. and Horvitz, H. R. (1998). The *C. elegans* protein EGL-1 is required for programmed cell death and interacts with the Bcl-2-like protein CED-9. *Cell* **93**, 519-529.

Consoulas, C., Duch, C., Bayline, R. J. and Levine, R. B. (2000). Behavioral transformations during metamorphosis: Remodeling of neural and motor systems. *Brain Res. Bull.* **53**, 571-583.

Consoulas, C., Restifo, L. L. and Levine, R. B. (2002). Dendritic remodeling and growth of motoneurons during metamorphosis of *Drosophila melanogaster*. *J. Neurosci.* **22**, 4906-4917.

Cory, S. and Adams, J. M. (2002). The Bcl-2 family: regulators of the cellular life-or-death switch. *Nat. Rev. Cancer* **2**, 647-656.

Cruz Reyes, J. and Tata, J. R. (1995). Cloning, characterization and expression of two *Xenopus* bcl-2-like cell-survival genes. *Gene* **158**, 171-179.

Dai, J.-D. and Gilbert, L. I. (1998). Juvenile hormone prevents the onset of programmed cell death in the prothoracic glands of *Manduca sexta*. *Gen. Comp. Endocrinol.* **109**, 155-165.

Daish, T. J., Mills, K. and Kumar, S. (2004). *Drosophila* caspase DRONC is required for specific developmental cell death pathways and stress-induced apoptosis. *Dev. Cell* **7**, 909-915.

Danial, N. N. and Korsmeyer, S. J. (2004). Cell death: Critical control points. *Cell* **116**, 205-219.

Datta, S. (1999). Activation of neuroblast proliferation in explant culture of the *Drosophila* larval CNS. *Brain Res.* **818**, 77-83.

Desagher, S., Osen-Sand, A., Nichols, A., Eskes, R., Montessuit, S., Lauper, S., Maundrell, K., Antonsson, B. and Martinou, J. C. (1999). Bid-induced

conformational change of Bax is responsible for mitochondrial cytochrome c release during apoptosis. *J. Cell Biol.* **144**, 891–901.

Dodd, M. H. I. and Dodd, J. M. (1976). The biology of metamorphosis. Physiology of the Amphibia, ed. Lofts, B., Academic Press, New York, **3**, 467-599.

Dorstyn, L., Colussi, P. A., Quinn, L. M., Richardson, H. and Kumar, S. (1999). DRONC, and ecdysone-inducible *Drosophila* caspase. *Proc. Natl. Acad. Sci. USA* **96**, 4307-4312.

Dorstyn, L., Read, S., Cakouros, D., Huh, J. R., Hay, B. A. and Kumar, S. (2002). The role of cytochrome c in caspase activation in *Drosophila melanogaster* cells. *J. Cell Biol.* **156**, 1089-1098.

Draizen, T. A., Ewer, J. and Robinow, S. (1999). Genetic and hormonal regulation of the death of peptidergic neurons in the *Drosophila* central nervous system. *J. Neurobiol.* **38**, 455-465.

Du, C., Fang, M., Li, Y., Li, L. and Wang, X. (2000). Smac, a mitochondrial protein that promotes cytochrome c-dependent caspase activation by eliminating IAP inhibition. *Cell* **102**, 33–42.

Dubrovsky, E. B., Dubrovskaya, V. A., Bilderback, A. L. and Berger, E. M. (2000). The isolation of two juvenile hormone-inducible genes in *Drosophila melanogaster*. *Dev. Biol.* **224**, 486-495.

Ellis, H. M. and Horvitz, H. R. (1986). Genetic control of programmed cell death in the nematode *C. elegans*. *Cell* **44**, 817-829.

Emery, I. F., Noveral, J. M., Jamison, C. F. and Siwicki, K. K. (1997). Rhythms of *Drosophila period* gene expression in culture. *Proc. Natl. Acad. Sci. USA* **94**, 4092-4096.

Enari, M., Sakahira, H., Yokoyama, H., Okawa, H., Iwamatsu, A. and Nagata, S. (1998). A caspase-activated DNase that degrades DNA during apoptosis, and its inhibitor ICAD. *Nature* **391**, 43-50.

Ewer, J and Reynolds, S. (2002). Neuropeptide control of molting in insects. In: *Hormone, brain and behavior*, vol. 35 (ed. D.W. Pfaff, A. P. Arnold, S.E. Fahrbach, A. M. Etgen and R. T. Rubin), pp1-92. San Diego, CA: Academic Press.

Ewer, J., Wang, C.-M., Klukas, K. A., Mesce, K. A., Truman, J. W. and Fahrbach, S. E. (1998). Programmed cell death of identified peptidergic neurons involved in ecdysis behavior in the moth, *Manduca sexta*. *J. Neurobiol.* **37**, 265-280.

Fadok, V. A., Bratton, D. L., Rose, D. M., Pearson, A., Ezekewitz, R. A. and Henson, P. M. (2000). A receptor for phosphatidylserine-specific clearance of apoptotic cells. *Nature* **405**, 85–90.

Foley, K. and Cooley, L. (1998). Apoptosis in late stage *Drosophila* nurse cells does not require genes within the *H99* deficiency. *Development* **125**, 1075-1082.

Franc, N. C., Heitzler, P., Ezekowitz, R. A. B. and White, K. (1999). Requirement for Croquemort in phagocytosis of apoptotic cells in *Drosophila*. *Science* **284**, 1991-1994.

Furlow, J. D. and Neff, E. S. (2006). A developmental switch induced by thyroid hormone: *Xenopus laevis* metamorphosis. *Trends Endocrinol. Metab.* **17**, 38-45.

Giordano, E., Rendina, R., Peluso, I. and Furia, M. (2002). RNAi triggered by symmetrically transcribed transgenes in *Drosophila melanogaster*. *Genetics* **160**, 637-648.

Glücksmann, A. (1951) Cell death in normal vertebrate ontogeny. *Biol. Rev.* **26**, 59-86.

Gordon, A. S., Goldsmith, E. D. and Charipper, H. A. (1943) Effect of thiourea on the development of the amphibian. *Nature* **152**, 504–505.

Gorski, S. M., Chittaranjan, S., Pleasance, E. D., Freeman, J. D., Anderson, C. L., Varhol, R. J., Coughlin, S. M., Zuyderduyn, S. D., Steven, J. M., Jones, S. J. M. et al. (2003). A SAGE approach to discovery of genes involved in autophagic cell death. *Curr. Biol.* **13**, 358-363.

Goyal, L., McCall, K., Agapite, J., Hartwieg, E. and Steller, H. (2000). Induction of apoptosis by *Drosophila reaper*, *hid*, and *grim* through inhibition of IAP function. *EMBO J.* **19**, 589-597.

Graur, D. and Li, W.-H. (1999). Fundamentals of Molecular Evolution. Sunderland, MA: Sinauer.

Grether, M. E., Abrams, J. M., Agapite, J., White, K. and Steller, H. (1995). The *head involution defective* gene of *Drosophila melanogaster* functions in programmed cell death. *Genes Dev.* **9**, 1694-1708.

Gudernatsch, J. F. (1912). Feeding experiments on tadpoles. *Arch Entwicklungsmech Org* **35**, 457–483.

Gumienny, T. L., Brugnera, E., Tosello-Trampont, A. C., Kinchen, J. M., Haney, L. B., Nishiwaki, K., Walk, S. F., Nemergut, M. E., Macara, I. G., Francis, R. et al. (2001). CED-12/ELMO, a novel member of the CrkII/Dock180/Rac pathway, is required for phagocytosis and cell migration. *Cell* **107**, 27–41.

Hansen, I. A., Sehnal, F., Meyer, S. R. and Scheller, K. (2001). Corazonin gene expression in the wax moth *Galleria mellonella*. *Insect Mol. Biol.* **10**, 341-346.

Hao, H., Glossop, N. R., Lyons, L., Qiu, J., Morrish, B., Cheng, Y., Helfrich-Förster, C. and Hardin, P. (1999). The 69 bp circadian regulatory sequence (CRS) mediates per-like developmental, spatial, and circadian expression and behavioral rescue in Drosophila. *J. Neurosci.* **19**, 987-994.

Hartenstein, V. (1993). Atlas of *Drosophila* development. Cold Spring Harbor Laboratory Press, Plainview, NY.

Hasegawa, E. and Tanaka, S. (1994). Genetic control of albinism and the role of juvenile hormone in pigmentation in *Locusta migratoria*. *Jap. J. Entomol.* **62**, 315-324.

Hay, B. A., Wasserman, D. A. and Rubin, G. M. (1995). *Drosophila* homologs of baculovirus inhibitor of apoptosis proteins function to block cell death. *Cell* **83**, 1253-1262.

Helfrich-Förster, C. (1995). The period clock gene is expressed in central nervous system neurons which also produce a neuropeptide that reveals the projections of circadian pacemaker cells within the brain of *Drosophila melanogaster*. *Proc. Natl. Acad. Sci. USA* **92**, 612-616.

Helfrich-Förster, C. (1998). Robust circadian rhythmicity of *Drosophila melanogaster* requires the presence of lateral neurons: a brain-behavioral study of *disconnected* mutants. *J. Comp. Physiol. A* **182**, 435-453.

Hengartner, M. O., Ellis, R. E. and Horvitz, H. R. (1992). *Caenorhabditis elegans* gene *ced-9* protects cells from programmed cell death. *Nature* **356**, 494-499.

Hua, Y., Ishibashi, J., Saito, H., Tawfik, A. I., Sakakibara, M., Tanaka, Y., Derua, R., Waelkens, E., Baggerman, G., De Loof, A. et al. (2000). Identification of [Arg^7] corazonin in the silkworm, *Bombyx mori* and the cricket, *Gryllus bimaculatus*, as a factor inducing dark color in an albino strain of the locust, *Locusta migratoria*. *J. Insect Physiol.* **46**, 853-860.

Huang, Y., Erdmann, N., Peng, H., Zhao, Y. and Zheng, J. (2005). The role of TNF related apoptosis-inducing ligand in neurodegenerative diseases. *Cell Mol. Immunol.* **2**, 113-122.

Huh, J. R., Foe, I., Muro, I., Chen, C. H., Seol, J. H., Yoo, S. J., Guo, M., Park, J. M., and Hay, B. A. (2006). The *Drosophila* IAP DIAP2 is dispensable for cell survival, required for the innate immune response to Gram-negative bacterial infection, and can be negatively regulated by the Reaper/Hid/Grim family of IAP-binding apoptosis inducers. *J.Biol. Chem.* In Press.

Huh, J. R., Guo, M. and Hay, B. A. (2004). Compensatory Proliferation induced by cell death in the *Drosophila* wing disc requires activity of the apical cell death caspase Dronc in a nonapoptotic role. *Curr. Biol.* **14**, 1262-1266.

Hyun, S., Lee, Y., Hong, S.-T., Bang, S., Paik, D., Kang, J., Shin, J., Lee, J., Jeon, K. and Hwang, S. et al. (2005). *Drosophila* GPCR Han is a receptor for the circadian clock neuropeptide PDF. *Neuron* **48**, 267-278.

Igaki, T., Kanuka, H., Inohara, N., Sawamoto, K., Núñez, G., Okano, H. and Miura, M. (2000). Drob-1, a *Drosophila* member of the bcl-2/CED-9 family that promotes cell death. *Proc. Natl. Acad. Sci. USA* **97**, 662-667.

Jacobson, M. D., Weil, M. and Raff, M. C. (1997). Programmed cell death in animal development. *Cell* **88**, 347-354.

Janiak, F., Leber, B. and Andrews, D. W. (1994). Assembly of Bcl-2 into microsomal and outer mitochondrial membranes. *J. Biol. Chem.* **269**, 9842-9849.

Jiang, C., Baehrecke, E. and Thummel, C. (1997). Steroid regulated programmed cell death during *Drosophila* metamorphosis. *Development* **124**, 4673-4683.

Jiang, C., Lamblin, A.-F. J., Steller, H. and Thummel, C. S. (2000). A steroid-triggered transcription hierarchy controls salivary gland cell death during *Drosophila* metamorphosis. *Mol. Cell* **5**, 445-455.

Jursnich, V. A., Fraser, S. E., Held JR., L. I., Ryerse, J. and Bryant, P. J. (1990). Defective gap-junctional communication associated with imaginal disc overgrowth and degeneration caused by mutations of the *dco* gene in *Drosophila*. *Dev. Biol*. **140,** 413-429.

Kaiser, W. J., Vucic, D. and Miller, L. K. (1998). The *Drosophila* inhibitor of apoptosis D-IAP1 suppresses cell death induced by the caspase drICE. *FEBS Lett.* **440**, 243-248.

Kerr, J. F. R., Wyllie, A. H. and Currie, A. R. (1972) Apoptosis: a basic biological phenomenon with wide-ranging implications in the tissue kinetics. *Br. J. Cancer* **26**, 239-257.

Kiess, W. and Gallaher, B. (1998). Hormonal control of programmed cell death/ apoptosis. *Eur. J. Endocrinol.* **138**, 482-491.

Kim, Y.-J., Spalovska-Valachova, I., Cho, K.-H., Zitnanova, I., Park, Y., Adams, M. E. and Zitnan, D. (2004). Corazonin receptor signaling in ecdysis initiation. *Proc. Natl. Acad. Sci. USA* **101**, 6704-6709.

Kimura, K. I. and Truman, J. W. (1990). Post-metamorphic cell death in the nervous and muscular systems of *Drosophila melanogaster*. *J. Neurosci.* **10**, 403–411.

King-Jones, K. and Thummel, C. S. (2005). Nuclear receptors-A perspective from *Drosophila*. *Nat. Rev. Genet.* 6, 311-323.

Kischkel, F. C., Hellbardt, S., Behrmann, I., Germer, M., Pawlita, M., Krammer, P. H. and Peter, M. E. (1995). Cytotoxicity-dependent APO-1 (Fas/CD95)-associated proteins form a death-inducing signaling complex (DISC) with the receptor. *EMBO J.* **14**, 5579–5588.

Klionsky, D. J. and Emr, S. D. (2000). Autophagy as a regulated pathway of cellular degradation. *Science* **290**, 1717-1721.

Kornbluth, S. and White, K. (2005). Apoptosis in *Drosophila*: neither fish nor fowl (nor man, nor worm). *J. Cell Sci.* **118**, 1779-1787.

Kozopas, K. M., Yang, T., Buchan, H. L., Zhou, P. and Craig, R. W. (1993). MCL1, a gene expressed in programmed myeloid cell differentiation, has sequence similarity to BCL2. *Proc. Natl. Acad. Sci. USA* **90**, 3516–3520.

Kraft, R., Levine, R. B. and Restifo, L. L. (1998). The steroid hormone 20-hydroxyecdysone enhances neurite growth of *Drosophila* mushroom body neurons isolated during metamorphosis. *J. Neurosci.* **18**, 8886-8899.

Kumar, S. and Doumanis, J. (2000). The fly caspases. *Cell Death Differ.* **7**, 1039-1044.

Laski, F. A., Rio, D. C. and Rubin, G. M. (1986). Tissue specificity of Drosophila P element transposition is regulated at the level of mRNA splicing. *Cell* **44**, 7-19.

Laundrie, B., Peterson, J. S., Baum, J. S., Chang, J. C., Fileppo, D., Thompson, S. R. and McCall, K. (2003). Germline cell death is ihibited by *P*-element insertions disrupting the *dcp-1/pita* nested gene pair in Drosophila. *Genetics* **165**, 1881-1888.

Lee, C.-Y., Cooksey, B. A. K. and Baehrecke, E. H. (2002a). Steroid regulation of midgut cell death during *Drosophila* development. *Dev. Biol.* **250**, 101-111.

Lee, C.-Y., Simon, C. R., Woodard, C. T. and Baehrecke, E. H. (2002b). Genetic mechanism for the stage- and tissue-specific regulation of steroid triggered programmed cell death in *Drosophila*. *Dev. Biol.* **252**, 138-148.

Lee, C-Y, Clough, E. A., Yellon, P., Teslovich, T. M., Stephan, D. A. and Baehrecke, E. H. (2003). Genome-wide analyses of steroid- and radiation-triggered programmed cell death in *Drosophila*. *Curr. Biol.* **13**, 350-357.

Lee, G. and Park, J. H. (2004). Hemolymph sugar homeostasis and starvation-induced hyperactivity affected by genetic manipulations of the adipokinetic hormone-encoding gene in *Drosophila melanogaster*. *Genetics* **167**, 311-323.

Lee, G., Foss, M., Goodwin, S. F., Carlo, T., Taylor, B. J. and Hall, J. C. (2000a). Spatial, temporal, and sexually dimorphic expression patterns of the *fruitless* gene in the *Drosophila* central nervous system. *J. Neurobiol.* **43**, 404-426.

Lee, T and Luo, L. (1999). Mosaic analysis with a repressible cell marker for studies of gene function in neuronal morphogenesis. *Neuron* **22**, 451-461.

Lee, T., Marticke, S., Sung, C., Robinow, S. and Luo, L. (2000b). Cell-autonomous requirement of the USP/EcR-B ecdysone receptor for mushroom body neuronal remodeling in *Drosophila*. *Neuron* **28**, 807-818.

Leulier, F., Lhocine, N., Lemaitre, B. and Meier, P. (2006a) The *Drosophila* IAP DIAP2 functions in innate immunity and is essential to resist Gram-negative bacterial infection. *Mol Cell Biol.* In press.

Leulier, F., Ribeiro, P. S., Palmer, E., Tenev, T., Takahashi, K., Robertson, D., Zachariou, A., Pichaud, F., Ueda, R. and Meier, P. (2006b). Systematic *in vivo* RNAi analysis of putative components of the *Drosophila* cell death machinery. *Cell Death Differ.* 1-12.

Leulier, F., Rodriguez, A., Khush, R. S., Abrams, J. M. and Lemaitre, B. (2000). The *Drosophila* caspase Dredd is required to resist Gram-negative bacterial infection. *EMBO reports* **1**, 353-358.

Levine, R. B., Morton, D. B. and Restifo, L. L. (1995). Remodeling of the insect nervous system. *Curr. Opin. Neurobiol.* **5**, 28-35.

Libmbach, K. J. and Wu, R. (1985). Characterization of two *Drosophila melanogaster* cytochrome c genes and their transcripts. *Nucleic Acids Res.* **13**, 631-644.

Lisi, S., Mazzon, I. and White, K. (2000). Diverse domains of THREAD/DIAP1 are required to inhibit apoptosis induced by REAPER and HID in *Drosophila*. *Genetics* **154**, 669-678.

Liu, Q. A. and Hengartner, M. O. (1998). Candidate adaptor protein CED-6 promotes the engulfment of apoptotic cells in *C. elegans*. *Cell* **93**, 961–972.

Liu, X., Kim, C. N., Yang, J., Jemmerson, R. and Wang, X. (1996). Induction of apoptotic program in cell-free extracts: requirement for dATP and cytochrome c. *Cell* **86**, 147-157.

Lockshin, R. A., and Williams, C. M. (1964) Programmed cell death. II. Endocrine potentiation of the breakdown of the intersegmental muscles of silkmoths. *J Insect Physiol.* **10**, 643-649.

Ludwig, M. Z. (2002). Functional evolution of noncoding DNA. *Curr. Opin. Genet. Dev.* **12**, 634-639.

Luo, X., Budihardjo, I., Zou, H., Slaughter, C. and Wang, X. (1998). Bid, a Bcl2 interacting protein, mediates cytochrome c release from mitochondria in response to activation of cell surface death receptors. *Cell* **94**, 481–490.

McCarthy, J. V. and Dixit, V. M. (1998). Apoptosis induced by *Drosophila reaper* and *grim* in a human system. Attenuation by inhibitor of apoptosis proteins (cIAPs). *J. Biol. Chem.* **273**, 24009-24015.

McDonald, M. J. and Rosbash, M. (2001). Microarray analysis and organization of circadian gene expression in *Drosophila*. *Cell* **107**, 567-578.

McDonnell, T. J., Deane, N., Platt, F. M., Nunez, G., Jaeger, U., McKearn, J. P. and Korsmeyer, S. J. (1989). *bcl-2*-immunoglobulin transgenic mice demonstrate extended B cell survival and follicular lymphoproliferation. *Cell* **57**, 79–88.

Means, J. C., Muro, I. and Clem, R. J. (2006). Lack of involvement of mitochondrial factors in caspase activation in a *Drosophila* cell-free system. *Cell Death Differ.* **13**, 1222-1234.

Meier, P., Silke, J., Leevers, S. J. and Evan, G. I. (2000). The *Drosophila* caspase DRONC is regulated by DIAP1. *EMBO J.* **19**, 598-611.

Melchers, F., ten Boekel, E., Seidl, T., Kong, X. C., Yamagami, T., Onishi, K., Shimizu, T., Rolink, A. G. and Anderson, J. (2000). Repertoire selection by pre-B-cell receptors and B-cell receptors, genetic control of B-cell development from immature to mature B cells. *Immunol. Rev.* **175**, 33-46.

Mills, K., Daish, T., Harvey, K. F., Pfleger, C. M., Hariharan, I. K. and Kumar, S. (2006). The *Drosophila melanogaster* Apaf-1 homologue ARK is required for most, but not all, programmed cell death. *J. Cell Biol.* **172**, 809-815.

Muro, I., Berry, D. L., Huh, J. R., Chen, C. H., Huang, H., Yoo, S. J., Guo, M., Baehrecke, E. H. and Hay, B. A. (2006). The *Drosophila* caspase Ice is important for many apoptotic cell deaths and for spermatid individualization, a nonapoptotic process. *Development* **133**, 3305-3315.

Muro, I., Hay, B. A. and Clem, R. J. (2002). The *Drosophila* DIAP1 protein is required to prevent accumulation of a continuously generated, processed form of the apical caspase DRONC. *J. Biol. Chem.* **277**, 49644-49650.

Muro, I., Monser, K. and Clem, R. J. (2004). Mechanism of Dronc activation in *Drosophila* cells. *J. Cell Sci.* **117**, 5035-5041.

Muzio, M., Chinnaiyan, A. M., Kischkel, F. C., O'Rourke, K., Shevchenko, A., Ni, J., Scaffidi, C., Bretz, J.D., Zhang, M., Gentz, R. et al. (1996). FLICE, a novel FADD-homologous ICE/CED-3-like protease, is recruited to the CD95 (Fas/APO-1) death–inducing signaling complex. *Cell* **85**, 817–827.

Nagata, S. (2005). DNA degradation in development and programmed cell death. *Annu. Rev. Immunol.* **23**, 853–875.

Nakajima, K., Fujimoto, K. and Yaoita, Y. (2005). Programmed cell death during amphibian metamorphosis. *Sem. Cell Dev. Biol.* **16**, 271-280.

Nakajima, K., Takahashi, A. and Yaoita, Y. (2000). Structure, expression, and function of the *Xenopus laevis* caspase family. *J. Biol. Chem.* **275**, 10484-10491.

Nakano, K. and Vousden, K. H. (2001). PUMA, a novel pro-apoptotic gene, is induced by p53. *Mol. Cell* **7**, 683–694.

Nässel, D. R. (2002). Neuropeptides in the nervous system of *Drosophila* and other insects: multiple roles as neuromodulators and neurohormones. *Prog. Neurobiol.* **68**, 1-84.

Nässel, D. R. and Ekström, P. (1997). Detection of neuropeptides by immunocytochemistry. *Methods Mol. Biol.* **72**, 71-101.

Nieuwkoop, P. D. and Faber, J. (1956). Normal table of *Xenopus laevis*, North-Holland Publishing Company, Amsterdam.

O'Neil, M. T. and Belote, J. M. (1992). Interspecific comparison of the *transformer* gene of Drosophila reveals an unusually high degree of evolutionary divergence. *Genetics* **131**, 113-128.

O'Shea, M. and Rayne, R. C. (1992). Adipokinetic hormones: Cell and molecular biology. *Experientia* **48**, 430-438.

Oltvai, Z. N., Milliman, C. L. and Korsmeyer, S. J. (1993). Bcl-2 heterodimerizes *in vivo* with a conserved homolog, Bax, that accelerates programmed cell death. *Cell* **74**, 609–619.

Park, J. H. and Hall, J. C. (1998). Isolation and chronobiological analysis of a neuropeptide pigment-dispersing factor gene in *Drosophila melanogaster*. *J. Biol. Rhythms* **13**, 219-228.

Park, J. H., Helfrich-Förster, C., Lee, G., Li, L., Rosbash, M. and Hall, J. C. (2000). Differential regulation of circadian pacemaker output by separate clock genes in *Drosophila*. *Proc. Natl. Acad. Sci. USA* **97**, 3608-3613.

Park, J. H., Schroeder, A. J., Helfrich-Förster, C., Jackson, F. R. and Ewer, J. (2003). Targeted ablation of CCAP neuropeptide-containing neurons of *Drosophila* causes specific defects in execution and circadian timing of ecdysis behavior. *Development* **130**, 2645-2656.

Peterson, C., Carney, G. E., Taylor, B. J. and White, K. (2002). *reaper* is required for neuroblast apoptosis during *Drosophila* development. *Development* **129**, 1467-1476.

Phelps, C. B. and Brand, A. H. (1998). Ectopic gene expression in *Drosophila* using GAL4 system. *Methods* **14**, 367-379.

Ping, Y., Stoleru, D., Levine, J. D., Hall, J. C. and Rosbash, M. (2003). *Drosophila* free-running rhythms require intercellular communication. *PloS Biol.* **1**, 32-40.

Porras, M. G., De Loof, A., Breuer, M. and Arechiga, H. (2003). Corazonin promotes tegumentary pigment migration in the crayfish *Procambarus clarkii*. *Peptides* **24**, 1581-1589.

Powell, J. R. (1997). Progress and Prospects in Evolutionary Biology: The Drosophila Model. New York: Oxford University Press.

Predel, R. (2001). Peptidergic neurohemal system of an insect: Mass spectrometric morphology. *J. Comp. Neurol.* **436**, 363-375.

Predel, R., Agricola, H., Linde, D., Wollweber, L., Veenstra, J. A. and Penzlin, H. (1994). The insect neuropeptide corazonin: Physiological and immunocytochemical studies in *Blattariae*. *Zoology* **98**, 35-50.

Prochazkova, J., Kylarova, D., Vranka, P. and Lichnovsky, V. (2003). Comparative study of apoptosis-detecting techniques: TUNEL, apostatin, and lamin B. *BioTechniques* **35**, 528-533.

Quinn, L., Coombe, M., Mills, K., Daish, T., Colussi, P., Kumar, S. and Richardson, H. (2003). Buffy, a Drosophila Bcl-2 protein, has anti-apoptotic and cell cycle inhibitory functions. *EMBO J.* **22**, 3568-3579.

Quinn, L., Dorstyn, L., Mills, K., Colussi, P., Chen, P., Coombe, M., Abrams, J., Kumar, S. and Richardson, H. (2000). An essential role for the caspase dronc in developmentally programmed cell death in *Drosophila*. *J. Biol. Chem.* **275**, 40416-40424.

Raff, M. C., Barres, B. A., Burne, J. F., Coles, H. S., Ishizaki, Y. and Jacobson, M. D. (1993). Programmed cell death and the control of cell survival: lessons from the nervous system. *Science* **262**, 695-700.

Ranz, J. M., Castillo-Davis, C. I., Meiklejohn, C. D. and Hartl, D. L. (2003). Sex-dependent gene expression and evolution of the *Drosophila* transcriptome. *Science* **300**, 1742-1745.

Rathmell, J. C. and Thompson, C. B. (2002). Pathways of apoptosis in lymphocyte development, homeostasis, and disease. *Cell* **109**, S97-S107.

Reddien, P. W. and Horvitz, H. R. (2000). CED-2/CrkII and CED-10/Rac control phagocytosis and cell migration in *Caenorhabditis elegans. Nat. Cell Biol.* **2**, 131–136.

Reddien, P. W. and Horvitz, H. R. (2004). The engulfment process of programmed cell death in *Caenorhabditis elegans*. *Annu. Rev. Cell Dev. Biol.* **20**, 193-221

Reed, R. and Maniatis, T. (1985). Intron sequences involved in lariat formation during pre-mRNA splicing. *Cell* **41**, 95-105.

Renn, S. C. P., Park, J. H., Rosbash, M., Hall, J. C. and Taghert, P. H. (1999). A *pdf* neuropeptide gene mutation and ablation of PDF neurons each cause severe abnormalities of behavioral circadian rhythms in *Drosophila*. *Cell* **99**, 791-802.

Restifo, L. L. and Wilson, T. G. (1998). A juvenile hormone agonist reveals distinct developmental pathways mediated by ecdysone-inducible Broad Complex transcription factors. *Dev. Genet.* **22**, 141-159.

Riddiford, L. M. (1993). Hormones and *Drosophila* development. In *Development of Drosophila melanogaster* (ed. M. Bate and A. M. Arias), pp. 899-939. New York: Cold Spring Harbor Laboratory Press.

Riddiford, L. M., Cherbas, P. and Truman, J. W. (2001). Ecdysone receptors and their biological actions. *Vitam. Horm.* **60**, 1-73.

Ringo, J., Werczberger, R., Altaratz, M. and Segal, D. (1991). Female sexual receptivity is defective in juvenile hormone-deficient mutants of the *apterous* gene of *Drosophila melanogaster*. *Behav. Genet.* **21**, 453-469.

Robinow, S. and White K. (1991). Characterization and spatial distribution of the ELAV protein during *Drosophila melanogaster* development. *J. Neurobiol.* **22**, 443-461.

Robinow, S., Draizen, T. A. and Truman, J. W. (1997). Genes that induce apoptosis: Transcriptional regulation in identified, doomed neurons of the *Drosophila* CNS. *Dev. Biol.* **190**, 206-213.

Robinow, S., Talbot, W. S., Hogness, D. S. and Truman, J. W. (1993). Programmed cell death in the *Drosophila* CNS is ecdysone-regulated and coupled with a specific ecdysone receptor isoform. *Development* **119**, 1251-1259.

Rodriguez, A., Chen, P., Oliver, H. and Abrams, J. M. (2002). Unrestrained caspase-dependent cell death caused by loss of *Diap1* function requires the *Drosophila* Apaf-1 homolog, *Dark*. *EMBO J.* **21**, 2189-2197.

Rodriguez, A., Oliver, H., Zou, H., Chen, P., Wang, X. and Abrams, J. (1999). Dark, a *Drosophila* homolog of Apaf-1/ced-4, functions in an evolutionarily conserved death pathway. *Nat. Cell Biol.* **1**, 272-279.

Roller, L., Tanaka, Y. and Tanaka, S. (2003). Corazonin and corazonin-like substances in the central nervous system of the Pterygote and Apterygote insects. *Cell Tissue Res*. **312**, 393-406.

Rot-Nikcevic, I. and Wassersug, R. J. (2003). Tissue sensitivity to thyroid hormone in athyroid *Xenopus laevis* larvae. *Dev Growth Differ* **45**, 321–325.

Rubin, G. M. and Spradling, A. C. (1982). Genetic transformation of *Drosophila melanogaster* with transposable element vectors. *Science* **218**, 348-353.

Ryoo, H. D., Bergmann, A., Gonen, H., Ciechanover, A. and Steller, H. (2002). Regulation of *Drosophila* IAP1 degradation and apoptosis by *reaper* and *ubcD1*. *Nat. Cell Biol.* **4**, 432-438.

Sachs, L. M., Abdallah, B., Hassan, A., Levi, G., De Luze, A., Reed, J. C. and Demeneix, B. A. (1997). Apoptosis in *Xenopus* tadpole tail muscles involves Bax-dependent pathways. *FASEB J.* 11, 801-808.

Sakai, T., Satake, H., Minakata, H. and Takeda, M. (2004). Characterization of crustacean cardioactive peptide as a novel insect midgut factor: Isolation, localization, and stimulation of α-amylase activity and gut contraction. *Endocrinol.* **145**, 5671-5678.

Salvesen, G. S. and Abrams, J. M. (2004) Caspase activation - stepping on the gas or releasing the brakes? Lessons from humans and flies. *Oncogene* **23**, 2774-2784.

Saunders, D. S., Henrich, V. C. and Gilbert, L. I. (1989). Induction of diapause in *Drosophila melanogaster*: Photoperiodic regulation and the impact of arrhythmic clock mutations on time measurement. *Proc. Natl. Acad. Sci. USA* **86**, 3748-3752.

Savill, J. and Fadok, V. (2000). Corpse clearance defines the meaning of cell death. *Nature* **407**, 784–788.

Schin, K. S. and Clever, U. (1965). Lysosomal and free acid phosphatase in salivary glands of *Chironomus tentans*. *Science* **150**, 1053-1055.

Schoofs, L., Baggerman, G., Veelaert, D., Breuer, M., Tanaka, S., DeLoof, A. (2000). The pigmentotropic hormone [His^7]-corazonin, absent in a *Locusta migratoria* albino strain, occurs in an albino strain of *Schistocerca gregaria*. *Mol. Cell. Endocrinol.* **168**, 101-109.

Schreiber, A. M. and Brown, D. D. (2003). Tadpole skin dies autonomously in response to thyroid hormone at metamorphosis. *Proc. Natl. Acad. Sci. USA* **100**, 1769-1774.

Schubiger, M., Tomita, S., Sung, C., Robinow, S. and Truman, J. W. (2003). Isoform specific control of gene activity in vivo by the *Drosophila* ecdysone receptor. *Mech. Dev.* **120**, 909-918.

Schubiger, M., Wade, A. A., Carney, G. E., Truman, J. W. and Bender, M. (1998). *Drosophila* EcR-B ecdysone receptor isoforms are required for larval molting and for neuron remodeling during metamorphosis. *Development* **125**, 2053-2062.

Sehnal, F. and Bryant, P. J. (1993). Delayed Pupariation in *Drosophila* imaginal disc overgrowth Mutants is associated with reduced ecdysteroid titer. *J. Insect physiol.* **39**, 1051-1059.

Sharma, Y., Cheung, U., Larsen, E. W. and Eberl, D. F. (2002). pPTGAL, a convenient Gal4 *P*-element vector for testing expression of enhancer fragments in *Drosophila*. *Genesis* **34**, 115-118.

Shiga, S. (2003). Anatomy and functions of brain neurosecretory cells in Diptera. *Micro. Res. Tech.* **62**, 114-131.

Shiga, S., Davis, N. T., Hildebrand, J. G. (2003). Role of neurosecretory cells in the photoperiodic induction of pupal diapause of the tobacco hornworm *Manduca sexta*. *J. Comp. Neurol.* **462**, 275-285.

Slama, K., Sakai, T. and Takeda, M. (2006). Effect of corazonin and crustacean cardioactive peptide on heartbeat in the adult American cockroach (*Periplaneta americana*). *Arch. Insect Biochem. Physiol.* **62**, 91-103.

Song, Z., Guan, B., Bergman, A., Nicholson, D. W., Thornberry, N. A., Peterson, E. P. and Steller, H. (2000). Biochemical and genetic interactions between *Drosophila* caspases and the proapoptotic genes *rpr*, *hid*, and *grim*. *Mol. Cell. Biol.* **20**, 2907-2914.

Song, Z., McCall, K. and Steller, H. (1997). DCP-1, a *Drosophila* cell death protease essential for development. *Science* **275**, 536-540.

Sonnenfeld, M. J. and Jacobs, J. R. (1995). Macrophages and glia participate in the removal of apoptotic neurons from the *Drosophila* embryonic nervous system. *J. Comp. Neurol.* **359**, 644-652.

Srinivasula, S.M., Datta, P., Kobayashi, M., Wu, J.-W., Fujioka, M., Hegde, R., Zhang, Z., Mukattash, R., Fernandes-Alnemri, T., Shi, Y., et al. (2002). *Sickle*, a novel *Drosophila* death gene in the r*eaper/hid/grim* region, encodes an IAP-inhibitory protein. *Curr. Biol.* **12**, 125–130.

Stanewsky, R. (2002). Clock mechanisms in *Drosophila. Cell Tissue Res.* **309**, 11-26.

Stangier, J., Hilbich, C., Beyreuther, K., Keller, R. (1987). Unusual cardioactive peptide (CCAP) form pericardial organs of the shore crab *Carcinus maenas*. *Proc. Natl. Acad. Sci. USA* **84**, 575-579.

Sternberg, P. W. and Horvitz, H. R. (1981). Gonadal cell lineages of the nematode *Panagrellus redivivus* and implications for evolution by the modification of cell lineage. *Dev. Biol.* **88**, 147-166.

Streichert, L. C., Pierce, J. T., Nelson, J. A. and Weeks, J. C. (1997). Segment-specific programmed cell death of identified motoneurons triggered directly by steroid hormones in vitro. *Dev. Biol.* **183**, 95-107.

Suda, T., Takahashi, T., Golstein, P. and Nagata, S., (1993). Molecular cloning and expression of the Fas ligand, a novel member of the tumor necrosis factor family. *Cell* **75**, 1169–1178.

Sulston, J. E. (1976). Post-embryonic development in the ventral cord of *Caenorhabditis elegans*. *Philos. Trans. R. Soc. Lond. B Biol. Sci.* **275**, 287-297.

Suzuki, Y., Imai, Y., Nakayama, H., Takahashi, K., Takio, K. and Takahashi, R. (2001). A serine protease, HtrA2, is released from the mitochondria and interacts with XIAP, inducing cell death. *Mol. Cell* **8**, 613–621.

Taghert, P. H. and Schneider, L. E. (1990). Interspecific comparison of a *Drosophila* gene encoding FMRFamide-related neuropeptides. *J. Neurosci.* **10**, 1929-1942.

Talbot, W. S., Swyryd, E. A. and Hogness, D. S. (1993). *Drosophila* tissues with different metamorphic responses to ecdysone express different ecdysone receptor isoforms. *Cell* **73**, 1323-1337.

Tanaka, S. (2000a). The role of [His^7]-corazonin in the control of body-color polymorphism in the migratory locust, *Locusta migratoria* (Orthoptera: Acrididae). *J. Insect Physiol.* **46**, 1169-1176.

Tanaka, S. (2000b). Induction of darkening by corazonins in several species of Orthoptera and their possible presence in ten insect orders. *Appl. Entomol. Zool.* **35**, 509-517.

Tanaka, S. and Pener, M. P. (1994). A neuropeptide controlling the dark pigmentation in color polymorphism of the migratory locust, *Locusta migratoria*. *J. Insect Physiol.* **40**, 997-1005.

Tanaka, Y., Hua, Y. J., Roller, L. and Tanaka, S. (2002). Corazonin reduces the spinning rate in the silkworm, *Bombyx mori.* *J. Insect Physiol.* **48**, 707-714.

Tanaka, Y., Ishibashi, J. and Tanaka, S. (2003). Comparison of structure-activity relations of corazonin using two different bioassay systems. *Peptides* **24**, 837-844.

Tartaglia, L. A., Ayres, T. M., Wong, G. H. and Goeddel, D. V. (1993). A novel domain within the 55 kD TNF receptor signals cell death. *Cell* **74**, 845–853.

Tawfik, A. I., Tanaka, S., De Loof, A., Schoofs, L., Baggerman, G., Waelkens, E., Derua, R., Milner, Y., Yerushalmi, Y. and Pener, M. P. (1999). Identification of the gregarization-associated dark-pigmentotropin in locusts through an albino mutant. *Proc. Natl. Acad. Sci. USA* **96**, 7083-7087.

Tenev, T., Zachariou, A., Wilson, R., Paul, A. and Meier, P. (2002). Jafrac2 is an IAP antagonist that promotes cell death by liberating Dronc from DIAP1. *EMBO J.* **21**, 5118–5129.

Thevissen, K., Francois, I. E., Winderichx, J., Pannecougue, C., Cammue, B. P. (2006). Ceramide involvement in apoptosis and apoptotic diseases. *Mini Rev. Med. Chem.* **6**, 699-709.

Thummel, C. S. (1996). Flies on steroids-*Drosophila* metamorphosis and the mechanisms of steroid hormone action. *Trends Genet.* **12**, 306-310.

Tissot, M. and Stocker, R. F. (2000). Metamorphosis in *Drosophila* and other insects: the fate of neurons throughout the stages. *Prog. Neurobiol.* **62**, 89-111.

Truman, J. W. (1990). Metamorphosis of the central nervous system of *Drosophila*. *J. Neurobiol.* **21**, 1072-1084.

Truman, J. W., Talbot, W. S., Fahrbach, S. E. and Hogness, D. S. (1994). Ecdysone receptor expression in the CNS correlates with stage-specific responses to ecdysteroids during *Drosophila* and *Manduca* development. *Development* **120**, 219-234.

Truman, J. W., Taylor, B. J. and Awad, T. A. (1993). Formation of the adult nervous system. In *Development of Drosophila melanogaster* (ed. M. Bate and A. M. Arias), pp. 1234-1275. New York: Cold Spring Harbor Laboratory Press.

Trump, B. F., Valigorsky, J. M., Dess, J. H., Mergner, J. W., Kim, K. M., Jones, R. T., Pendergrass, R. E., Garbus, J. and Cowley, R. A. (1973). Cellular change in human disease: A new method of pathological analysis. *Hum. Pathol.* **4**, 89-109.

Tsujimoto, Y., Cossman, J., Jaffe, E. and Croce, C. M. (1985). Involvement of the *bcl-2* gene in human follicular lymphoma. *Science* **228**, 1440–1443.

Varkey, J., Chen, P., Jemmerson, R. and Abrams, J. M. (1999). Altered cytochrome-c display precedes apoptotic cell death in *Drosophila*. *J. Cell Biol.* **144**, 701-710.

Vaux, D. L., Cory, S. and Adams, J. M. (1988). Bcl-2 gene promotes haemopoietic cell survival and cooperates with c-myc to immortalize pre-B cells. *Nature* **335**, 440–442.

Veenstra, J. A, and Davis, N. T. (1993). Localization of corazonin in the nervous system of the cockroach *Periplaneta americana*. *Cell Tissue Res.* **274**, 57-64.

Veenstra, J. A. (1989). Isolation and structure of corazonin, a cardioactive peptide from the American cockroach. *FEBS Lett.* **250**, 231-234.

Veenstra, J. A. (1991). Presence of corazonin in three insect species, and isolation and identification of [His^7] corazonin from *Schistocerca americana*. *Peptides* **12**, 1285-1289.

Veenstra, J. A. (1994). Isolation and structure of the *Drosophila* corazonin gene. *Biochem. Biophys. Res. Commun.* **204**, 292-296.

Veis, D. J., Sorenson, C. M., Shutter, J. R. and Korsmeyer, S. J. (1993). *bcl-2*-deficient mice demonstrate fulminant lymphoid apoptosis, polycystic kidneys, and hypopigmented hair. *Cell* **75**, 229–240.

Verleyen, P., Baggerman, G., Mertens, I., Vandersmissen, T., Huybrechts, J., Lommel, A. V., Loof, A. D. and Schoofs, L. (2006). Cloning and characterization of a third isoform of corazonin in the honey bee *Apis mellifera*. *Peptides* **27**, 493-499.

Vernooy, S. Y., Chow, V., Su, J., Verbrugghe, K., Yang, J., Cole, S., Olsen, M. R. and Hay, B. A. (2002). *Drosophila* Bruce can potently suppress Rpr-and Grim-dependent but not Hid-dependent cell death. *Curr. Biol.* **12**, 1164-1168.

Vucic, D., Kaiser, W. J. and Miller, L. K. (1998). Inhibitor of apoptosis proteins physically interact with and block apoptosis induced by *Drosophila* proteins HID and GRIM. *Mol. Cell Biol.* 18, 3300-3309.

Wang, J., Zheng, L., Lobito, A., Chan, F. K.-M., Dale, J., Sneller, M., Yao, X., Puck, J. M., Straus, S. E. and Lenardo, M. J. (1999a). Inherited human caspase 10 mutations underlie defective lymphocyte and dendritic cell apoptosis in Autoimmune Lymphoproliferative Syndrome type II. *Cell* **98**, 47-58.

Wang, S. L., Hawkins, C. J., Yoo, S. J., Muller, H. A. J. and Hay, B. A. (1999b). The *Drosophila* caspase inhibitor DIAP1 is essential for cell survival and is negatively regulated by HID. *Cell* **98**, 453-463.

Wang, Z and Brown, D. D. (1993). Thyroid hormone-induced gene expression program for amphibian tail resorption. *J. Biol. Chem.* **268**, 16270–16278.

Watts, R. J., Hoopfer, E. D. and Luo, L. (2003). Axon pruning during *Drosophila* metamorphosis: Evidence for local degeneration and requirement of the ubiquitin-proteasome system. *Neuron* **38**, 871-885.

Watts, R. J., Schuldiner, O., Perrino, J., Larsen, C. and Luo, L. (2004) Glia engulfs degenerating axons during developmental axon pruning. *Curr. Biol.* **14**, 678-684.

Weeks, J. C. (2003). Thinking globally, acting locally: steroid hormone regulation of the dendritic architecture, synaptic connectivity and death of an individual neuron. *Prog. Neurobiol.* **70**, 421-442.

Weeks, J. C. and Truman, J. W. (1984a). Neural organization of peptide−activated ecdysis behaviors during the metamorphosis of *Manduca sexta*. I. Conservation of the peristalsis motor pattern at the larval–pupal transformation. *J. Comp. Physiol. A* **155**, 407–422.

Weeks, J. C. and Truman, J. W. (1984b). Neural organization of peptide-activated ecdysis behaviors during the metamorphosis of *Manduca sexta*. II. Retention of the proleg motor pattern despite loss of the prolegs at pupation. *J. Comp. Physiol. A* **155**, 423–433.

White, K., Grether, M. E., Abrams, J. M., Young, L., Farrell, K. and Steller, H. (1994). Genetic control of programmed cell death in *Drosophila*. *Science* **264**, 677-683.

Williams, J. A., Su, H. S., Bernards, A., Field, J. and Sehgal, A. (2001). A circadian output in *Drosophila* mediated by neurofibromatosis-1 and Ras/MAPK. *Science* **293**, 2251-2256.

Wilson, R., Goyal, L., Ditzel, M., Zachariou, A., Baker, D. A., Agapite, J., Steller, H. and Meier, P. (2002). The DIAP1 RING finger mediates ubiquitination of Dronc and is indispensable for regulating apoptosis. *Nat. Cell Biol.* **4**, 445-450.

Wing, J. P., Karres, J. S., Ogdahl, J. L., Zhou, L., Schwartz, L. M. and Nambu, J. R. (2002). *Drosophila* sickle is a novel grim-reaper cell death activator. *Curr. Biol.* **12**, 131-135.

Wing, J. P., Zhou, L., Schwartz, L. M. and Nambu, J. R. (1998). Distinct cell killing properties of the *Drosophila reaper*, *head involution defective*, and *grim* genes. *Cell Death Differ.* **5**, 930-939.

Wu, D., Wallen, H. D., Inohara, N. and Nunez, G (1997). Interaction and regulation of the *Caenorhabditis elegans* death protease CED-3 by CED-4 and CED-9. *J. Biol. Chem.* **272**, 21449-21454.

Wu, Y. C. and Horvitz, H. R. (1998a). The *C. elegans* cell corpse engulfment gene ced-7 encodes a protein similar to ABC transporters. *Cell* **93**, 951–960

Wu, Y. C. and Horvitz, H. R. (1998b). *C. elegans* phagocytosis and cell-migration protein CED-5 is similar to human DOCK180. *Nature* **392**, 501–504

Wyllie, A. H. (1980). Glucocorticoid-induced thymocyte apoptosis is associated with endogenous endonuclease activation. *Nature* **284**, 555-556.

Xu, D., Li, Y., Arcaro, M., Lackey, M. and Bergmann, A. (2005). The CARD-carrying caspase Dronc is essential for most, but not all developmental cell death in *Drosophila*. *Development* **132**, 2125-2134.

Xue, D., Shaham, S. and Horvitz, H. R. (1996). The *Caenorhabditis elegans* cell-death protein CED-3 is a cysteine protease with substrate specificities similar to those of the human CPP32 pretease. *Genes Dev.* **10**, 1073-1083.

Yan, N., Gu, L., Kokel, D., Chai, J., Li, W., Han, A., Chen, L., Xue, D. and Shi, Y. (2004). Structural, biochemical, and functional analyses of CED-9 recognition by the proapoptotic proteins EGL-1 and CED-4. *Mol. Cell* **15**, 999-1006.

Yang, X., Chang, H. Y. and Baltimore, D. (1998). Essential role of CED-4 oligomerization in CED-3 activation and apoptosis. *Science* **281**, 1355-1357.

Yin, V. P. and Thummel, C. S. (2004). A balance between diap1 death inhibitor and reaper and hid death inducers controls steroid-triggered cell death in *Drosophila*. *Proc. Natl. Acad. Sci. USA* **101**, 8022-8027.

Yoo, S. J., Huh, J. R., Muro, I., Yu, H., Wang, L., Wang, S. L., Feldman, R. M., Clem, R. J., Muller, H. A. and Hay, B. A. (2002). Hid, Rpr and Grim negatively regulate DIAP1 levels through distinct mechanisms. *Nat. Cell Biol*. **4**, 416-24.

Yuan, J. and Horvitz, H. R. (1990). The *Caenorhabditis elegans* genes *ced-3* and *ced-4* act cell autonomously to cause programmed cell death. *Dev. Biol.* **138**, 33-41.

Yuan, J., Shaham, S., Ledoux, S., Ellis, H. M. and Horvitz, H. R. (1993). The *C. elegans* cell death gene *ced-3* encodes a protein similar to mammalian interleukin-1beta-converting enzyme. *Cell* **75**, 641-652.

Zachariou, A., Tenev, T., Goyal, L., Agapite, J., Steller, H. and Meier, P. (2003). IAP-antagonists exhibit non-redundant modes of action through differential DIAP1 binding. *EMBO J.* **22**, 6642-6652.

Zaidi, A. U., Enomoto, H., Milbrandt, J. and Roth, K. A. (2000). Dual fluorescent *in situ* hybridization and immunohistochemical detection with tyramide signal amplification. *J. Histochem. Cytochem.* **48**, 1369-1375.

Zee, M. C. and Weeks, J. C. (2001). Developmental change in the steroid hormone signal for cell-autonomous, segment-specific programmed cell death of a motoneuron. *Dev. Biol.* **235,** 45–61.

Zha, J., Harada, H., Yang, E., Jockel, J. and Korsmeyer, S. J. (1996). Serine phosphorylation of death agonist BAD in response to survival factor results in binding to 14–3-3 not BCL-X(L). *Cell* **87**, 619–628.

Zhang, Z. and Gerstein, M. (2003). Of mice and men: phylogenetic footprinting aids the discovery of regulatory elements. *J. Biol.* **2**, 11.

Zheng, X., Wang, J., Haerry, T. E., Wu, A. Y.-H., Martin, J., O'Connor, M. B., Lee, C.-H. J. and Lee, T. (2003). TGF-β signaling activates steroid hormone receptor expression during neuronal remodeling in the *Drosophila* brain. *Cell* **112**, 303-315.

Zhou, L., Schnitzler, A., Agapite, J., Schwartz, L. M., Steller, H. and Nambu, J. R. (1997). Cooperative functions of the *reaper* and *head involution defective* genes in the programmed cell death of *Drosophila* central nervous system midline cells. *Proc. Natl. Acad. Sci. USA* **94**, 5131-5136.

Zhou, L., Song, Z., Tittel, J. and Steller, H. (1999). Hac-1, a *Drosophila* homolog of APAF-1 and CED-4, functions in developmental and radiation-induced apoptosis. *Mol. Cell* **4**, 745-755.

Zhou, Z., Hartwieg, E., and Horvitz, H. R. (2001). CED-1 is a transmembrane receptor that mediates cell corpse engulfment in *C. elegans*. *Cell* **104**, 43-56.

Zuzarte-Luís, V. and Hurlé, J. M. (2002). Programmed cell death in the developing limb. *Int. J. Dev. Biol*. **46**, 871-876.

Vita

Youn-Jeong Choi was born in Seoul, South Korea. She attended Yonsei University in Seoul and earned a Bachelor of Science degree in Biology in 1992 and a Master of Science degree in Molecular Biology and Microbiology in 1994. She met her husband, came to the United States, attended Pellissippi State Technical Community College in Knoxville and earned a certificate for Environmental Technology and Safety while she was pregnant. She came back to South Korea in 1997 and worked in the field of cell biology and biochemistry at Korea Research Institute of Bioscience and Biotechnology in Daejeon. She was admitted to Ph.D. program in Biochemistry and Cellular and Molecular Biology department at the University of Tennessee, Knoxville in 2001 and will graduate as a Ph.D. in the field of neurogenetics in fall 2006.